NUCLEAR SPACE POWER SYSTEMS

H. M. Dieckamp
Director, Space Systems Department
ATOMICS INTERNATIONAL
A Division of North American Aviation, Inc.

RUSS VICKERS

DISCLAIMER

PART I
STATE-OF-THE-ART – 1963

1. INTRODUCTION

There is at the present time a vigorous national program devoted to the development of extremely high-thrust space vehicle booster systems. These large and expensive booster systems will have the capability of placing large vehicles and payloads into space. The successful utilization of these large payloads will only be realized with the concurrent availability of lightweight, long-lived, high-power, reliable, electrical generating systems. The availability of large boosters coupled with nuclear auxiliary power sources will allow the space program to progress beyond the current era of space exploration. The future era of space utilization will reap untold benefits to all of mankind through world-wide communications, weather forecasts, navigational aids, etc. As nuclear power sources grow in power output and reliability, the promising ion and plasma forms of electric propulsion will allow interplanetary exploration without the fantastic size and cost of pure chemical systems.

For significant electrical power loads, which are required for missions in excess of several days, only solar and nuclear systems can be considered. The applicable range of various power systems is illustrated in Figure 1. Batteries and other chemical systems are ruled out on the basis of the large weights associated with these systems. At power levels of the order of a few kilowatts, both the various solar and nuclear power systems offer their own specific advantages and disadvantages, and the selection of a particular solar or nuclear power system can only be accomplished in the context of specific mission requirements, payload considerations, reliability, costs, etc. In this evaluation, the nuclear system offers definite advantages of ruggedness, high power per unit area, no collector deployment, no orientation, continuous power, minimum power storage requirement, etc. In many cases, the added power availability of a nuclear system should offer significant operational flexibility and improved reliability through application of more conventional circuitry and instrumentation and through redundancy. As the power requirements are increased to the order of tens of kilowatts, the nuclear systems have an increasingly favorable weight, size, and

TABLE I

SNAP DEVELOPMENT PROGRAMS

	SNAP 10A	SNAP 2	NASA SNAP 8	SPUR SNAP 50
Power, kwe	0.5	3	35 to 50*	350†
Reactor power, kwt	30	50	600*	2500†
Efficiency, %	1.6	6	8	14
Reactor outlet temperature, °F	1000	1200	1300*	~2000
Reactor	$U\text{-}ZrH_x$ Thermal	$U\text{-}ZrH_x$ Thermal	$U\text{-}ZrH_x$ Thermal	UC fast
Primary coolant	NaK-78	NaK-78	NaK-78	Lithium
Power conversion	Ge-Si Thermoelectric	Hg Rankine	Hg Rankine	K Rankine
Boiling temperature, °F	-	930	1070	-
Turbine inlet temperature, °F	-	1150	1250	1950†
Condensing temperature, °F	-	600	700*	1300 to 1400†
Hot junction temperature, °F	930	-	-	-
Cold junction temperature, °F	615	-	-	-
Radiator temperature, °F	615	600	580*	1300 to 1400
Radiator area, ft^2	62.5	120	1800*	700†
ft^2/kwe	125	40	45	2†
System unshielded weight, lb	650	1200	>3500*	5000
lb/kwe	1300	400	>100*	15
Available	1964	1966	1970	1975/1980
Development agency	AEC	AEC	AEC/NASA	AEC/AF
Flight test agency	AF	AF	NASA	AF
System contractor	Atomics International	Atomics International	Aerojet General	Pratt & Whitney
Power conversion contractor	Radio Corp. of America	Thompson Ramo Wooldridge	Aerojet General	AiResearch
Reactor contractor	Atomics International	Atomics International	Atomics International	Pratt & Whitney
Flight test contractor	Lockheed	Lockheed	-	-

*Nucleonics, Vol 21, No. 7, July 1936, p 79
†SPUR High Temperature Space Radiator, Parker and Stone, ARS Paper 2549-62, September 1962

cost advantage over any of the presently envisioned solar power systems. For power levels in the hundreds of kilowatts and above, a nuclear system is the only one which appears at all feasible. Despite the lack of specific plans for near term application of nuclear power, the SNAP (Systems for Nuclear Auxiliary Power) program has initiated the development and demonstration of a spectrum of units to fill future needs. The currently identified systems under development are described in Table I.

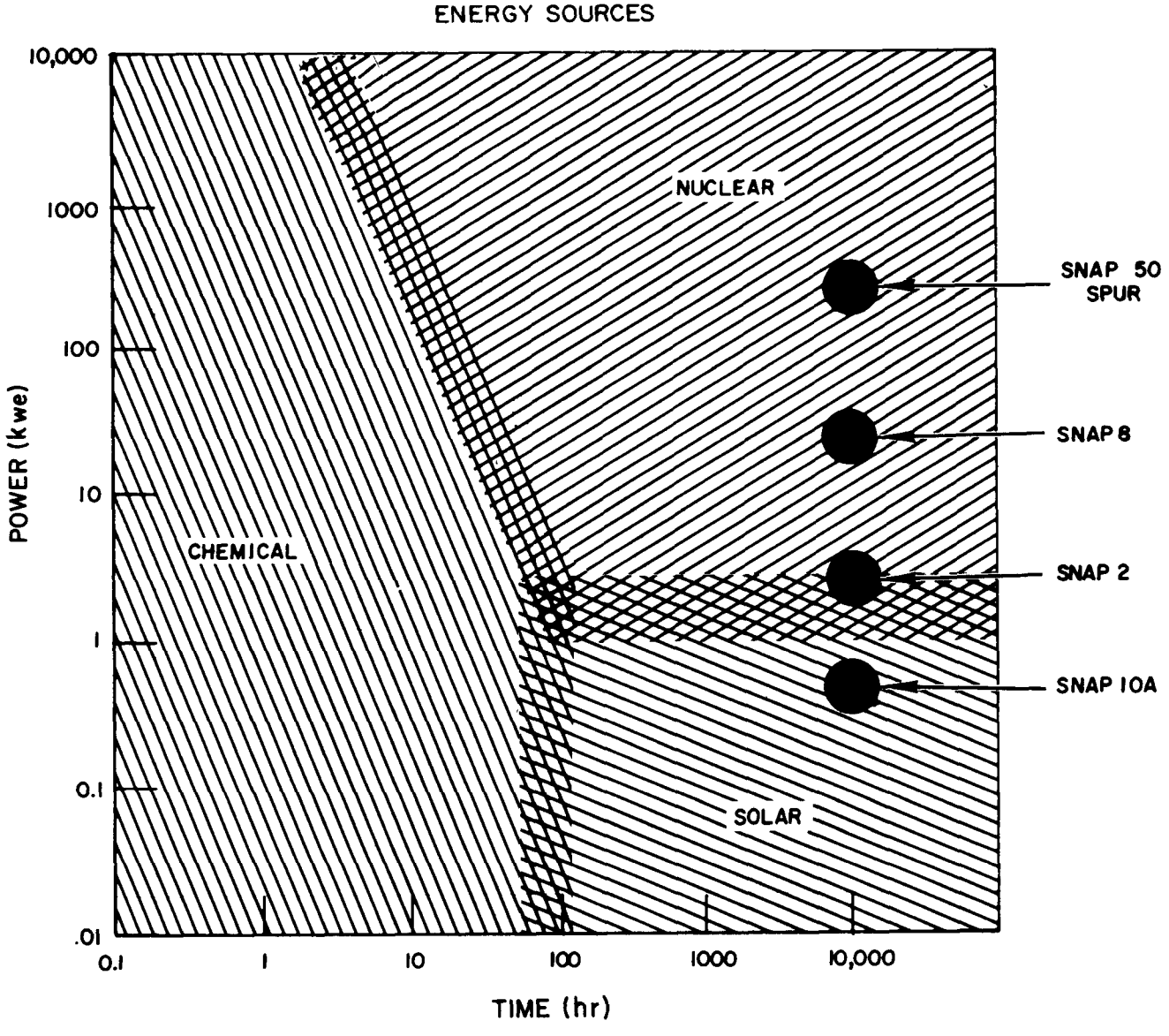

7-19-62 7561-0016

Figure 1. Power and Duration Regions for Various Energy Sources. (Chemical includes storage batteries, fuel cells, and cryogenic H_2-O_2 engine. Solar includes both photovoltaic as well as solar mirror systems. The circles indicate objectives of the current SNAP systems under development).

2. DEVELOPMENT STATUS

A. REACTORS

The SNAP hydride ($U\text{-}ZrH_x$) thermal reactor concept is employed in SNAP 10A, 2, and 8. Two full-power test reactors have integrated a total operating time in excess of two years at temperature and power conditions up to, and including, the SNAP 10A and SNAP 2 requirements. A third power reactor test, designed for the SNAP 8 higher power and temperature conditions, is critical and in the early test phases. A uranium carbide fast reactor concept is currently considered the prime choice for SNAP 50. The SNAP 50 program is proceeding with the LCRE (Lithium Cooled Reactor Experiment). This test is a residual of the ANP program and bears only a coolant temperature and structural materials technology relationship to SNAP 50. It is significant to note that the total operating reactor experience near the SNAP 50 temperature requirements is just a few minutes.

B. POWER CONVERSION

The SNAP 10A system employs silicon-germanium alloy materials for thermoelectric direct power conversion. The lower figure of merit, $S^2/\rho k$ of the Si-Ge alloys, was accepted in order to achieve better fabricability and higher temperature capability than the more familiar Pb-Te. The Hg Rankine cycle turbomachinery development for SNAP 2 has overcome the structural and thermal distortion problems that were limiting the reliability of the Hg lubricated bearings. Recent rotating machinery endurance accomplishments on SNAP 2 and Sunflower have demonstrated the complete engineering feasibility of a hermetic machine with working fluid lubrication. In a recent redirection of the SNAP 8 program, these advantages of the SNAP 2 concept have been abandoned. The NASA feels that the redirection to utilize rotating shaft seals and organic lubricants will allow a separation of development variables and will provide a closer relationship to existing technology for SNAP 8. In comparison to SNAP 2, which employs direct condensation of the Hg in a combination condenser-radiator, SNAP 8 now includes a compact condenser with a liquid metal heat transfer loop coupling the condenser to the radiator. In addition, SNAP 8 now includes an organic loop and radiator to cool the lubricant. The immediate SNAP 8 turbomachinery development will reveal the practicability of attempting to apply conventional conversion

machinery technology to space power. The power conversion for SNAP 50 should be considered to be in the research phase. Considerable research has been initiated by several agencies in the problems relating to alkali metal power conversion systems. The effort must certainly be considered as dominated and paced by high temperature (refractory metals) materials and fabrication technology.

C. SYSTEM

The system and boost vehicle integration design have been completed for SNAP 10A. Prototype flight systems have been fabricated and the program is proceeding into the system preflight qualification phase. SNAP 2 is well into component development and the early stages of system development. SNAP 8 should be characterized as in the component development and system definition phase and SNAP 50 as research.

D. FLIGHT TESTS

SNAP 10A and 2 will be flight tested as part of a joint AEC/AF program during 1964 and 1966, respectively. The Atlas/Agena combination will be used in these test flights. The NASA has postponed specific flight test plans for SNAP 8 until there is a better definition of the mission. It is expected that SNAP 50 flight testing will again be a joint AEC/AF program; any schedule planning has not been disclosed.

3. OPERATIONAL FACTORS

A. SHIELDING

The shield weight is a stronger function of the mission and allowable integration configuration then it is of the power unit. In the case of payloads comprised of semiconductor devices, dose levels below 10^{11} nvt and 10^{6} r probably require very minor restrictions on component selection. Payload hardening for 10^{12} nvt and 10^{7} r can be accommodated if properly considered from the outset of payload design.

The shield weight for simple conical shadow shield geometry can be in the region of 200 to 500 lb for SNAP 10A, 2, and 8. In the case of manned applications, the shield weight varies from 4000 to 7000 lb for a simple conical shadow shield configuration of a small (10 ft diameter) space station to 15,000 to 20,000 lb for a large (150 ft diameter) toroidal station.

B. RELIABILITY

The high-energy density advantage of nuclear heat sources directly implies that long life is a necessary requirement to achieve the full advantage of nuclear power systems. The only unique, self-imposed, environment that could influence reliability is radiation. The more important influences of high temperature, corrosion, creep, high vacuum, micrometeors, etc., are shared by other approaches to high performance space power. The major problem becomes apparent when one considers the unreasonable time and cost associated with a statistical demonstration of reliability or with the corollary identification of failure modes with confidence. This basic dilema is shared by many other aspects of the space program. The ultimate solution must rely upon simplicity, basic phenomenological understanding, and sound engineering. Basic system development must progress to a level which allows a valid judgment of inherent reliability and considerable experience will have to come from interim usage.

C. COST

The SNAP 10A and 2 programs have progressed to the point where reasonably accurate cost estimates can be made. The basic cost of a SNAP 10A unit is estimated at less than one million dollars and the SNAP 2 unit should cost between 1 and 1.5 million dollars. An estimate of 3 to 5 million dollars for a SNAP 8 unit seems reasonable.

D. SAFETY

Thus far in the SNAP program, no insurmountable safety problems have been identified. The AEC has established an Aerospace Safety Program for the specific purpose of developing the technology necessary to minimize any nuclear safety problems. The SNAP systems have been designed to meet operational factory-to-flight sequence requirements. In general, the reactor powered SNAP unit can be transported, stored, installed, checked-out, etc., without nuclear hazard or personnel exposure. In general, the use of a reactor powered unit need not perturb the normal launch operations. During launch, the normal chemical exclusion radius is adequate to protect launch personnel from any unlikely nuclear hazard introduced by a vehicle malfunction or abort. During the entire prelaunch and launch sequence the reactor is basically inert and contains a negligible inventory of radioactivity. After startup and operation in orbit, the system can be shut down and the accumulated radioactivity will decay to a safe level during the remaining time in orbit prior to reentry. A recent suborbital flight test indicates that reentry heating will assist in the safe dispersal of any remaining inventory at reentry. It is clear that the use of nuclear power units in earth orbits will not constitute a radiological hazard to the general public.

4. FUTURE DIRECTION

The key to improved performance (watts/lb or watts/ft^2) of all space power systems including the SNAP units is heat source temperature. In general, the performance advancements will be paced by the availability of the materials technology required by a given operating temperature. In the reactor, temperature and fuel material selection will determine the useful power output of the reactor before failure due to fission product induced fuel swelling. In the remainder of the system, temperature and material selection will limit life due to corrosion, creep, sublimation, etc. It is clear that temperature is the key to improved performance, however detrimental it may be to system life and reliability.

The performance of SNAP 10A and subsequent thermoelectric systems improves rapidly with source temperature. The watts/ft^2 of radiator area are proportional to the fifth power of the source temperature. The low efficiency disadvantage of thermoelectric systems will probably be offset by the inherent reliability of static power conversion up to multikilowatt power levels.

The performance of the Hg Rankine cycles is limited by the practical working pressure limit and the thermodynamic properties of Hg. The major improvement in Rankine cycles occurs with the change in working fluid which unfortunately involves a discrete temperature step of about 600 to 800°F to the SNAP 50 conditions. In the future, Hg systems will probably be used beyond their region of optimum size because of the more immediate availability of the lower temperature technology. Thus, large Hg Rankine systems or multiple smaller systems may well be used in the several hundred kilowatt power range.

The discrete temperature applicability of Rankine cycles introduces a significant aspect of the Brayton cycle which is not currently part of the nuclear space power program. Even though the Brayton cycle requires a larger radiator area at a given heat source temperature limit, the cycle and the machinery are probably more versatile in accepting the increased heat source temperature capability that time and technological improvements will yield. The potential of a more continuous performance growth could have a significant influence on long-term reliability achievement.

As a backup to the SNAP 50 program, the AEC has initiated a development program at ORNL to evaluate the feasibility of a system employing a fast reactor

with direct alkali metal boiling in the reactor core. The maximum performance system of the future, 5 to 10 lb/kw, is the reactor thermionic system. Even though this concept has been called SNAP 70, no system development program has been established. Two system concepts are being advanced. One system employs vacuum diodes outside the reactor, perhaps in the radiator. This concept forces the entire reactor structure, control, coolant, pumps, etc., to operate in the 2000 to 2500°F region. The other approach places the diodes directly in the core as an integral subassembly of the fuel element. The nuclear material operates at the cathode temperature of the space charge neutralized diode of about 3000°F, while the remaining reactor structure, control, coolant, pumps, etc., operate at the anode temperature of about 1500°F. There have been many independent and government sponsored research efforts in the field of thermionic conversion. The basic phenomenon is reasonably well understood as evidenced by demonstrated conversion efficiency and power density accomplishments. The problems of materials selection for the environment and for useful diode life are less well understood. The technology necessary for the selection of a reactor fuel material with appropriate physical properties and high energy output capability is currently far from the status required to support serious system design and development.

5. COMPETITIVE POSITION

A partial appreciation of the comparison between nuclear power plants and the alternate energy sources can be derived from the following figures. Figure 2 shows a comparison with chemical energy storage devices of various watt-hr/lb ratings. The ordinate shows the time duration at which the weight of the chemical sources exceeds the weight of a nuclear plant for a given power. The nuclear devices currently occur only at discrete power levels but for the purposes of this comparison, a continuum is implied between these powers. It is apparent from Figure 2 that nuclear devices become competitive from a weight point of view for rather short durations of large amounts of power. Figure 3 compares the weight of the current nuclear power plants with the approximate weight of solar cell systems as a function of power. It can be seen that the weight crossover occurs at about one kilowatt. Since weight alone is not the complete picture, Figure 4 compares the required solar cell area with the nuclear power plant radiator area requirements. The area crossover occurs at a few hundred watts. It should be remembered that the nuclear power plant requires no continuous orientation and no energy storage to cover operation while in the earth's shadow. The area comparison further favors nuclear power when one considers far planet operations where the solar intensity is significantly lower. From a dollar cost point of view, SNAP 10A will cost about one million dollars which is competitive with an equivalent solar cell system. At high power levels the nuclear systems will have a significant cost advantage (see Figure 5).

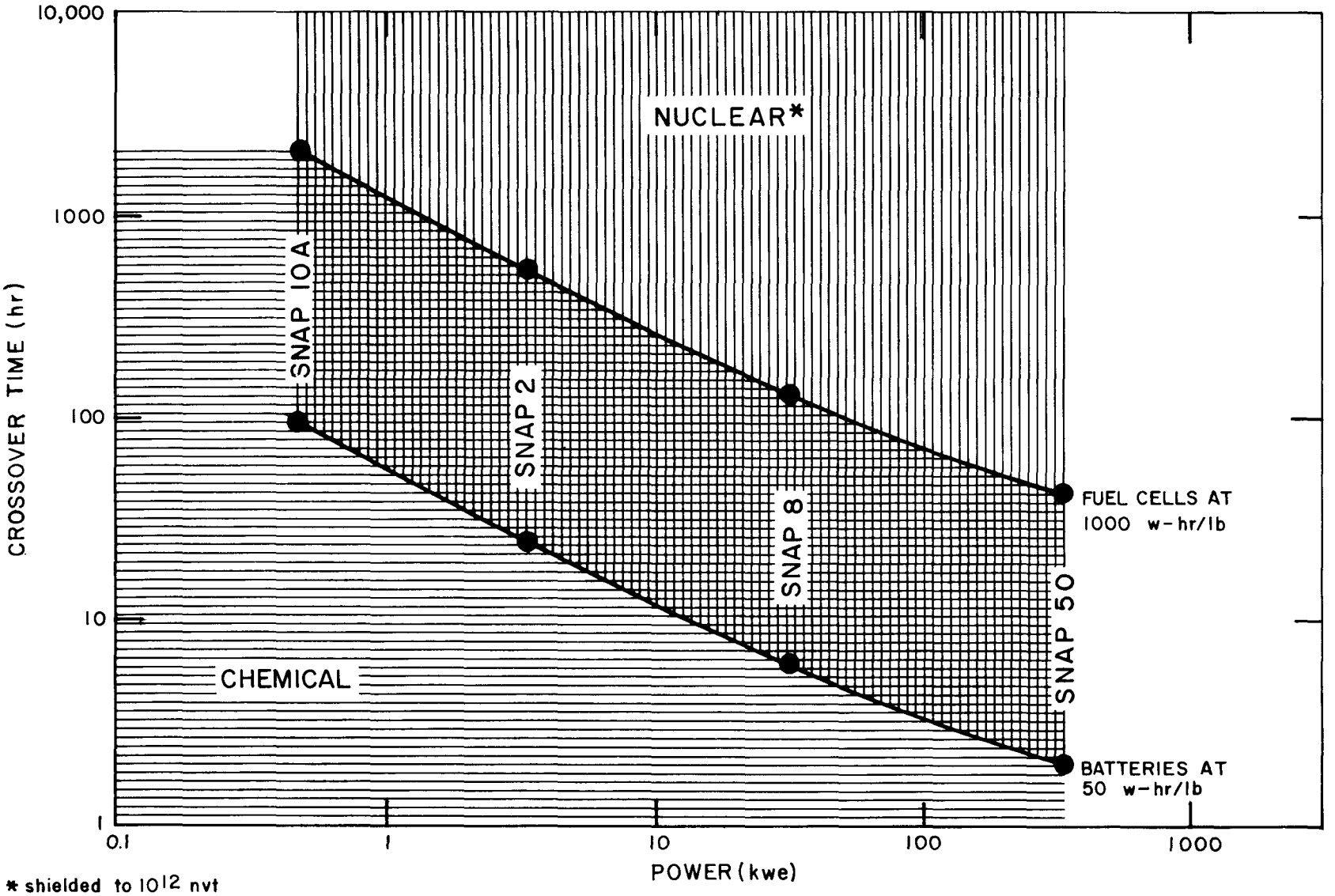

10-9-63

7561-0749

Figure 2. Weight Crossover Between Chemical and Nuclear Power Systems as a Function of Power and Endurance. (The crossover time is defined as the time at which the weight of a chemical system at a given watt-hr/lb rating exceeds the weight of a nuclear system.)

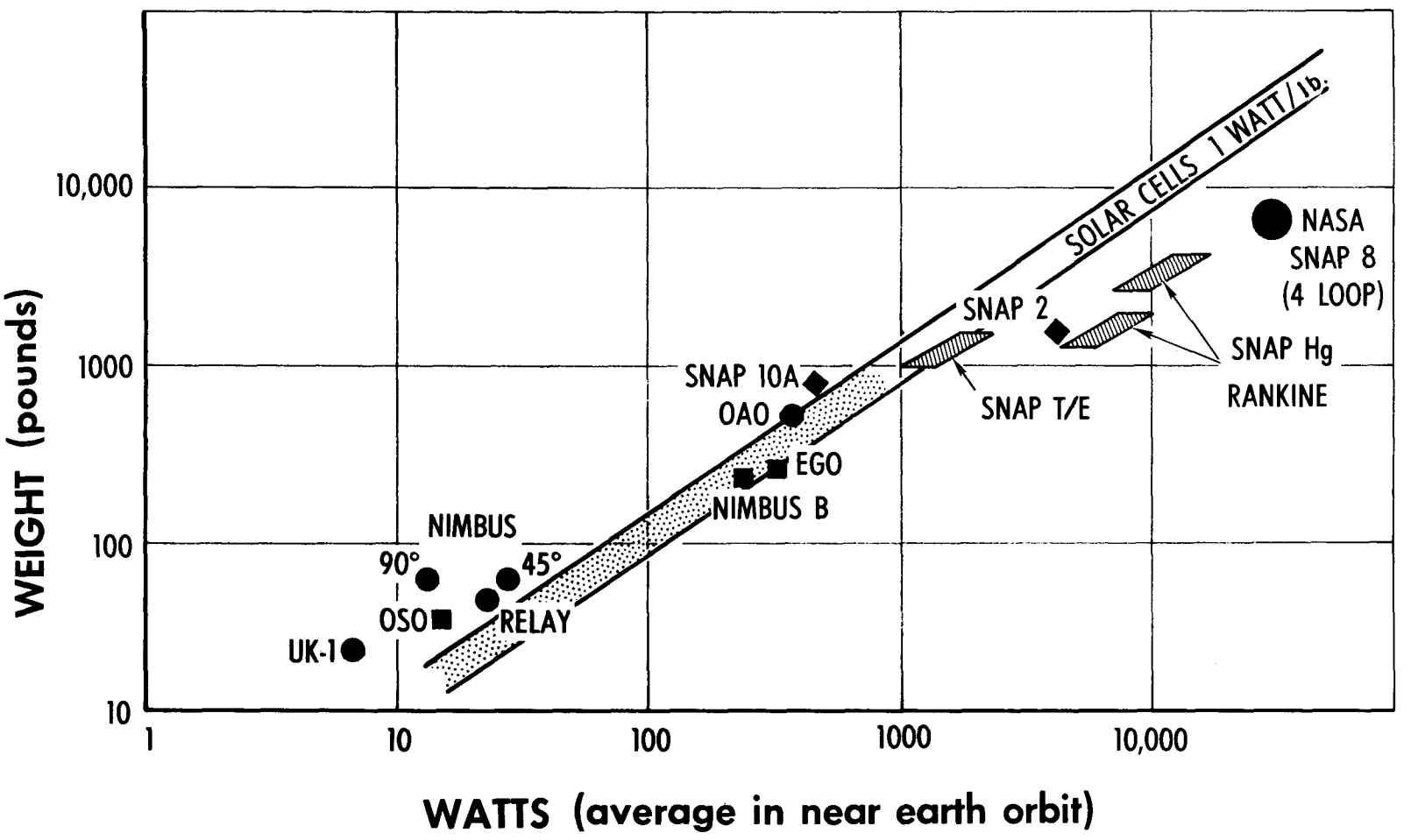

6-24-63

7561-0482

Figure 3. Comparison of Weight of Solar Cell and Nuclear APU's as a Function of Power. (The solar cell weights do not include the weight of orientation propellant for long durations. The nuclear system weights include shielding for electronic payloads, 10^{12} nvt. Solar cell data: Cherry, Wm. R., Astronautics and Aerospace Engineering, May 1963)

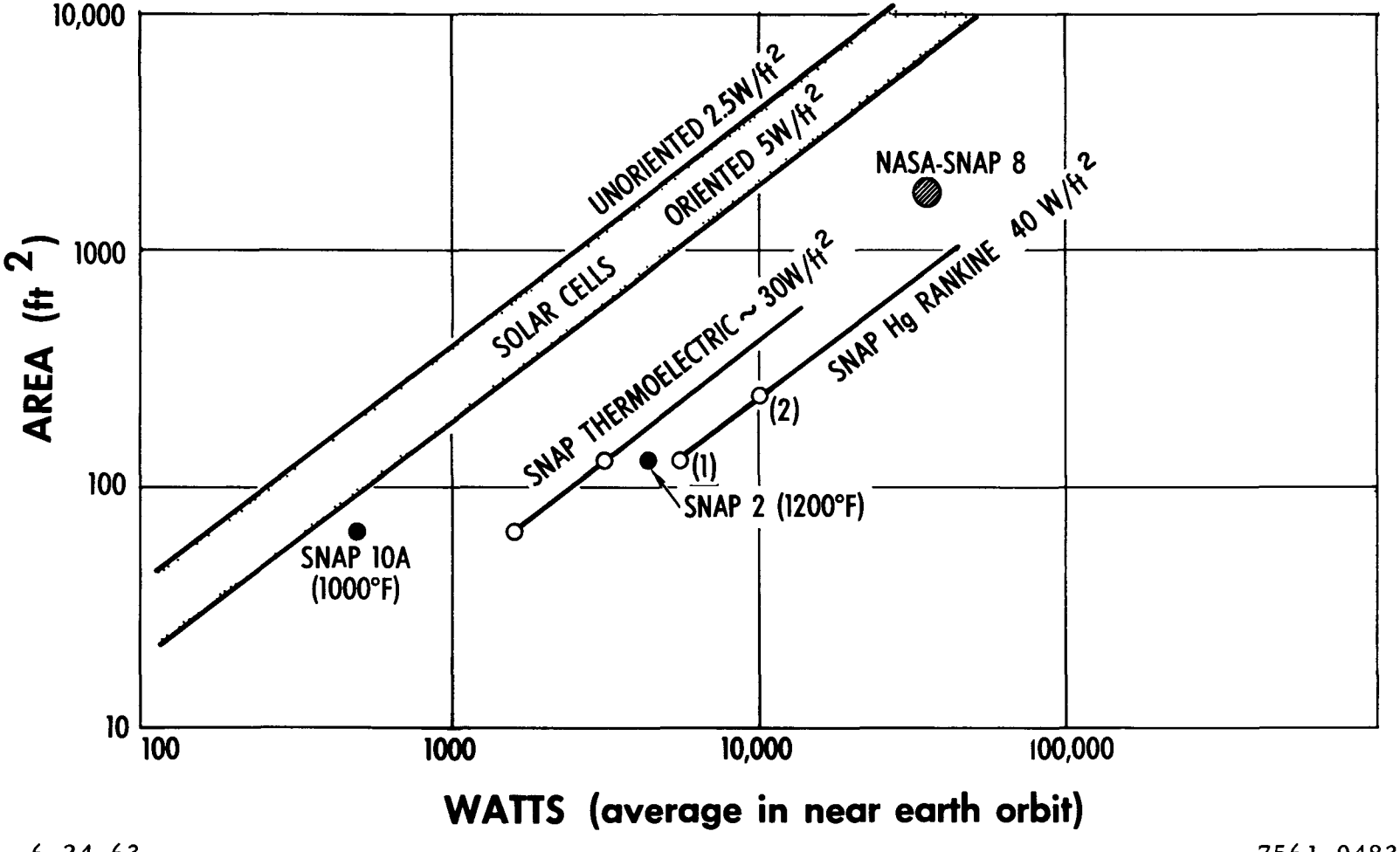

6-24-63

7561-0483

Figure 4. Area Requirements for Solar Cell Arrays and Nuclear Systems as a Function of Power

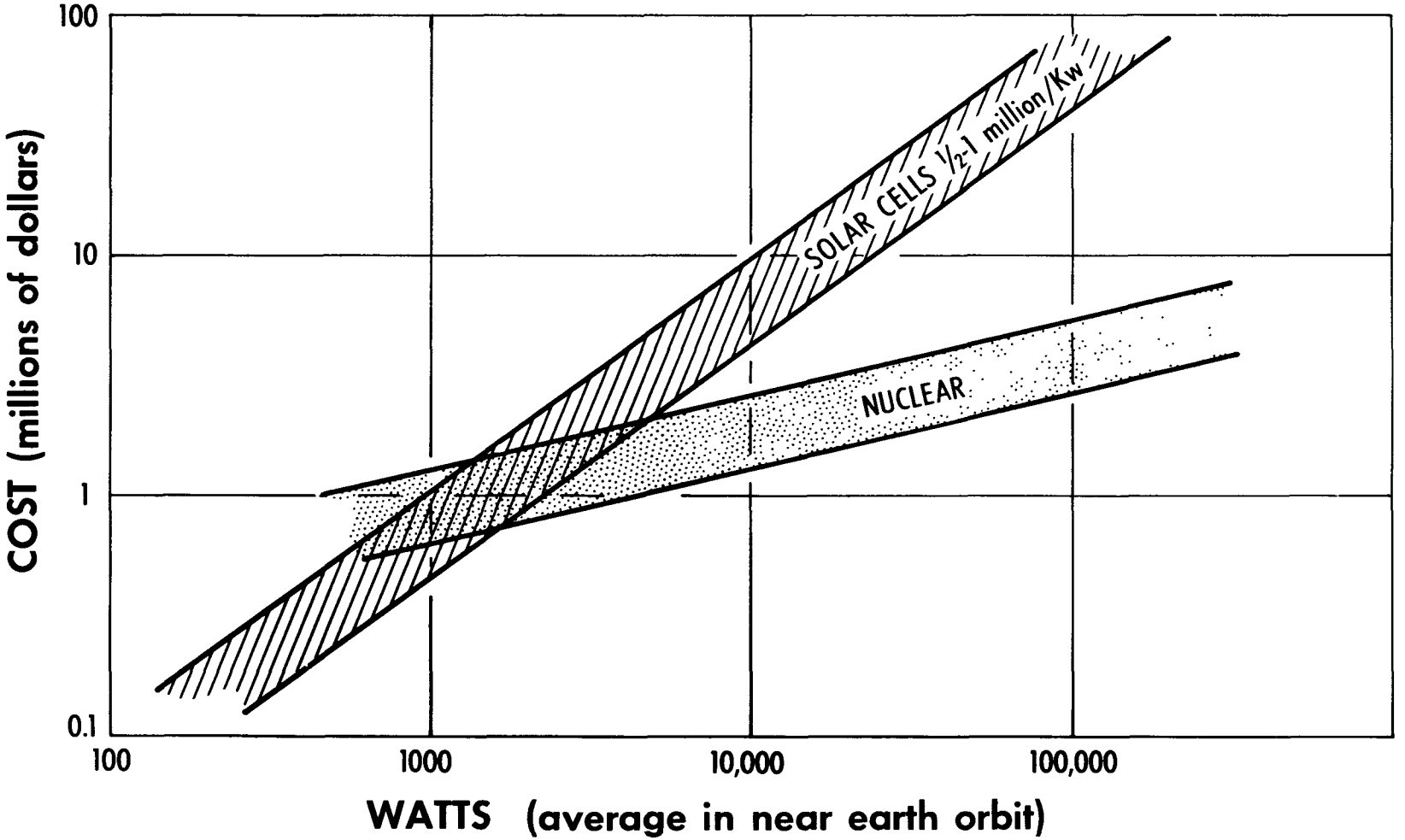

Figure 5. Cost Comparison Between Nuclear and Solar Cell Systems as a Function of Power

PART II
SYSTEM TECHNOLOGY

1. INTRODUCTION

A nuclear power supply for space vehicle applications is composed of three major subsystems:

a) Nuclear reactor heat source

b) Power-conversion system

c) Heat-rejection system

These three major subsystems are closely interrelated in the selection of a power system concept and the subsequent system optimization and design point selection. The unique space limitation of radiative heat rejection only results in an extreme premium on high heat source temperature and a system Carnot cycle efficiency optimum (η_c = 0.2 to 0.25) for minimum heat-rejection radiator area. These considerations coupled with the efficiency and temperature requirements of the power-conversion subsystem define the reactor heat source temperature and power. The reactor temperature and power requirements in turn determine the reactor concept, materials, size, and configuration. In addition, many unique considerations and requirements are imposed on the space power system.

The more significant ones are:

a) Operation at high temperature to provide for efficient radiative heat rejection

b) Capability of withstanding the severe shocks, vibrations, gravity, pressure, and temperature transients during vehicle launch

c) Operation in high vacuum

d) Operation in zero-gravity

e) Operation in presence of space radiations and rain of micrometeorite particles

f) Minimum weight and size

g) Long unattended life

h) High reliability

i) Remote startup in orbit

j) Completely automatic control

k) Capability of operating without subjecting the vehicle to excessive disturbing torques

l) Design and installation to permit efficient low weight shadow shielding of payloads

m) Packaging and installation to permit prelaunch startup and checkout with maximum safety and minimum vehicle and facility modification

n) Packaging for installation within vehicle structural and flight stability constraints

o) Reentry burnup of systems which may operate in low-altitude reentering orbits

The purpose of the following material is to indicate the basic capabilities and limitations of nuclear reactor heat sources and to survey the reactor requirements imposed by the currently applicable power-conversion subsystems, i.e., turboelectric, thermoelectric, and thermionic. The approach toward satisfying the unique operational requirements of space nuclear power plants will be introduced by a description of the current systems under development.

2. NUCLEAR FISSION

A. FISSION PROCESS

In the fission process the nucleus absorbs a neutron and the resulting compound nucleus is so unstable that it immediately breaks up into two parts of more or less equal mass, called fission fragments. Most of the fragments are radioactive, decaying at different rates, with the emission of negative beta particles and gamma radiation, to form products which are themselves usually radioactive. In the fission of U-235, for example, there are formed more than 80 primary products, with mass numbers ranging from 72 to 160. Each of these undergoes, on the average, three stages of radioactive decay before being converted into a stable nucleus. As a result, there are over 200 radioactive isotopes of 30 or more different elements present among the fission products after a short time.

Nuclear fission as a result of neutron capture occurs only with the heaviest elements. Whereas certain isotopes, notably uranium-233, uranium-235, and plutonium-239 undergo fission with thermal (low-energy) neutrons as well as with fast (high-energy) neutrons, others, such as thorium-232 and uranium-238 require fast neutrons to cause fission. In general, the cross section (neutron capture probability) is largest for thermal neutrons; it then decreases with increasing neutron energy, according to $(\text{velocity})^{-1}$, and becomes relatively small for fast neutrons.

From the point of view of the utilization of nuclear energy, the importance of fission lies in two facts. First, the process is associated with the release of considerable amounts of energy, and second, the reaction initiated by neutrons is also accompanied by the liberation of neutrons. It is thus possible, under proper conditions, for the process to be self-sustaining and for energy to be generated continuously, once the fission reaction has been started.

B. RELEASE OF NEUTRONS

Most of the nuclear fragments formed when fission occurs have too many neutrons for stability, and so there is a tendency for some of them to expel neutrons almost instantaneously. These are the neutrons which appear to accompany the fission process. The average number, ν, of neutrons liberated for each thermal neutron absorbed in a fission reaction by U-235, U-233, and Pu-239 is given in Table II. It will be noted that the average numbers of neutrons liberated are not integers.

TABLE II

AVERAGE NUMBER OF NEUTRONS LIBERATED PER THERMAL NEUTRON ABSORBED IN FISSION

Fissionable Nucleus	Number of Neutrons (ν)
U-233	2.41 ± 0.03
U-235	2.51 ± 0.03
Pu-239	2.91 ± 0.04

This is because the nucleus splits in many different ways as already mentioned. Although the number of neutrons expelled in any individual act of fission must be integral, the average over a large number of fissions is not necessarily a whole number. A typical distribution of the number of neutrons per fission of U-235 is shown in Figure 6.

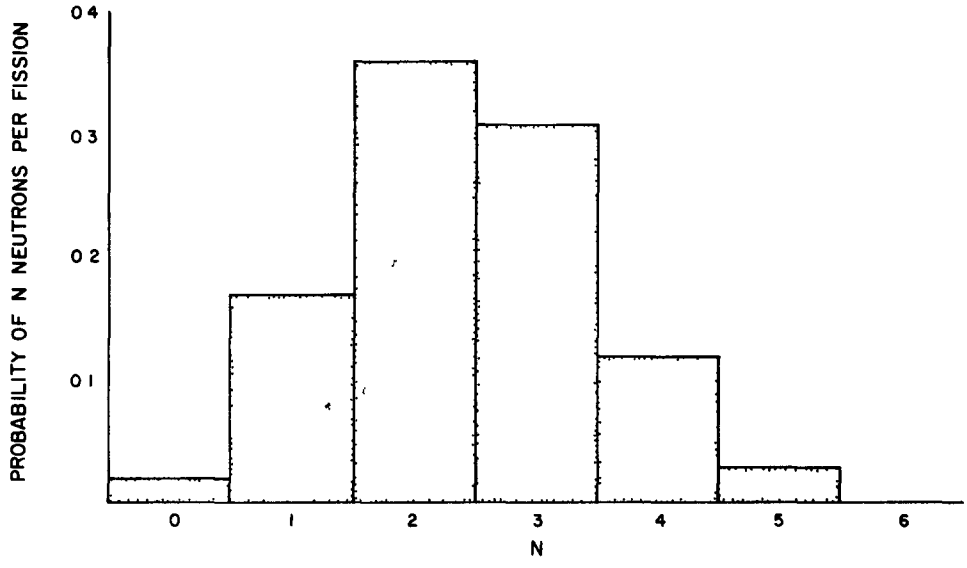

Figure 6. Neutron Yield from the Fissioning of U-235. (Even though the number of neutrons from any one fission event is an integer, the average over a large number is not.)

The neutrons emitted as a result of the fission process can be divided into two categories, namely, prompt neutrons and delayed neutrons. The prompt neutrons, which constitute over 98% of the fission neutrons, are released within

an extremely short interval of time, probably about 10^{-14} sec (or less), of the instant of fission. The energy of these neutrons covers a considerable range, from over 10 Mev down to quite small values; the average energy of the prompt neutrons is about 2 Mev. The energy distribution for U-235 fission neutrons is shown in Figure 7. The energy of the prompt fission neutrons is an insignificant

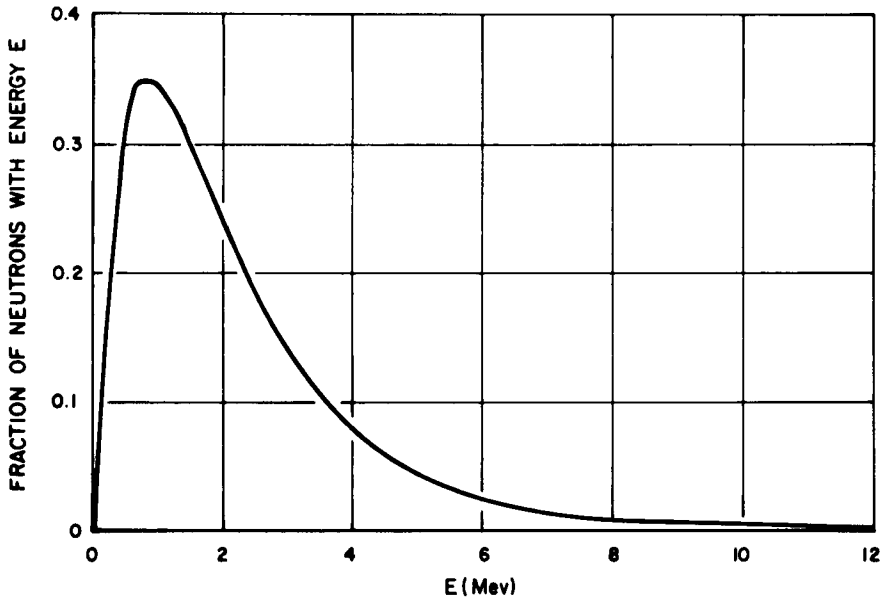

Figure 7. Energy Distribution of Prompt Fission Neutrons

fraction of the total fission energy. However, the neutron energy is very significant to the subsequent fission that a neutron can induce. In a "fast" reactor the prompt neutrons are utilized near their energy of origin. In the "thermal reactor" the neutrons must be slowed down from millions of electron volts to energies less than 1/10 of an electron volt before they can enter into a subsequent fission event. It will be seen later that this neutron slowing-down process has a strong influence on the size and composition of a thermal reactor.

The delayed neutrons, as their name implies, are emitted over a period of a few seconds to minutes, the intensity falling off rapidly with time. The delayed neutrons accompanying fission fall into unique groups according to characteristic delay times. The rate of decay of the intensity in each delayed-neutron group is exponential, as it is for radioactive change. Because the delayed neutrons are a result of nuclear decomposition of fission fragments, they

fall into the same groups for different fissioning nuclei. The six generally accepted delayed neutron groups have half lives of 54, 22, 5.6, 2.12, 0.45, and 0.15 seconds. In a time period equal to one half-life, one-half of the neutrons remaining at the start of that period are emitted. The fraction of delayed neutrons is a function of the fissioning nucleus and is 0.3, 0.75, and 0.23% for U-233 U-235, and Pu-239 respectively. The energy of the delayed neutrons falls in the region of 0.25 to 0.6 Mev. Figure 8 shows the fraction of fission neutrons remaining to be emitted as a function of time for U-235. The delayed neutrons have an important bearing on the time-dependent behavior of nuclear reactors. Were it not for these neutrons, the safe control of nuclear reactors would be much more difficult than it is.

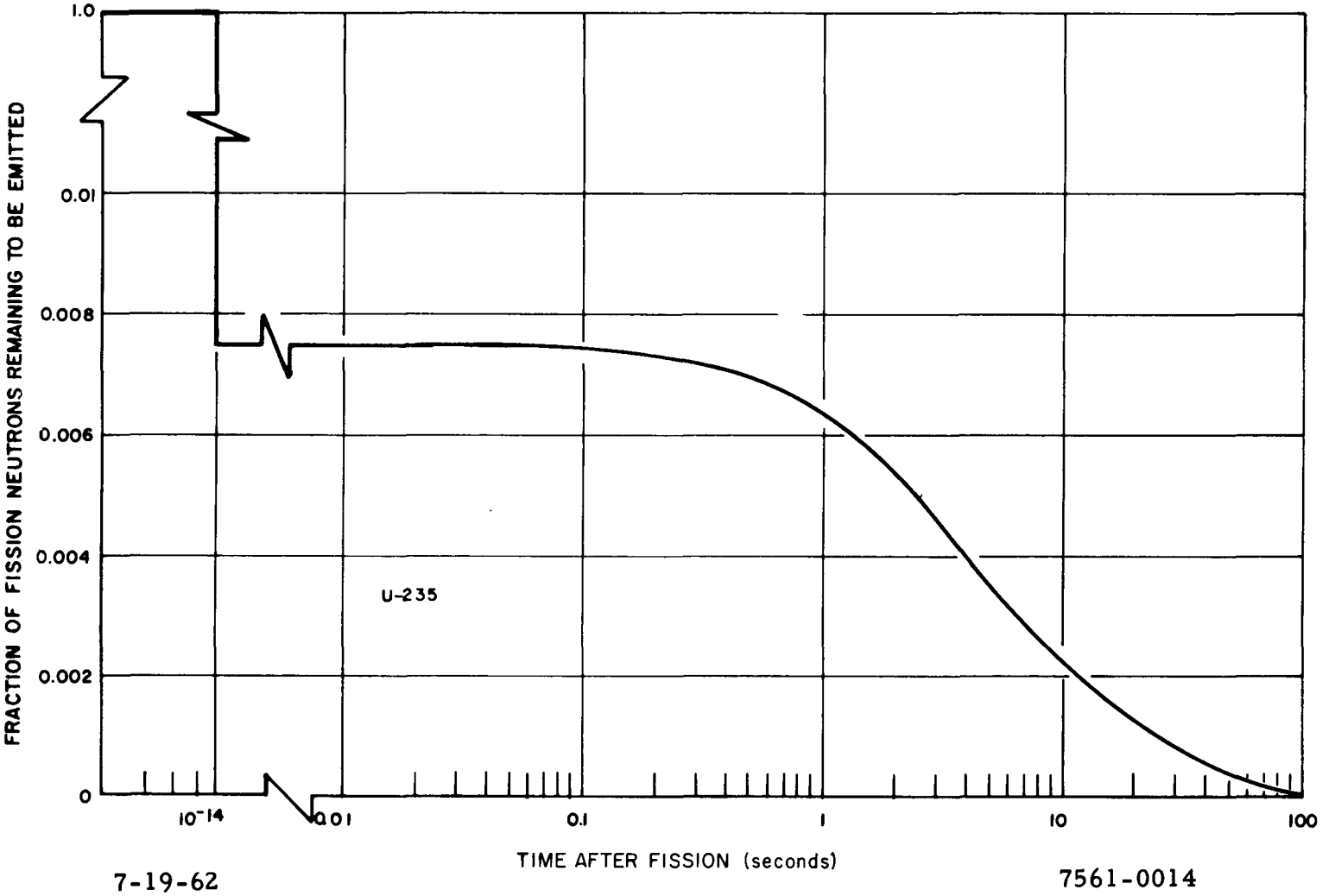

Figure 8. Time Dependence of Neutron Emission From Fissioning of U-235 (The fact that 3/4 of 1% of the U-235 fission neutrons are delayed by a significant time greatly simplifies reactor control.)

C. FISSION ENERGY

The fission process is remarkable for the magnitude of the energy released; it is about 200 Mev for each nucleus undergoing fission, which may be compared with a few electron volts for each atom reacting in chemical processes, such as the combustion of coal or oil, or up to 20 Mev for nonfission nuclear reactions. The large energy release in fission is associated with the fact that the products of the reaction have an appreciably smaller total mass than that of the nucleus undergoing fission plus the neutron causing fission. Because of the equivalence of mass and energy, which has now been firmly established from the study of many nuclear processes, the considerable decrease in mass in the fission reaction must be accompanied by the liberation of a large amount of energy.

The relationship between energy E and the equivalent mass m is given by the Einstein equation

$$E = mc^2,$$

where c is the velocity of light. If m is in grams, and c in cm/sec, i.e., 3×10^{10} cm/sec, then E will be in ergs. For the present purpose it is more useful to express m in atomic mass units; the equation then becomes:

$$E(\text{ergs}) = m(\text{amu}) \times 1.49 \times 10^{-3}.$$

1 Mev = 1.60×10^{-6} erg, and so the energy equivalent is expressed in Mev by:

$$E(\text{Mev}) = m(\text{amu}) \times 931.$$

The magnitude of the energy released in nuclear fission will be estimated for the fission of U-235, making the simplifying assumption that the products are nuclei with mass number 95 and 139, since these are known to be obtained in greatest amount. In order to balance the mass numbers, it is evident that two fission neutrons are liberated in this case, as may be seen from the following equation.

$$U^{235} + n^1 \rightarrow X^{95} + Y^{139} + 2n^1,$$

The neutron on the left is the one which initiates fission, and the two on the right are formed as a result of fission.

The mass of the U-235 atom is known to be 235.124 amu, whereas that of the neutron is 1.00897 amu, which may be approximated to 1.009 for the present purpose. By comparison with known stable species, the masses of the two fission products postulated above will be 94.945 and 138.955 amu, respectively. Hence the following balance sheet of the masses before and after fission may be drawn up:

Masses Before Fission		Masses After Fission	
U-235	235.124	Mass number-95	94.945
1 neutron	1.009	Mass number-139	138.955
Total	236.133	2 neutrons	2.018
		Total	235.918

Mass converted into energy = 236.133 - 235.918 = 0.215 amu.

As seen above, 1 amu is equivalent to 931 Mev, and so the energy released per fission is given by:

Energy released per fission = (0.215)(931) = 198 Mev.

Although this calculation was made for one particular mode of fission, it may be regarded as quite typical. While there are slight variations from one mode to another, it appears, on the whole, that an estimate of about 200 Mev of energy released per U-235 nucleus undergoing fission is satisfactory. The same value may also be taken as applying to the fission of U-233 and Pu-239.

D. ENERGY DISTRIBUTION

The major proportion — over 80% — of the energy of fission appears as kinetic energy of the fission fragments, and this immediately manifests itself as heat within less than 0.01 mm of the point of fission. Part of the remaining 20% or so is liberated in the form of instantaneous gamma rays and as kinetic energy of the fission neutrons. The rest is released gradually as energy carried by the beta particles and gamma rays emitted by the radioactive fission products as they decay over a period of time.

The approximate distribution of the fission energy, which may be regarded as applying to all three of the important fissionable species, is given in Table III.

TABLE III

LIBERATION OF HEAT DUE TO FISSION

Instantaneous	Mev
Energy of fission fragments	168
Energy of fission neutrons	5
Instantaneous gamma rays	5
Capture gamma rays	7
	185
Delayed	
Beta particles from fission products	7
Gamma rays from fission products	6
Radiation from capture products	2
	15

Of the heat liberated instantaneously, about 90%, i.e., 168 Mev, will be produced at (or near) the point of fission, and only 17 Mev elsewhere. But of the delayed heat, the two amounts are approximately equal, i.e., about 7 Mev at the place where fission occurs and 8 Mev at a distance.

E. ENERGY EQUIVALENTS

In order to convert the fission energy into practical units, it should be recalled that 1 Mev is equal to 1.60×10^{-13} watt-sec. Hence the total energy (200 Mev) available per fission is about 3.2×10^{-11} watt-sec, so that it requires 3.1×10^{10} fissions to release 1 watt-sec of energy. In other words, fissions at the rate of 3.1×10^{10} per sec produce 1 watt of power, provided the reactor has been operating for some time.

One gram atom of an element, i.e., the atomic weight expressed in grams, of any element contains Avogadro number of individual nuclei (6.02×10^{23}); if all of these undergo fission, the energy liberated would be (6.02×10^{23}) times

$(3.2 \times 10^{-11}) = 1.9 \times 10^{13}$ watt-sec, or 5.3×10^{6} kwh. This is the amount of heat that would be released by the complete fission of 233 grams of U-233, or 235 grams of U-235, or 239 grams of Pu-239. Neglecting the relatively small differences between these weights, the results in Table IV may be regarded as applying to the heat produced by the fission of 1 lb of any of these materials. One pound of uranium is a cube which is 1.1 in. on a side.

TABLE IV

HEAT LIBERATED BY 1 LB OF FISSIONABLE MATERIAL

0.9×10^{13} cal
1.0×10^{7} kwh
2.8×10^{13} ft-lb
3.6×10^{10} Btu

A useful fact to remember is that the power production corresponding to the fission of 1 gram of material per day would be roughly 10^{6} watts or 1 Mw.

3. THE CHAIN REACTION

A. CONDITIONS FOR SELF-SUSTAINING

If a chain reaction is to be maintained, the minimum condition is that for each nucleus capturing a neutron and undergoing fission there shall be produced, on the average, at least one neutron which causes the fission of another nucleus. This condition can conveniently be expressed in terms of a multiplication factor or reproduction factor, defined as the ratio of the number of neutrons of any one generation to the number of corresponding neutrons of the immediately preceding generation. If the multiplication factor, represented by k, is exactly equal to or slightly greater than unity, a chain reaction will be possible. But if k is less than unity, even by a very small amount, the chain cannot be maintained.

Suppose, for example, a particular generation starts with 100 neutrons; if the multiplication factor is unity, there will be 100 corresponding neutrons at the beginning of the second generation, 100 at the third, and so on. Once it has started, the fission will continue at the same rate. For practical purposes, however, it is necessary that k be capable of exceeding unity, if power production is to be appreciable. The simplest way in which a required power level can be attained is for the multiplication factor to exceed unity; the number of neutrons present and, hence, the fission rate will then increase until the desired rate is reached.

B. NEUTRON BALANCE

The magnitude of the multiplication factor in any system consisting of fissionable material, e.g., uranium, and a moderator for slowing down the neutrons depends on the relative extents to which the neutrons take part in four main processes. These are: (1) complete loss or escape of neutrons from the system, generally referred to as leakage; (2) nonfission capture, by the fuel; (3) nonfission capture, sometimes called parasitic capture, by the moderator and by various extraneous substances ("poisons") such as structural materials, coolant, fission products, and impurities in the uranium and in the moderator; and finally, (4) fission capture of slow or of fast neutrons by the fuel.

In each of these four processes neutrons are removed from the system, but in the fourth process, i.e., in the fission reaction, other neutrons are generated to replace them. Hence, if the number of neutrons produced in the latter process is just equal to (or exceeds) the total number lost by escape and by fission and nonfission capture, the multiplication factor will equal (or exceed) unity and a chain reaction should be possible.

An illustration of the type of neutron balance that might exist in a system for which the multiplication factor is exactly unity is depicted below. It is assumed that fission results only from the capture of slow neutrons, and it is supposed, for simplicity, that exactly two neutrons are produced, on the average, in each fission process.

100 slow neutrons absorbed by U-235 to cause fission
↓
200 fission neutrons
↓ → 60 leak out during slowing down
140 neutrons slowed down
↓ → 10 leak out as slow neutrons
130 slow neutrons available for absorption
↓ → 30 absorbed by moderator, structure, poisons, etc.
100 slow neutrons (absorbed by U-235 to cause fission)

Since 100 slow neutrons are absorbed in fission processes at the beginning, and 100 are available for similar absorption at the end of the generation, the conditions for a self-sustaining chain are satisfied.

C. MULTIPLICATION FACTOR FOR THERMAL REACTORS

For the present, in order to avoid the problem of the loss of neutrons by leakage, it will be postulated that the multiplying system is infinite in extent. Suppose that, at a given instant representing the initiation of a generation, there are available n thermal neutrons which are captured in fuel. Let η be the average number of fast fission neutrons emitted as a result of the capture of one thermal neutron in fuel material. Then, due to the absorption of the n thermal neutrons $n\eta$ fast neutrons will be produced. It should be noted that since the neutrons captured in fuel do not all necessarily lead to fission, the value of η differs, in general, from the average number (see Table II) of fast neutrons released per slow neutron fission. If the latter number is represented by ν, then

$$\eta = \frac{\sigma_f}{\sigma_f + \sigma_c} \nu \quad ,$$

where σ_f is the macroscopic cross section for slow neutron fission, and σ_c is the cross section for absorption of thermal neutrons by nonfission processes in the fuel material (see Table V).

TABLE V

THERMAL NEUTRON CROSS SECTIONS

	Cross Sections (Barns)			Neutron Yield	
	Fission σ_f	Radiative Capture σ_c	Absorption $\sigma_a = \sigma_f + \sigma_c$	Per Fission ν	Per Absorption η
U^{233}	532	59	591	2.51	2.29
U^{235}	579	118	697	2.47	2.07
Pu^{239}	740	285	1025	2.91	2.09

Before the $n\eta$ fast neutrons have slowed down appreciably some will be captured by, and cause fission of, the fuel. Since more than one neutron is produced on the average in each fission, there will be an increase in the number of fast neutrons available. Allowance for this effect may be made by introducing the fast fission factor denoted by ϵ, and defined as the ratio of the total number of fast neutrons produced by fissions due to neutrons of all energies to the number resulting from thermal-neutron fissions.

$$\epsilon = \frac{\text{number of neutrons produced by all fissions}}{\text{number of neutrons produced by thermal fissions}}$$

Consequently, as a result of the capture of n thermal neutrons in fuel, $n\eta\epsilon$ fast neutrons will be formed.

As a result of collisions, mainly elastic, with the moderator, the fast neutrons will ultimately be slowed down or thermalized. However, during the slowing down process some of the neutrons are captured in nonfission processes, so that not all of the $n\eta\epsilon$ fast neutrons reach thermal energies. The fraction of the fast (fission) neutrons which escape capture while being slowed down is called the resonance escape probability, and is represented by p.

$$p = \frac{\text{number of neutrons which escape capture during slowing down}}{\text{total number of fast neutrons produced}}$$

Consequently, the number of neutrons which become thermalized is $n\eta\epsilon p$.

When the energy of the neutrons has been reduced to the thermal region, they will diffuse for some time, the energy distribution remaining essentially constant until they are ultimately absorbed by fuel, moderator, or such poisons as may be present. Of the thermal neutrons, therefore, a fraction f, called the thermal utilization, will be absorbed in fuel material; the value of f is represented by:

$$f = \frac{\text{thermal neutrons absorbed in fuel}}{\text{total thermal neutrons absorbed}},$$

where the denominator is the total number of thermal neutrons absorbed by fuel, moderator, and other materials present in the reactor. The number of thermal neutrons captured in fuel is consequently $n\eta\epsilon pf$.

For the present purpose, since the multiplication factor may be defined as the ratio of the total number of thermal neutrons absorbed, on the average, in one generation to the number of thermal neutrons absorbed in the preceding generation, on the average, in an infinite medium, it follows that:

$$k_\infty = \frac{n\eta\epsilon pf}{n} = \eta\epsilon pf \quad ,$$

where

k_∞ = infinite medium multiplication factor

η = neutron yield per fuel capture

ϵ = fast effect factor

p = resonance escape probability

f = thermal utilization.

This result is sometimes referred to as the four factor formula. As seen above, the condition for a self-sustaining chain reaction in a system is that the multiplication factor should be unity; the criterion for an infinite system is, therefore, that $\eta\epsilon pf = 1$. The neutron economy of an infinite medium is summarized in the diagram of Figure 9.

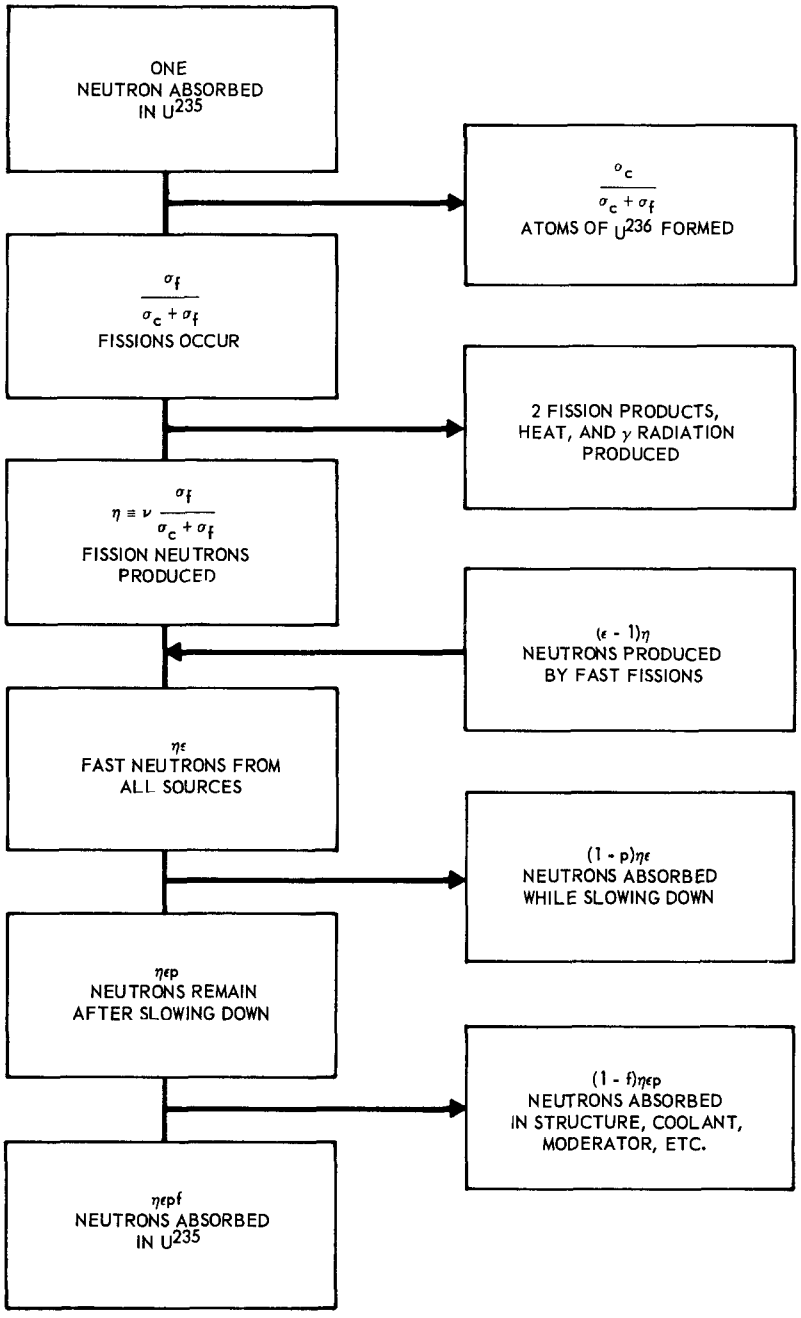

7-19-62 7561-0010

Figure 9. Neutron Economy for an Infinite Medium Containing U^{235}

In the case of a reactor in which the fuel material contains only U-235 and no U-238, both the fast fission factor, ϵ, and the resonance escape probability, p, will be virtually unity. Such a reactor can be made critical with a small proportion of fuel relative to moderator. In these circumstances,

$$k_\infty = \eta f \quad (U^{235} \text{ system}) \quad .$$

D. LEAKAGE OF NEUTRONS

For a reactor of finite size the condition that the infinite medium multiplication factor should be unity is no longer adequate for a self-sustaining chain reaction. It is required, in a finite system, that for every thermal neutron absorbed in fuel there shall be produced, on the average, one thermal neutron in addition to those lost by leakage from the reactor. If P is the total nonleakage probability, i.e., the probability that a neutron will not escape either during the slowing down process or while it diffuses as a thermal neutron, then the condition for a chain reaction to be maintained is:

$$k_\infty P = 1.$$

where

$P = P_f P_t$

P_f = fast neutron nonleakage probability

P_t = slow neutron nonleakage probability.

Only for the infinite system is the nonleakage probability unity, and then $k_\infty = 1$, satisfies the condition for the chain reaction. For a finite reactor, P is less than unity, and hence the infinite multiplication factor must exceed unity if the nuclear chain reaction is to be maintained.

The proportion of neutrons lost by escape from a finite reactor can be diminished by increasing the size of the system. The escape of neutrons occurs at the exterior, but absorption, leading to fission and neutron production, occurs throughout the whole of the interior of the reactor. The number of neutrons lost by escape thus depends on the external surface area, while the number formed is determined by the volume. To minimize the loss of neutrons and thereby increase the nonleakage probability, it is necessary to decrease tne ratio of area to volume; this can be done by increasing the size of the reactor. The

critical size is that for which the nonleakage probability P is such that $k_\infty P$ is just equal to unity. Since the area-to-volume ratio depends on the geometrical shape, the nonleakage probability will be determined by the shape of the reactor. For a given volume, a sphere has the smallest ratio of area to volume; hence, leakage from a spherical reactor will be less than for any other shape. The critical volume of such a reactor will consequently also be less.

As indicated above, the value of k_∞ is determined by the composition of the system, i.e., by the nature of the fuel and the proportion of moderator, and also by the arrangement of the material. Hence, if these are specified, a chain reaction will be possible only if P is large enough to make $k_\infty P$ equal to or greater than unity. The neutron economy of a finite U-235 system is summarized in the diagram of Figure 10.

E. CRITICAL SIZE OF REACTOR

The finite system must satisfy a neutron continuity equation which states

$$+ \text{Production} - \text{Leakage} - \text{Absorption} = \frac{dn}{dt} \quad .$$

The solution of this equation is dependent upon the model used to describe the slowing down of neutrons. For the case of the Fermi-Age or "continuous slowing down" model, it is assumed that a neutron loses a constant fraction of its incident energy with each collision. The physical quantity of principal interest is the average distance traveled by a neutron in the process of slowing down because the relationship between this distance and the reactor dimensions determines the fast leakage. In like manner the relationship between the distance traveled by a slow neutron prior to absorption and the reactor dimensions determines the slow leakage.

Solution of the continuity equation results in the following statement of the criticality condition:

CRITICALITY EQUATION

$$\frac{k_\infty e^{-B^2\tau}}{1 + L^2B^2} = 1 \quad .$$

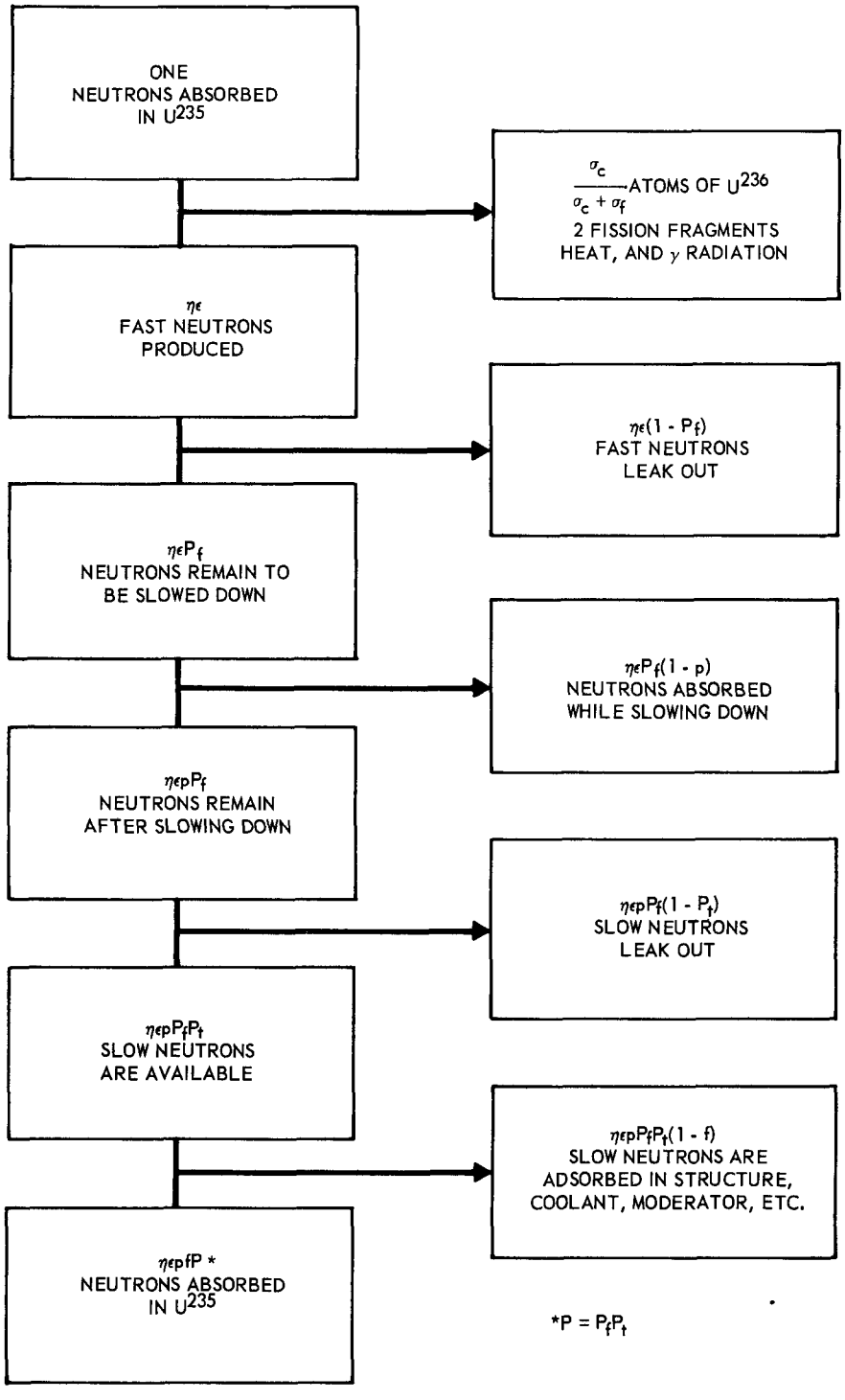

7-19-62 7561-0011

Figure 10. Neutron Economy for a Finite System Containing U^{235}

In the previous equation B^2 (called geometrical buckling) is related to the reactor shape and dimensions and is determined by the boundary conditions in the solution of the neutron diffusion equation

$$\nabla^2\varphi + B^2\varphi = 0 \quad .$$

The value of B^2 for various reactor configurations is given in Table VI.

TABLE VI

BUCKLING OF BARE REACTORS

Geometry	Buckling (B^2)	Minimum Volume
Sphere	$\left(\frac{\pi}{R}\right)^2$	$\frac{130}{B^3}$
Rectangular parallelepiped	$\left(\frac{\pi}{a}\right)^2 + \left(\frac{\pi}{b}\right)^2 + \left(\frac{\pi}{c}\right)^2$	$\frac{161}{B^3}$
Cylinder	$\left(\frac{2.405}{R}\right)^2 + \left(\frac{\pi}{H}\right)^2$	$\frac{148}{B^3}$

R = radius
H = cylinder height
a = length
b = width
c = height

In the criticality equation above $e^{-B^2\tau}$ is the fast neutron nonleakage probability. The Fermi Age, τ, is one sixth the mean square (crow flight) distance traveled by a neutron from the time of its emission to the time that it is slowed down.

In the criticality equation above $1/(1 + L^2B^2)$ is the thermal neutron nonleakage probability. The square of the diffusion length L^2 is one-sixth the mean square (crow flight) distance a neutron travels after slowing down and before absorption. In summary, then:

$$\text{Fast neutron nonleakage probability} = P_f = e^{-B^2\tau} \quad ;$$

$$\text{Slow neutron nonleakage probability} = P_t = \frac{1}{1 + L^2B^2} \quad ;$$

$$\text{Total nonleakage probability} = P = P_f P_t = \frac{e^{-B^2\tau}}{1 + L^2B^2} \quad .$$

The effective multiplication factor k_{eff} for a finite system is then

$$k_{eff} = \frac{k_\infty e^{-B^2\tau}}{1 + L^2B^2} \quad ,$$

and the criticality condition is

$$k_{eff} = 1.$$

If $B^2\tau$ is small enough that the expansion $e^{-B^2\tau} = (1 - B^2\tau) = (1 + B^2\tau)^{-1}$ is a good approximation, then the criticality condition can be reduced to:

$$k_{eff} \cong \frac{k_\infty}{(1 + L^2B^2)(1 + B^2\tau)} = 1 \quad ,$$

or

$$\frac{k_\infty}{\left[1 + B^2(L^2 + \tau)\right]} = 1 \quad .$$

If $(L^2 + \tau)$ is replaced by a quantity M^2 called the "migration area," then the criticality equation reduces to:

$$k_{eff} \cong \frac{k_\infty}{1 + M^2B^2} = 1 \quad ,$$

or

$$\frac{\eta\epsilon pf}{1 + M^2B^2} = 1 \quad .$$

The Fermi Age τ is a function of the moderator scattering cross section and mass number. The diffusion length (L) is a function of the neutron absorption cross section of the reactor. Some typical values of L^2, τ, and M^2 are given in Table VII.

TABLE VII

MODERATOR PROPERTIES

Moderator	Diffusion Length L_m (cm)	Fermi Age τ (cm^2)	Migration Length* M (cm)
H_2O	2.88	33	6.43
D_2O	100.	120	101.
Be	23.6	98	25.8
C	50.2	350	53.6

*$M = \sqrt{L^2 + \tau}$

The addition of fuel to the moderator does not significantly influence τ except to the degree of dilution, but it increases the neutron-absorption probability which decreases the distance a thermal neutron can wander about before being absorbed. Thus L is a function of fuel concentration. The effective L for the reactor medium can be expressed

$$L_{Reactor} = (1 - f)L_{Moderator}$$

where f is the thermal utilization.

It can be seen then that when f approaches unity, i.e., when practically all neutrons are absorbed in fuel, M^2 approaches τ. In a 100% enriched U^{235} reactor $\eta \cong 2$ and $\epsilon p \cong 1$;

therefore from

$$\frac{\eta \epsilon p f}{1 + M^2 B^2} = 1 \quad ,$$

becomes

$$\frac{2}{1 + B^2\tau} \cong 1 \quad ,$$

or

$$B^2\tau \cong 1 \quad ;$$

and since for a sphere of radius R

$$B^2 = \left(\frac{\pi}{R}\right)^2 \quad ,$$

$$\left(\frac{\pi}{R}\right)^2\tau \cong 1 \quad ,$$

$$R_{Critical} \cong \pi\sqrt{\tau} \quad .$$

Based on this approximation, the minimum size of various homogeneous U-235 spheres is shown in Table VIII.

TABLE VIII

MINIMUM SIZE OF BARE HOMOGENEOUS U-235 SPHERES

Moderator	$\pi\sqrt{\tau}$ (cm)	$R^*_{Critical}$ (cm)	Volume (ft^3)
H_2O	18	16	0.65
D_2O	34.5	32	5.
Be	31	29	3.6
C	59	55	23

*Adjusted for boundary condition (extrapolation distance).

F. REACTOR FLUX AND POWER DISTRIBUTION

The neutron flux distribution in a reactor is determined by the solution of the neutron diffusion equation

$$\nabla^2\varphi + B^2\varphi = 0$$

for appropriate coordinate systems and boundary conditions. The results for the common geometric shapes are given in Table IX. These solutions apply only to a critical reactor.

TABLE IX

FLUX DISTRIBUTION IN BARE CRITICAL REACTORS

Geometry	Critical Flux Distribution
Sphere	$\varphi(x) = \frac{A}{r} \sin\frac{\pi r}{R}$
Rectangular Parallelopiped	$\varphi(x,y,z) = A \cos\frac{\pi x}{a} \cos\frac{\pi y}{b} \cos\frac{\pi z}{c}$
Finite Cylinder	$\varphi(r,z) = A J_o \frac{2.405r}{R} \cos\frac{\pi z}{H}$

A comparison of the three functions, i.e., $\frac{1}{r} \sin\frac{\pi r}{R}$, $\cos\frac{\pi x}{a}$, and $J_o\left(\frac{2.405r}{R}\right)$ will reveal that a cosine function is a good approximation for all.

In a homogeneous reactor, wherein the fuel is uniformly dispersed throughout the reactor volume, the power distribution is the same as the flux distribution. The resulting ratio of maximum to average power in bare reactors is given in Table X.

TABLE X

PEAK-TO-AVERAGE POWER FOR BARE REACTORS

Geometry	P_{max}/P_{avg}
Sphere	3.29
Rectangular Parallelopiped	3.87
Finite Cylinder	3.64

The maximum-to-average power ratio must be considered in the detailed heat-transfer and fuel burnup design of a reactor.

G. REFLECTOR

In small reactors, criticality is a strong function of neutron leakage. The overall neutron economy of a reactor can be significantly improved by the addition of a nonfissionable blanket of material whose function is to reflect neutrons back into the reactor core and thus decrease the leakage. The best reflecting materials in general are those with high scattering cross sections and low neutron absorption characteristics. Whereas in the bare reactor the neutron flux approaches zero at the core boundary, in the reflected reactor the flux is increased at the core boundary and does not approach zero until some distance into the reflector region. The net result is that the effective reactor size is increased beyond the extent of the core. The flux distribution and effective core size change are illustrated in Figure 11.

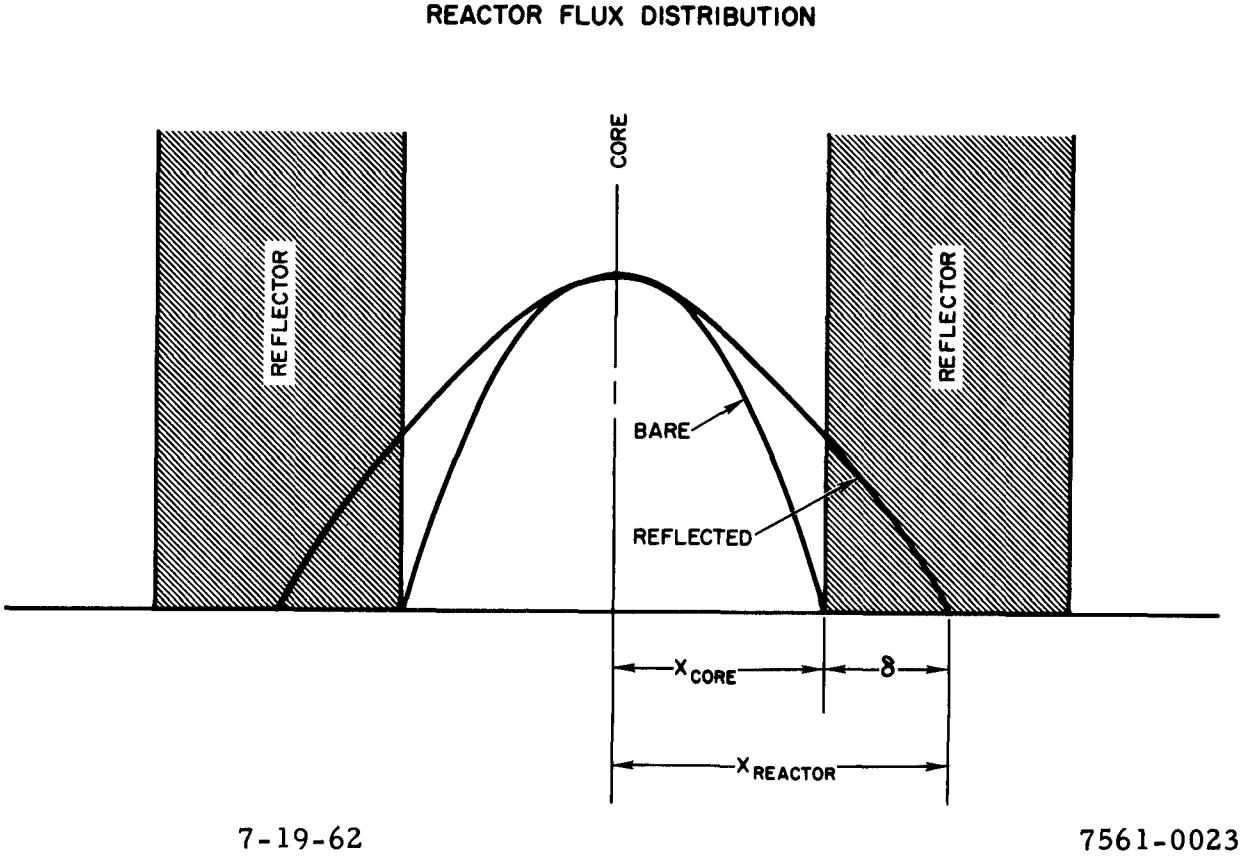

Figure 11. Effect of a Reflector on Neutron Flux Distribution and Effective Reactor Size

The increase in effective reactor size is called the "reflector savings," δ. The magnitude of δ is a function of the reflector thickness and the nuclear properties of the core and reflector regions. For small reflector thickness δ is a

fraction of the thickness. For large reflector thicknesses δ approaches a constant limit. This asymptotic value of δ is practically achieved when the reflector thickness is between 1.5 and 2 times the neutron-diffusion length in the reflector material. Therefore, as reflector thickness is increased the effective reactor dimensions increase or the core size can be decreased to maintain the same effective size. When the reflector is thick enough to yield the asymptotic value of δ, no further benefit results from increased reflector thickness. This point is illustrated in Figure 12.

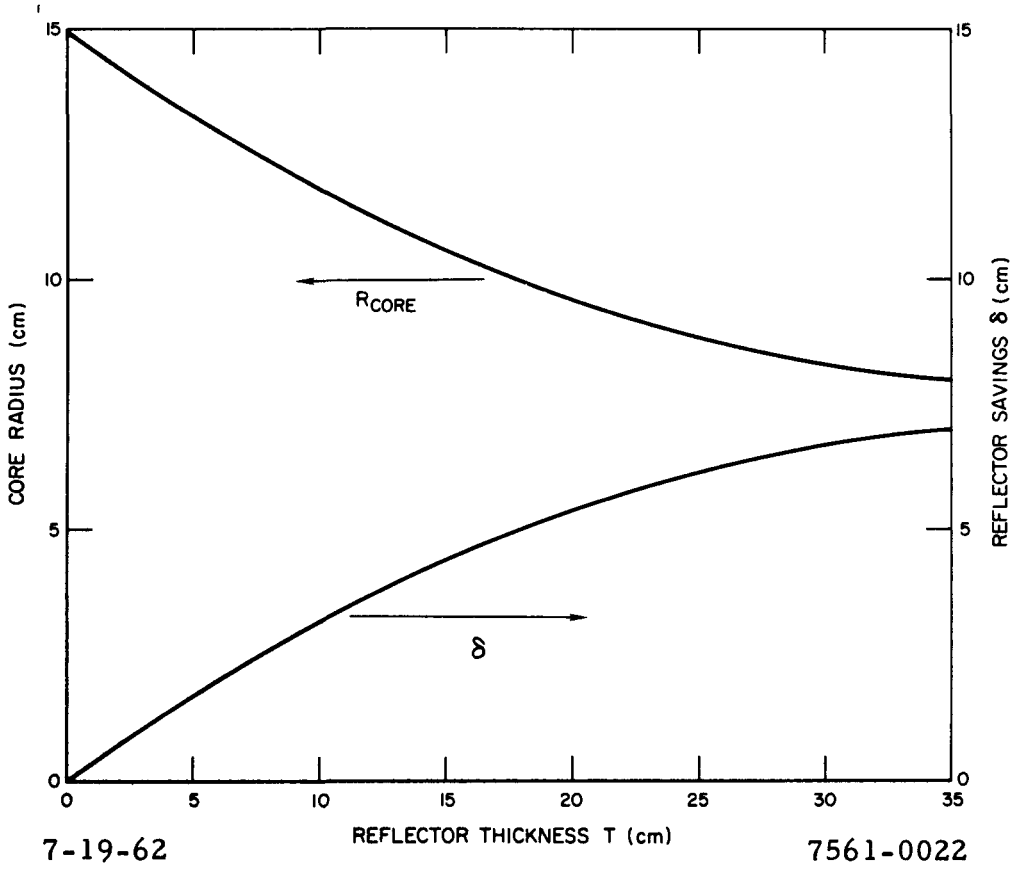

Figure 12. Effect of Reflector Thickness on Reactor Core Size and Reflector Savings as a Function of Thickness

The effective reactor dimension is then

$$X_{Reactor} = X_{Core} + \delta \quad .$$

This effective dimension is now used in calculating B^2 and leakage and also in describing the flux or power distribution.

For compact reactors the reflector has several significant advantages.

1) The critical mass or uranium inventory is decreased as a result of the smaller allowable core.

2) For certain material combinations the overall weight of the core plus reflector can be made less than the weight of the bare reactor by choosing an optimum reflector thickness.

3) The increased neutron flux at the core boundary decreases the peak-to-average power distribution in the reactor. In a compact reactor a decrease factor of 2 is reasonable.

4) Variations in reflector thickness can be used as an effective way to change leakage and thus control the reactor. This is especially true for compact reactors wherein δ can be an appreciable fraction of the effective reactor dimensions.

H. REACTOR KINETICS

The multiplication factor k is effectively the number of neutrons present at the end of a neutron generation for each neutron present at the beginning of that generation. Since one neutron is required to maintain the chain reaction, the number of neutrons will increase by k - 1 in a generation. Thus, if there are n neutrons present initially, the rate of increase will be n(k - 1) per generation. If ℓ is the average time between successive neutron generations in the system under consideration, then,

$$\frac{dn}{dt} = \frac{n(k-1)}{\ell} = \frac{nk_{ex}}{\ell} \quad ,$$

where k_{ex} is defined by

$$k_{ex} \equiv k - 1.$$

Upon integration of above, it is seen that,

$$n = n_o e^{t(k_{ex}/\ell)} \quad ,$$

where n_o is the initial number of neutrons and n is the number after the lapse of time t. It is seen, therefore, that if the multiplication factor is greater than unity, the number of neutrons will increase exponentially with time.

The generation time, ℓ, varies from about 10^{-9} sec for a fast reactor to 10^{-3} sec for very large reactors. If for example $k = 1.005$ and $\ell = 10^{-3}$ sec, the neutron increase per second equals e^5 or a factor of 150 per second.

The above calculation of the rate of neutron increase in a reactor with a multiplication factor exceeding unity gives the correct rate of neutron increase only if all the fission neutrons are released promptly, i.e., essentially at the instant of fission. About 0.75% of the fission neutrons are delayed, and this affects the calculation of the rate of neutron increase (or decrease).

The mean lives of the delayed neutrons range from about 0.6 sec to 80 sec. By weighting the values appropriately, according to the fraction in each group, the mean delay time, averaged over all the fission neutrons, is about 0.1 sec. The average time between the fission capture of a neutron in two successive generations is, consequently, about $0.1 + \ell$ sec; the first term is the average time elapsing between fission and the complete release of the neutron, whereas the second is that between release and capture in a fission process. In other words, the effective lifetime $\overline{\ell}$ of a neutron is roughly 0.1 sec.

Using the value 0.1 sec for $\overline{\ell}$, and taking k to be 1.005, as before, it is found that the number of neutrons actually increases by a factor of $e^{0.05}$, i.e., about 1.05 per second, as compared with a factor of 150 per second if all the neutrons were prompt. Clearly, the effect of the delayed fission neutrons, when the multiplication factor exceeds unity, is to make the rate of neutron increase much slower than it would have been had all the neutrons been released promptly.

When the effective multiplication factor is equal to 1.0075, the condition of a reactor is described as prompt critical, since the nuclear fission chain can be maintained by means of the prompt neutrons alone. If k exceeds this value, multiplication will occur due to the prompt neutrons, irrespective of those delayed, and the neutron density will increase rapidly right from the commencement. In this condition, a reactor is difficult to control and hence it is avoided in practice.

Just as the delayed fission neutrons affect the rate of increase of neutrons when the effective multiplication factor exceeds unity, so they influence the decay in the neutron density when the reactor is made subcritical, i.e., when it is being shut down. The delayed neutrons continue to be emitted for some time, and this maintains a fission rate that is considerably higher than would be the case if all the fission neutrons were prompt. The ultimate rate at which the neutron flux in a thermal reactor decreases after shutdown is determined essentially by the most delayed group of neutrons, i.e., by those with a mean life of 80 sec.

I. REACTOR CONTROL

For practical operation, a reactor must be constructed so that it is appreciably greater than the critical size. One reason is that an effective multiplication factor exceeding unity provides the only feasible means of increasing the number of neutrons, and hence the fission rate, up to the point where the required power level is attained. Once this has been reached, it is necessary to decrease the effective multiplication factor to unity, and then the reactor will remain in a steady state, neutrons being produced just as fast as they are used up by leakage and capture.

The adjustment of the multiplication of neutrons in a thermal reactor is achieved by the insertion of control rods of cadmium or boron steel. Both cadmium and boron have large capture cross sections for slow neutrons; hence, by varying the positions of the control rods the effective multiplication factor can be made to vary over a suitable range. In order to shut down the reactor, the control rods are inserted to an extent that permits them to absorb additional neutrons. The system now loses neutrons faster than they are formed by fission; the effective multiplication factor sinks below unity, and the chain reaction dies out.

The insertion of poison or control rods changes the effective multiplication factor, k_{eff}, by influencing the thermal utilization, f. A reactor can also be controlled by means of variation in the neutron leakage probability. In a reflected reactor this type of control called reflector control is achieved by moving portions of the reflector in order to vary the neutron leakage probability and thus the effective multiplication factor.

4. REACTOR DESIGN

A. SIZE

In the case of space reactors, wherein size and weight are of extreme importance, the dominant factor in the determination of reactor size is the leakage probability. In any reactor, whether it be thermal, epithermal, or fast, the leakage is dependent on a relationship between the reactor's physical size and the distance between succeeding fission events. For a thermal or nearly thermal reactor the distance between fission events is controlled by the number of neutron collisions or the distance necessary to slow the fission neutrons down from fission energy to the thermal energy at which they are captured by the fuel and results in the succeeding fission. This slowing down distance is a function of the moderator material scattering cross section and atomic mass. A moderator material property, known as the Fermi age (T), is related to the mean square slowing down distance and has units of cm^2. The influence of slowing down distance is revealed in Figure 13 which shows the critical volume of 100% dense bare spheres with critical mass in the range of 2.5 to 20 kg of U-235 as a function of Fermi age with the common moderator materials indicated on the abscissa. It is obvious that H_2O or hydrogenous moderation permits the smallest thermal reactor. The exceptional ability of water is a result of the hydrogen content. Since the hydrogen atom has the same mass as the neutron, a neutron can transfer up to all of its kinetic energy to the hydrogen atom in one collision. Thus, hydrogenous materials are very effective neutron moderators.

A more detailed survey of the relationship between critical mass and size of 100% dense bare spherical reactors is shown in Figure 14 for mixtures of U-235 and H_2O and of Be. Both curves begin at the zero moderator point which corresponds to the critical mass and size of a U-235 fast reactor. In the region to the left of the minimum critical mass point, the reactors are said to be "under moderated" and the average neutron energy causing fission is epithermal (greater than KT). In the region to the right of the critical mass minimum the reactors are over moderated and thermal. Figure 15 shows the weight of U-235-Be, U-235-H_2O, and U-235-ZrH_x reactors as a function of moderator to uranium ratio. Zirconium hydride (ZrH_x) has been included because it is a high temperature (1400°F) form of hydrogenous moderator. ZrH_x can have the same hydrogen density as cold water at temperatures of about 1200°F with a dissociation

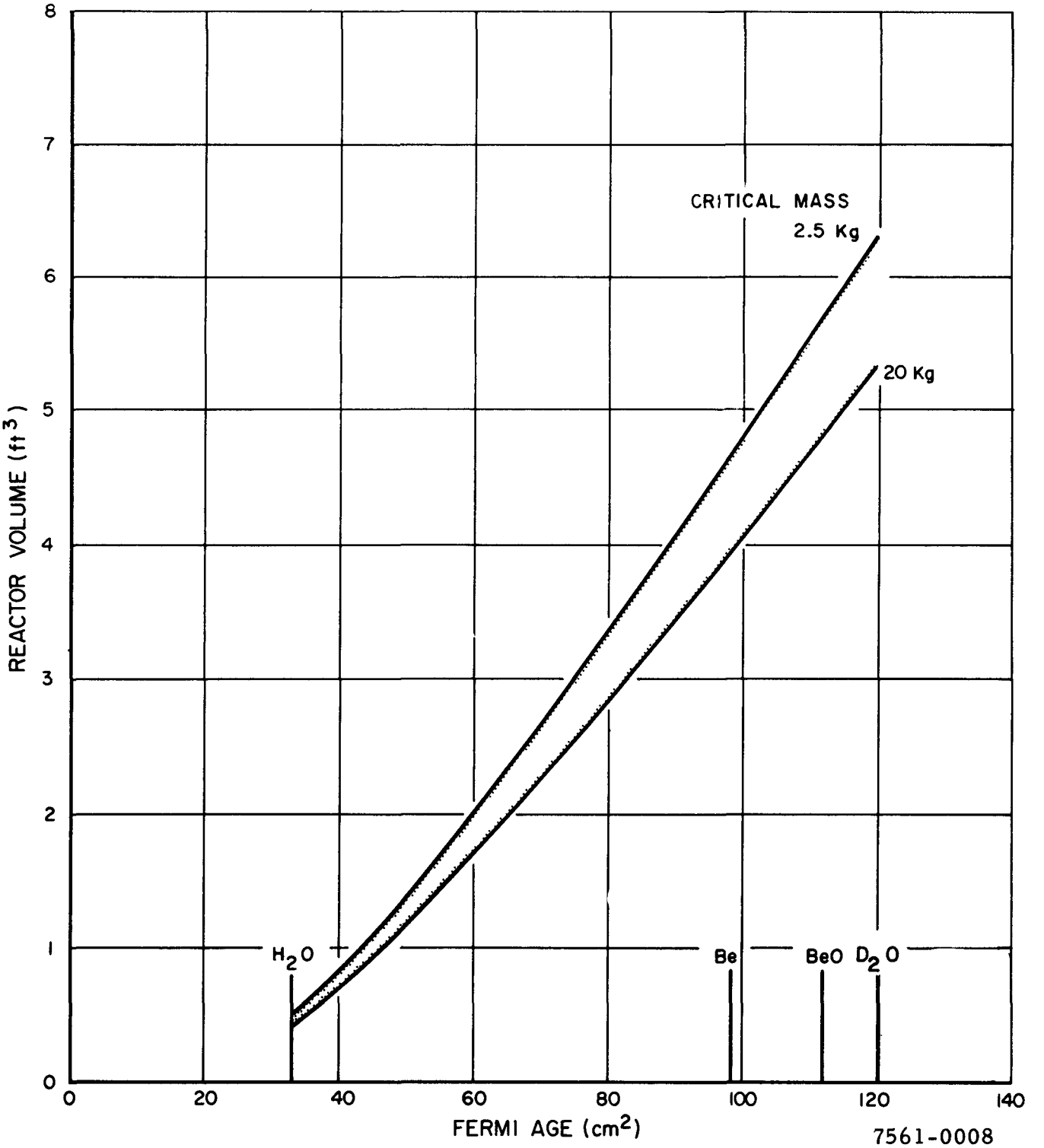

Figure 13. Volume of Bare 100% Dense Spherical Reactors with Critical Mass in the Range of 2.5 to 20 kg as a Function of Fermi Age

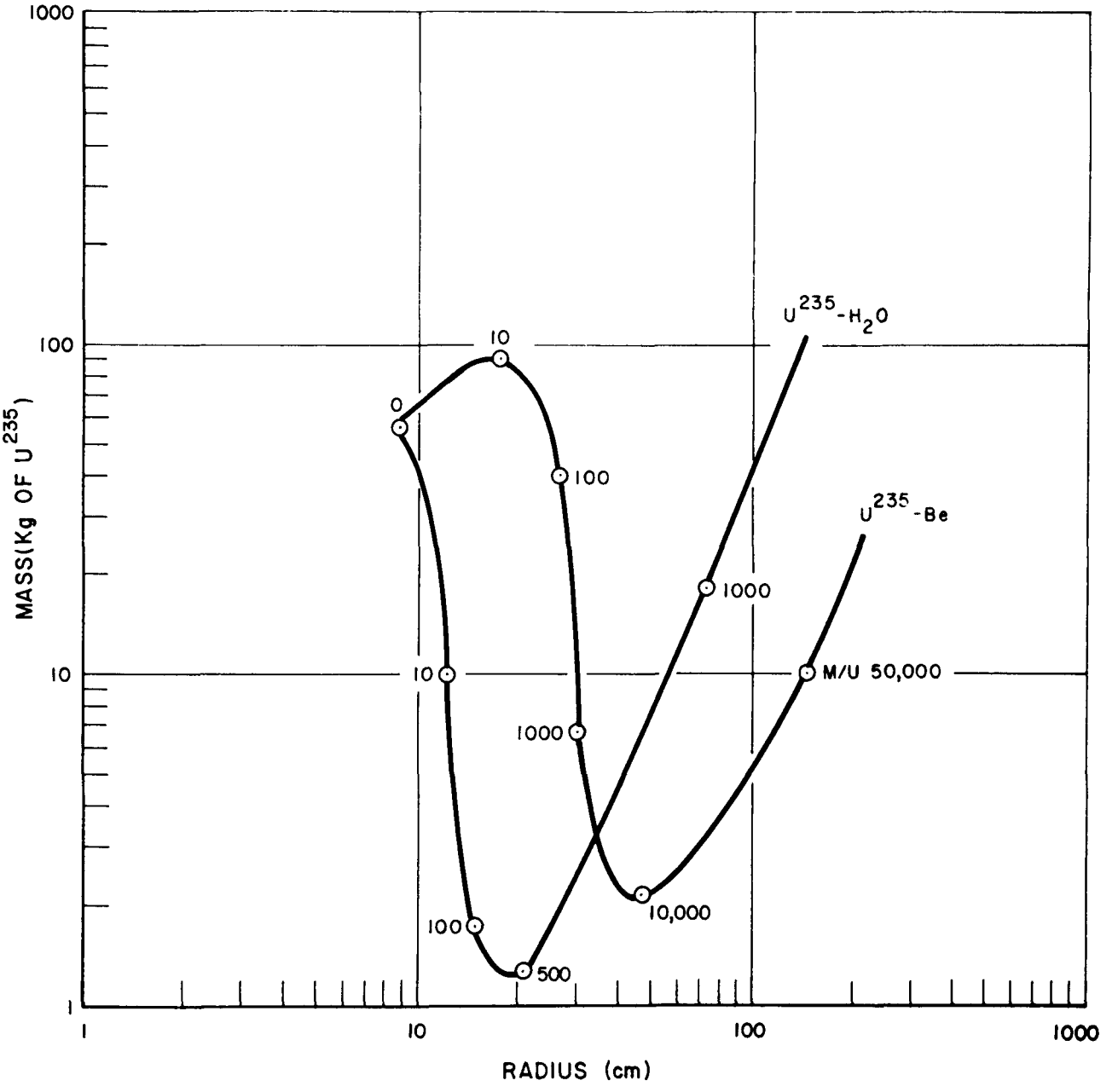

2-21-62 7590-A307

Figure 14. Critical Mass of Bare 100% Dense Homogeneous Spheres of U-235 Moderated by Water and by Be as a Function of Radius and Moderator to U Atom Ratio

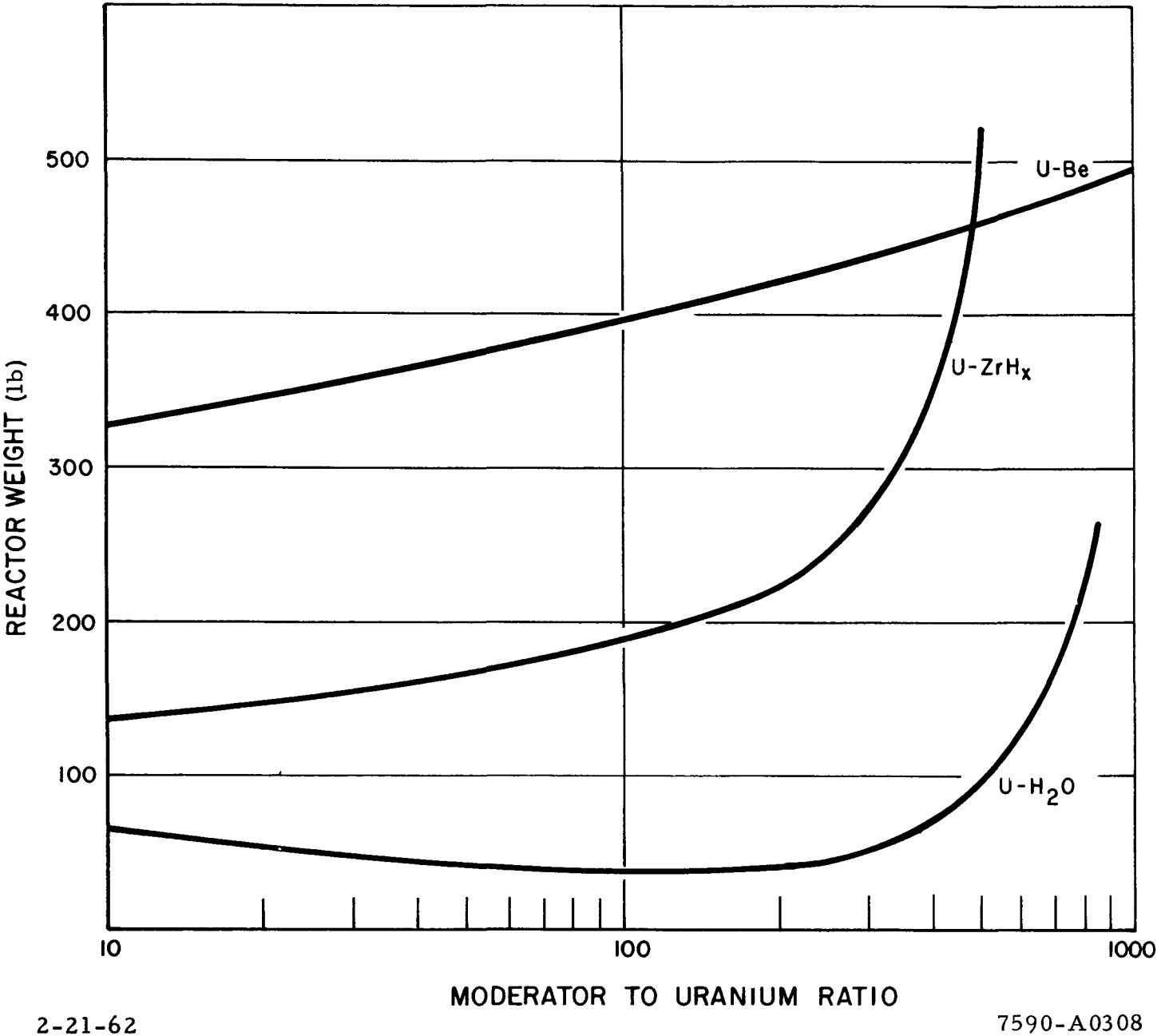

Figure 15. Weight of Bare 100% Dense Spherical Reactors as a Function of Moderator to Uranium Atom Radio

pressure of only 1 atmosphere (see Figure 16). The U-ZrH_x calculations were based on the critical size of a H_2O reactor but the difference arises from the fact that ZrH_x has a density of about 5.6.

The information discussed thus far has been for reactors of 100% density. A useful reactor must contain coolant passages for the removal of the reactor heat. The presence of such voids effectively decreases the density of the reactor. In order to maintain criticality the dimensions of a reactor must vary inversely as the density of the core material (fuel moderator). Therefore, since the volume varies as $(\text{density})^{-3}$ weight will be proportional to $(\text{density})^{-2}$. The result of density dependence is shown in Figure 17 which gives the weight of bare spherical fast reactors as a function of density. This type of density dependence holds for all reactors.

In addition to satisfying the basic criticality requirements for maintaining a chain reaction the reactor size is influenced by:

1) Operating temperature.

2) Excess reactivity requirements for compensation of fuel depletion, fission product poisons, etc.

3) Power density or heat transfer limitations.

4) Energy density or fuel burnup limitations.

B. TEMPERATURE

The size of a reactor is somewhat influenced by the operating temperature because the fuel and moderator material nuclear properties are a function of temperature. In addition as stated above, the reactor size is inversely proportional to density which varies with temperature. The most significant temperature limitations of a reactor are the materials strength, corrosion, compatibility, etc. limitations of the structural materials. Even though a reactor can theoretically produce power at any temperature, the engineering limitations of the fuel, moderator, and structure limit the available reactor outlet temperature. Even though it cannot be explicitly defined there is an intuitive relationship between operating temperature and lifetime. Figure 18 shows the lifetime-temperature relationship between current accomplishment and development objectives in nuclear power. This figure implies a state-of-the-art boundary for perhaps the next 10 to 20 years. This state-of-the-art boundary strongly influences the

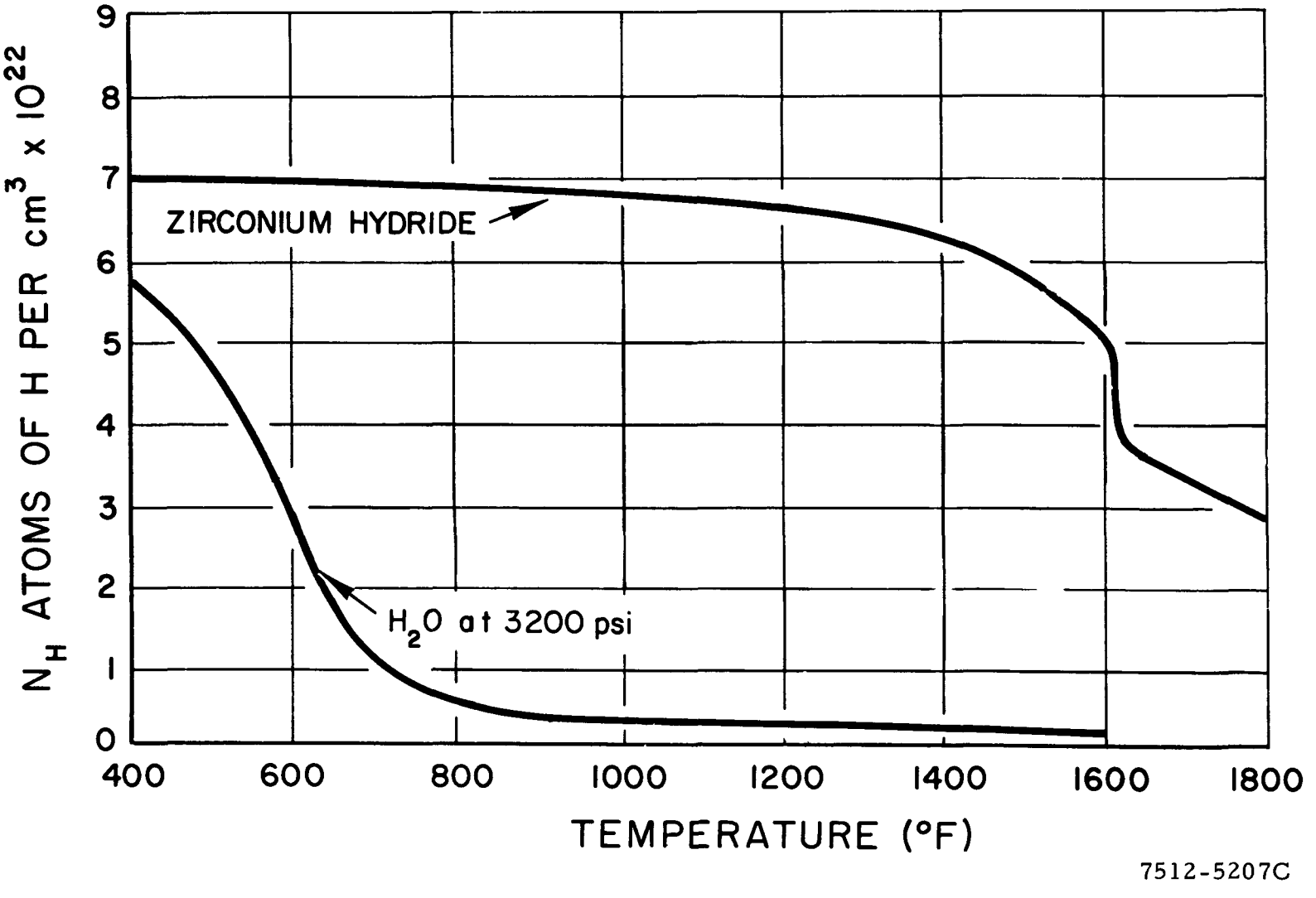

Figure 16. Hydrogen Density vs Temperature for Zirconium Hydride at One Atmosphere Dissociation Pressure and Water at the Critical Pressure

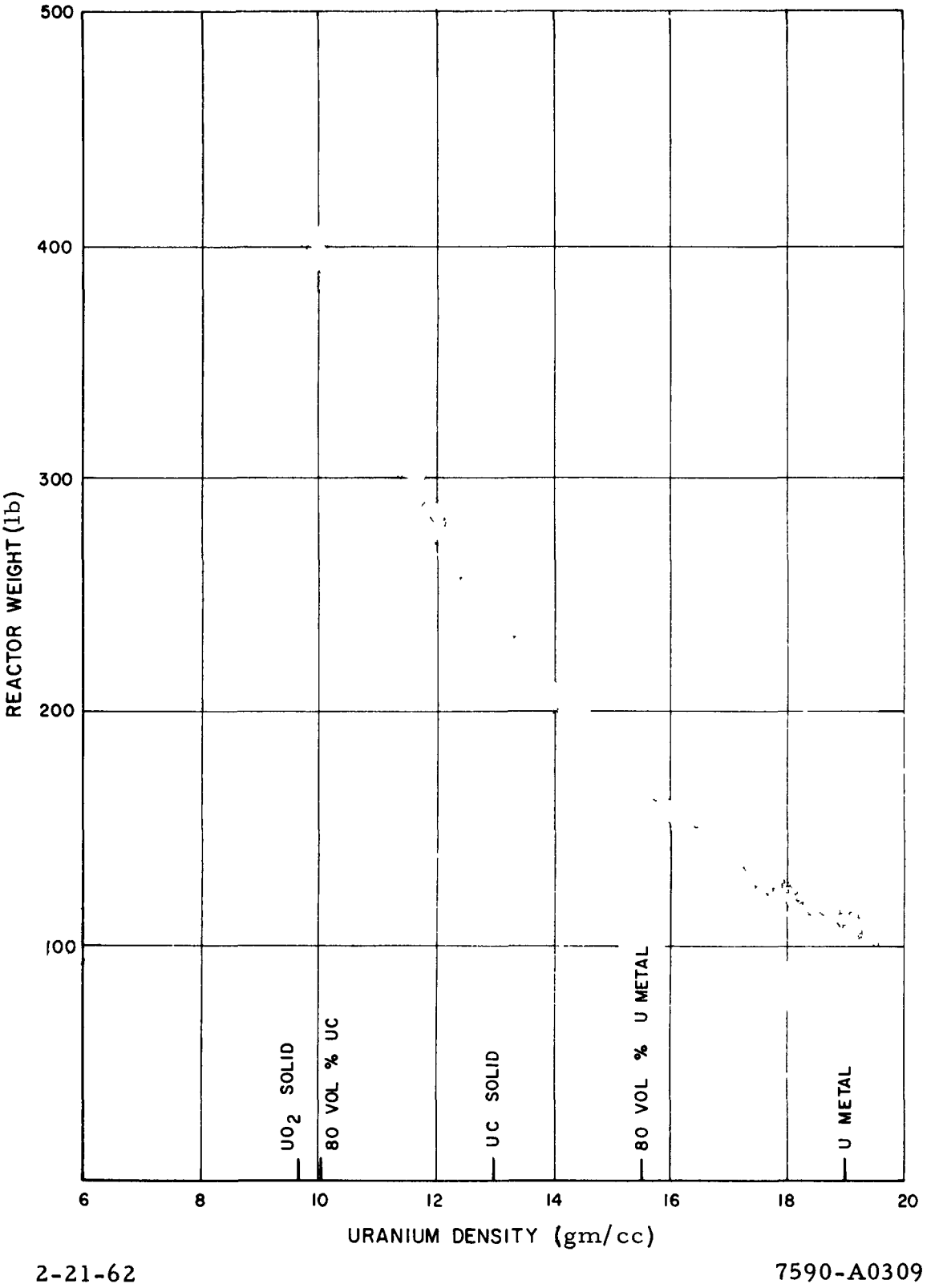

Figure 17. Weight of Bare Spherical Fast Reactors as a Function of Uranium Density

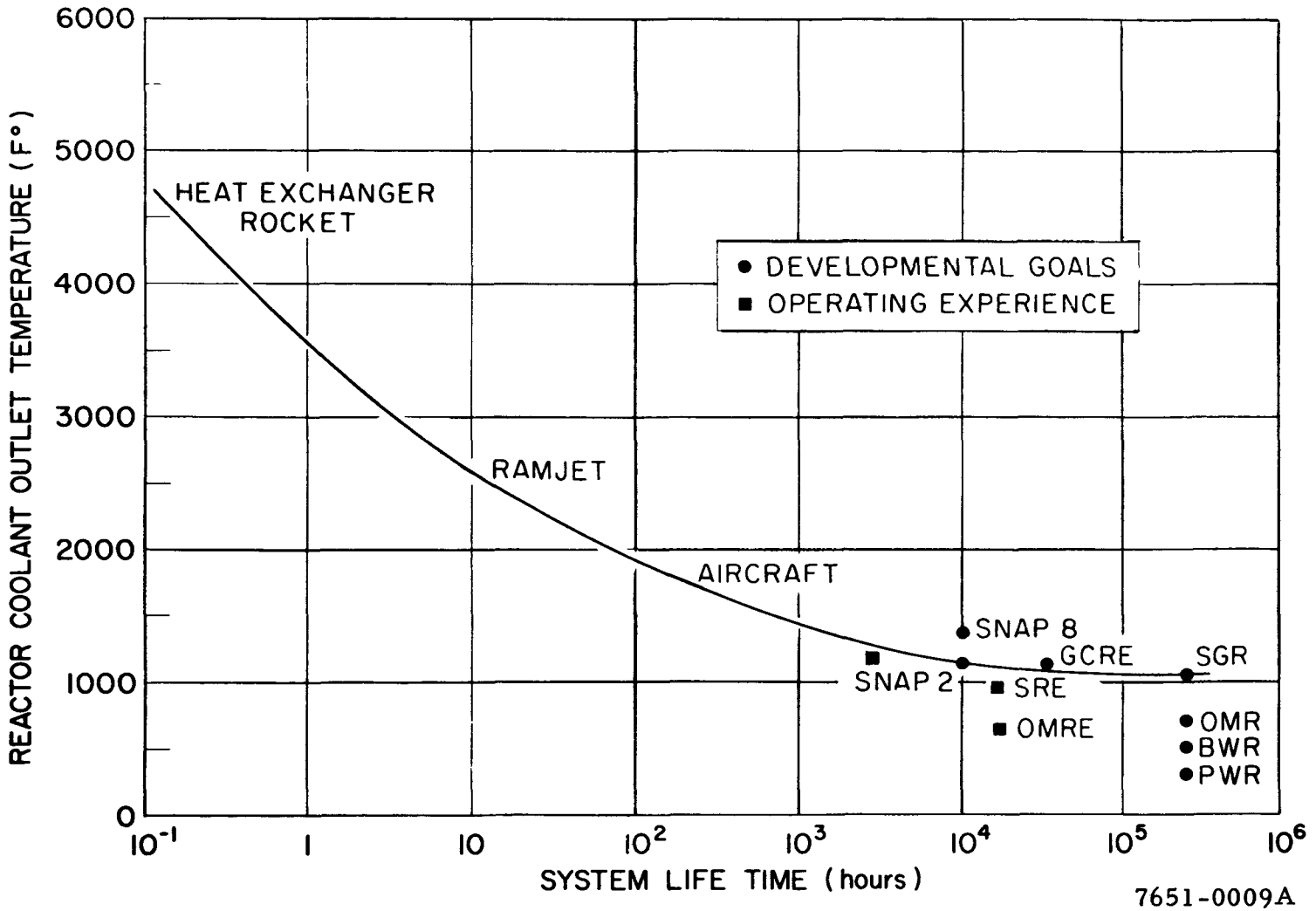

Figure 18. System Lifetime vs Operating Temperatures

reactor concept selection for immediate development and emphasizes the fact that high temperature materials development will pace the development of high temperature and high performance space systems of the future. A similar conclusion can be drawn about the state-of-the-art of high-temperature reactors from Figure 19 which shows the number of operating and planned reactors as a function of the reactor outlet temperature. Of course the choice of power reactor temperatures is greatly influenced by economics which may be considered as not applicable for space power. However, in effect, cost is probably one of the best direct measures of a state-of-the-art.

The approximate minimum weight of various reactors is shown as a function of temperature in Figure 20. The weights shown are for 100% dense spheres. Even though these weights could be reduced by the addition of a Be reflector, the inclusion of a void fraction for the reactor coolant would, in general, more than offset the weight reduction. Therefore, these weights can be considered representative, but by no means exact.

The aqueous homogeneous solution-type reactor is very light at low temperature but the moderator density decreases rapidly with temperature and the pressure necessary to suppress boiling soon becomes inconsistent with the objective of a lightweight reactor (the curve does not include the core vessel weight). The U-235 metal fast reactor is quite small; however, it must be limited to below 1200°F because of a large density change that accompanies a phase change at 1224°F. The U-ZrH_x system is similar in size to the H_2O moderated reactor because it can have the same hydrogen density as water below about 1200°F. Beyond 1200°F the size and weight increase because the hydrogen density must be decreased in order to control the thermal dissociation pressure of the compound. The UC and the UO_2 fast reactors are capable of up to 4200 and 5100°F respectively, the U-Be thermal reactor is limited in its temperature capability because of radiation damage induced swelling of Be at temperatures above about 1500°F.

C. CONTROL

In addition to the excess reactivity required to overcome the general reactivity decrease resulting from temperature, high power systems must have sufficient excess reactivity, and thus increased size, to compensate for burnup or depletion of the initial uranium inventory and the buildup of fission products of

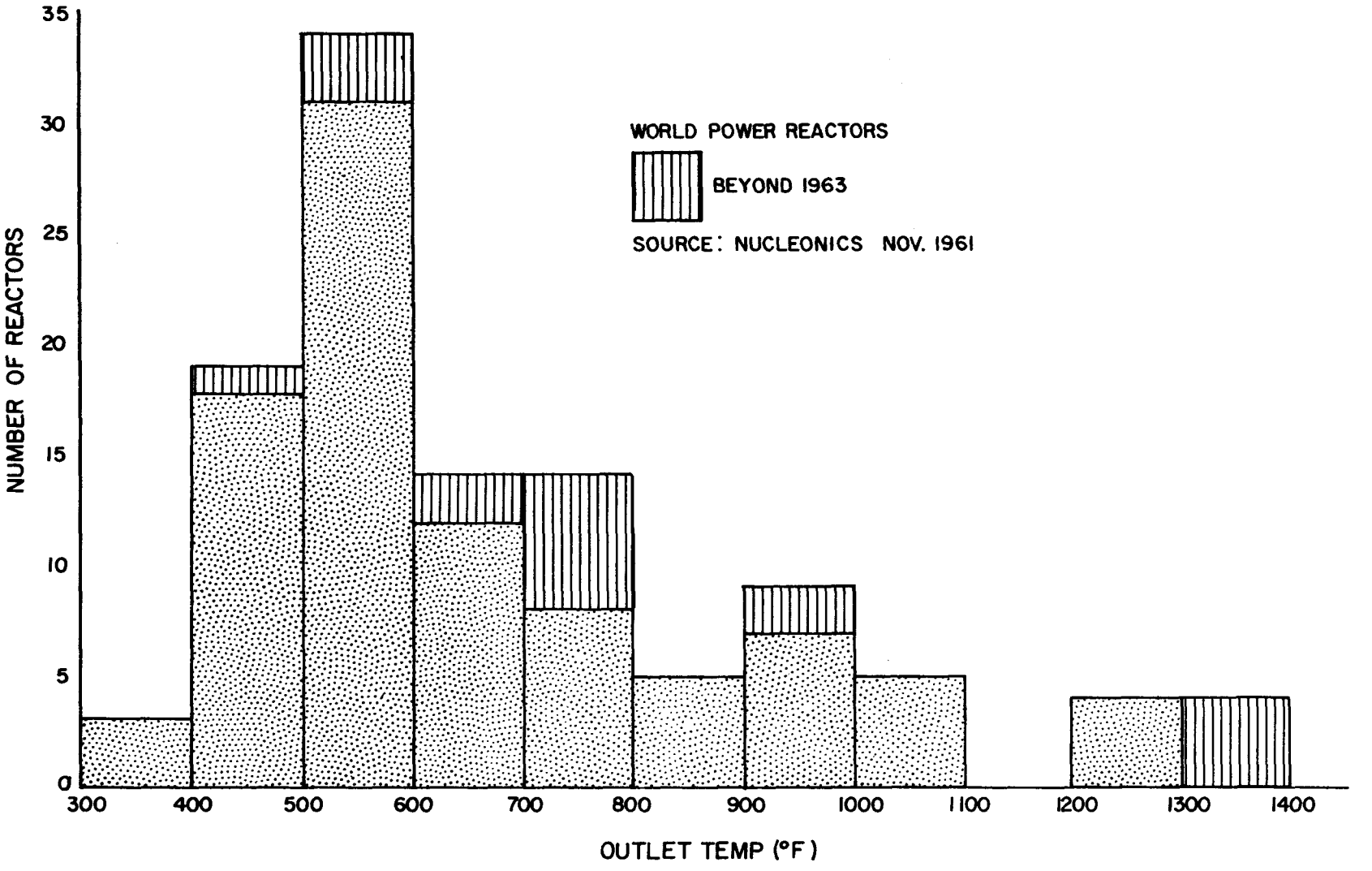

7-19-62

7561-0012

Figure 19. Number of Power Reactors in Operation or Planned for Immediate Future as a Function of Operating Temperature.

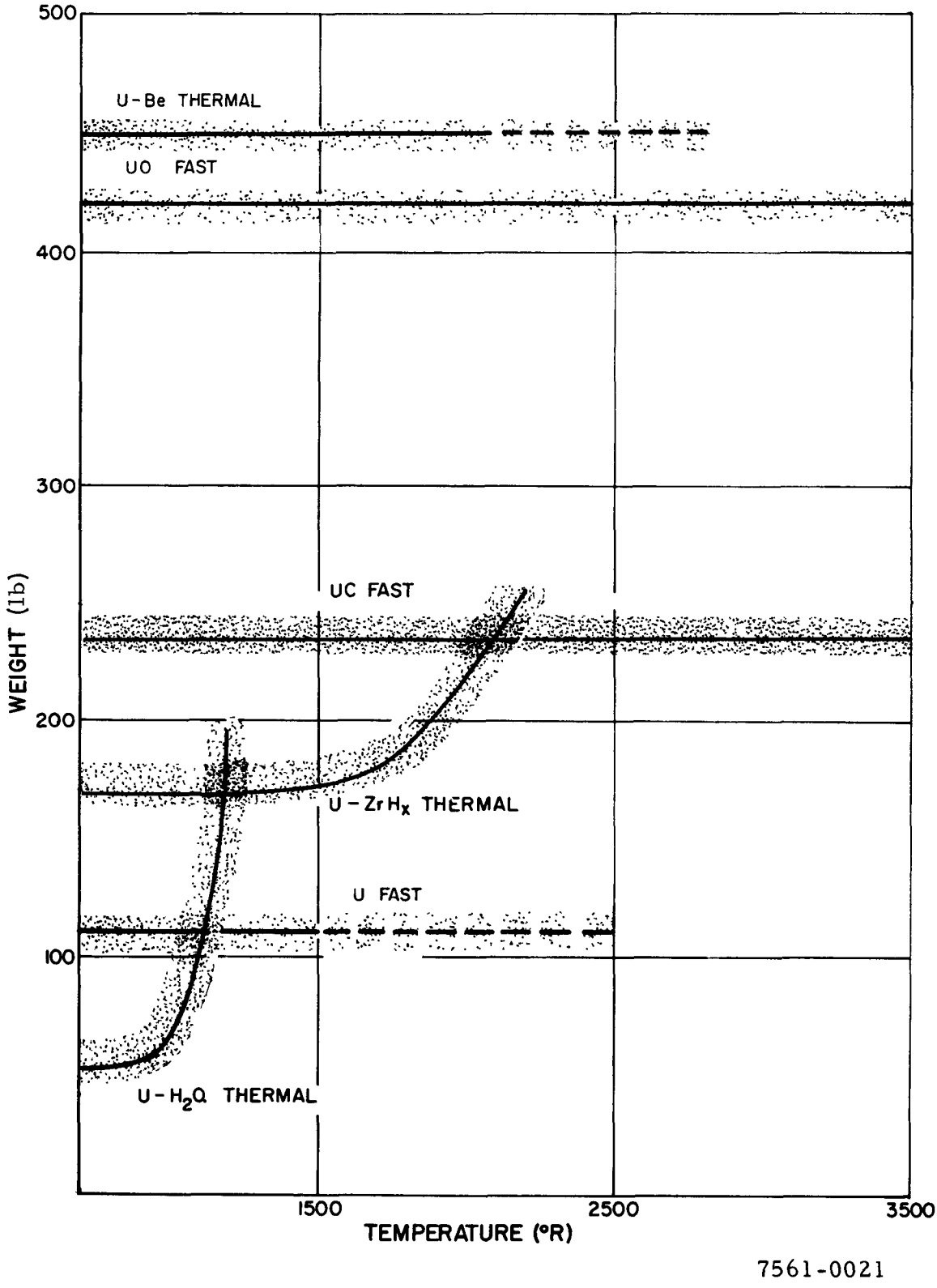

Figure 20. Weight of Bare 100% Dense Spherical Reactors as a Function of Operating Temperature

which some have high neutron absorption cross sections. The major fission product poisons are samarium and xenon. The most troublesome of these is xenon since the amount of poisoning is largest and since the poisoning increases rapidly and goes through a maximum after reactor shutdown or power decrease. This behavior imposes a serious limit on the allowable duty cycle of a high power density thermal reactor. Therefore it is very desirable to maintain reactor power constant. Fast reactors are not as greatly influenced by fission product poisons in general because the absorption cross sections are much lower at the neutron energy of the fast reactor.

These excess reactivity requirements impose a reactor control problem. In order to control the reactor from shutdown to operation throughout its lifetime the reactor must have more control worth than excess reactivity requirement. The amount of control that can be provided is a function of reactor size. Large reactors must be controlled by poison rods since leakage is small and provides little range for variation. Small reactors can be leakage controlled by varying the effective reflector thickness. However, the total amount of control available will decrease with increasing reactor size because the leakage decreases with size. Therefore, control requirements determine the appropriate control method and can limit the power density or energy content of a given reactor design.

D. POWER DENSITY

In addition to the fuel depletion and fission product poison considerations reactor size is a function of power density because: (1) the reactor density is decreased by the inclusion of coolant passages, and (2) surface or volumetric heat transfer and stress limitations can limit the power density.

In order to minimize both the reactor coolant fraction and the coolant pumping power, high temperature and high heat capacity coolants are desired. These conditions are best met by liquid metals. The properties of selected liquid metal coolants are shown in Table XI. It must be remembered that the reactor materials and the coolant must be compatible from a corrosion standpoint at the operating temperature.

If the reactor fuel element design or the coolant imposes a heat flux limitation, then the allowable reactor power density will be a function of the heat transfer surface per unit volume. It is therefore desirable for the reactor to contain the maximum amount of heat transfer surface consistent with the needs. The

TABLE XI

PHYSICAL PROPERTIES OF SOME SELECTED LIQUID METALS

	Sodium	NaK 44% K	Hg	Pb	Pb-Bi Eutectic	Li
Melting point, °F	208	65	-37	622	257	354
Boiling point, °F (14 7 psi)	1621	1518	675	3170	3038	2403
Liquid density, gm/cm^3	0 928-0 78	0 886-0 742	13 5-12 3	10 2	10	0 507-0 441
Specific heat, Btu/lb-°F	0 33-0 30	0 269-0 253	0 033	0 034	0 035	1 0
Thermal conductivity, Btu/ft^2	49. 8-34 5	14 8-16 7	5-9	8	5 3-6 5	22
Heat transfer coefficient, $Btu/hr-°F-ft^2$	6400	3500	5700	4100	3700	5800
Pumping power (water = 1 00)[1]	0 925	0 925	13 1	11 5	11 5	0 5
Probable temperature range, °F	250-1500	100-1400	-37-1000	650-1700	300-1700	400-2300

[1] At 10 ft/sec in 1 in diameter tube

core materials of a thermal reactor can be arranged in two ways. The heterogeneous reactor has the fuel separated from the moderator. Since a thermal reactor has only a few volume percent fuel and since practically all of the power is generated in the fuel, only a few volume percent are therefore available to provide or contain heat transfer surface. The homogeneous reactor has the fuel and moderator intimately mixed and power is produced throughout the entire core volume. Therefore the entire core volume of a homogeneous reactor is available for heat transfer surface. Since the core of a fast reactor contains fuel only, it has the same advantage as a homogeneous reactor. Thus for minimum weight high power density reactors the homogeneous arrangement of core materials is far superior.

If we consider a reactor whose core is composed of a bundle of mutually tangent cylindrical fuel elements, the heat transfer surface per unit volume is:

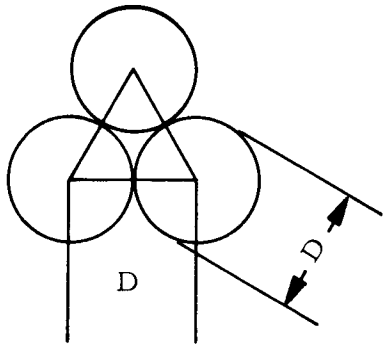

$$\frac{\text{Surface}}{\text{Volume}} = \frac{1/2\pi D}{1/2D\,\frac{\sqrt{3}}{2}D}$$

$$= \frac{2\pi}{\sqrt{3}\,D}$$

$$\frac{\text{Surface (ft}^2\text{)}}{\text{Volume (ft}^3\text{)}} = \frac{43.6}{D(\text{in.})}$$

If the limiting heat transfer flux is Q/A then

$$Q/V = \frac{A}{V}\,\frac{Q}{A} \quad ,$$

and

$$\frac{Q}{V}\left(\frac{Mw}{ft^3}\right) = \frac{12.8}{D(\text{in.})}\;\frac{Q}{A}\left(\frac{10^6\ \text{Btu}}{\text{hr-ft}^2}\right) \quad .$$

The maximum temperature drop across a given fuel element may be limited by maximum temperature considerations resulting from the fuel material melting point, phase change, etc., or it may be limited by a maximum allowable stress.

The temperature drop across a cylinder with uniform surface cooling and uniform volumetric heat generation is:

$$\Delta T = \frac{(Q/V)\, D^2}{16K} .$$

Therefore for a given ΔT limit

$$\frac{Q}{V} = \frac{16K\Delta T}{D^2} ,$$

$$\frac{Q}{V}\left(\frac{Mw}{ft^3}\right) = \frac{0.000675}{D^2_{(in.^2)}} \quad (K\Delta T) .$$

where K is the thermal conductivity in Btu/hr-ft-°F and ΔT is in °F. If there exists a ΔT limit, the power density is a function of the fuel element dimensions and $K\Delta T$ which is a material property. For example, uranium metal undergoes a phase change at about 1200°F which results in a 5% density decrease. This phase change must be avoided for metallurgical as well as reactivity reasons. If a uranium metal fast reactor is operating at a fuel surface temperature of 1000°F then the maximum ΔT can be only 200°F. The thermal conductivity of uranium metal is about 15 and therefore $K\Delta T = 3000$. The allowable power density for 1/4 in. diameter fuel rods is then $Q/V = \left[0.000675/(1/4)^2\right]3000 \cong 32$ Mw/ft^3. The volume of such a reactor might be about 1/10 ft^3. Thus, it could produce 3.2 Mw. If a higher power were desired the surface temperature would have to be reduced or the fuel rod diameter reduced, or the reactor made larger for heat transfer purposes. We might say the reactor size is criticality limited below 3.2 Mw and heat transfer limited beyond 3.2 Mw.

The temperature drop across a material leads to a stress. In the case of a cylinder the maximum tensile stress is:

$$\sigma = \frac{E\alpha\Delta T}{2(1-\nu)} ,$$

where

E = Young's modulus (psi)

α = linear coefficient of expansion $(°F)^{-1}$

ν = Poisson's ratio $\cong 1/3$

σ_{max} = allowable stress (psi) .

If the stress leads to brittle fracture in the material and the fracture influences heat transfer or mechanical integrity, then the stress must be kept below the fracture stress and the allowable ΔT is

$$\Delta T_{max} = \frac{4}{3} \frac{\sigma_{max}}{E\alpha} ,$$

and from above

$$Q/V = \frac{0.0009}{D^2} \frac{K\sigma_{max}}{E\alpha} .$$

The physical properties of two potential high temperature high power density fast reactor core materials are given in Table XII.

TABLE XII

FUEL PROPERTIES

	Metal	UO_2	UC
Density, gm/cc	19.0	10.96	13.63
U content, gm/cc	-	9.66	12.97
Melting point, °F	2070	5100	4200
Thermal conductivity, Btu/hr-ft-°F	15	1	14
Linear coefficient of expansion x 10^6	~20*	4	6.7
Modulus of elasticity, psi x 10^{-6}	20	25	30
Modulus of rupture, psi x 10^{-3}	-	25	25
$\sigma K/E\alpha = K\Delta T_{max}$	-	1/4 x 10^3	5/3 x 10^3

*Anisotropic

For example, consider a fast reactor which uses UO_2 for the fuel material and has 1/4 in. diameter fuel elements. Since the stress limited $K\Delta T$ for UO_2 is about $1/4 \times 10^3$, this reactor would be stress limited at a power density of

$$\frac{Q}{V} = \frac{0.0009}{(1/4)^2} (1/4 \times 10^3) = 3.6 \frac{Mw}{ft^3} .$$

If, however, it is determined that thermal stress induced fracture of the UO_2 does not impede heat transfer or mechanical integrity but that the fuel must be limited by central melting, then ΔT_{max} becomes $T_M - T_C$, where T_M = melting temperature and T_C = surface temperature, and

$$\frac{Q}{V} = \frac{0.000675}{(1/4)^2} K(T_M - T_C) ,$$

since K = 1 and T_M = 5100°F;

T_C (°F)	Q/V (Mw/ft^3)
1000	44
2000	33
3000	22

It is readily seen that the maximum power density under the above conditions is a function of the reactor operating temperature.

Figure 21 shows the relationship between power density, fuel element diameter, heat flux limit, and ΔT or stress limits for a homogeneous system with mutually tangent cylindrical fuel elements. Note that the above calculations are based totally on average values. No consideration has been given to the detailed power and temperature distribution in the reactor. These calculations are intended only to indicate the reactor design considerations and limitations.

E. ENERGY DENSITY

Burnup and resulting fuel depletion which are related to energy density impose control requirements and can limit reactor life. However, radiation damage is generally the most significant energy density limitation. Even

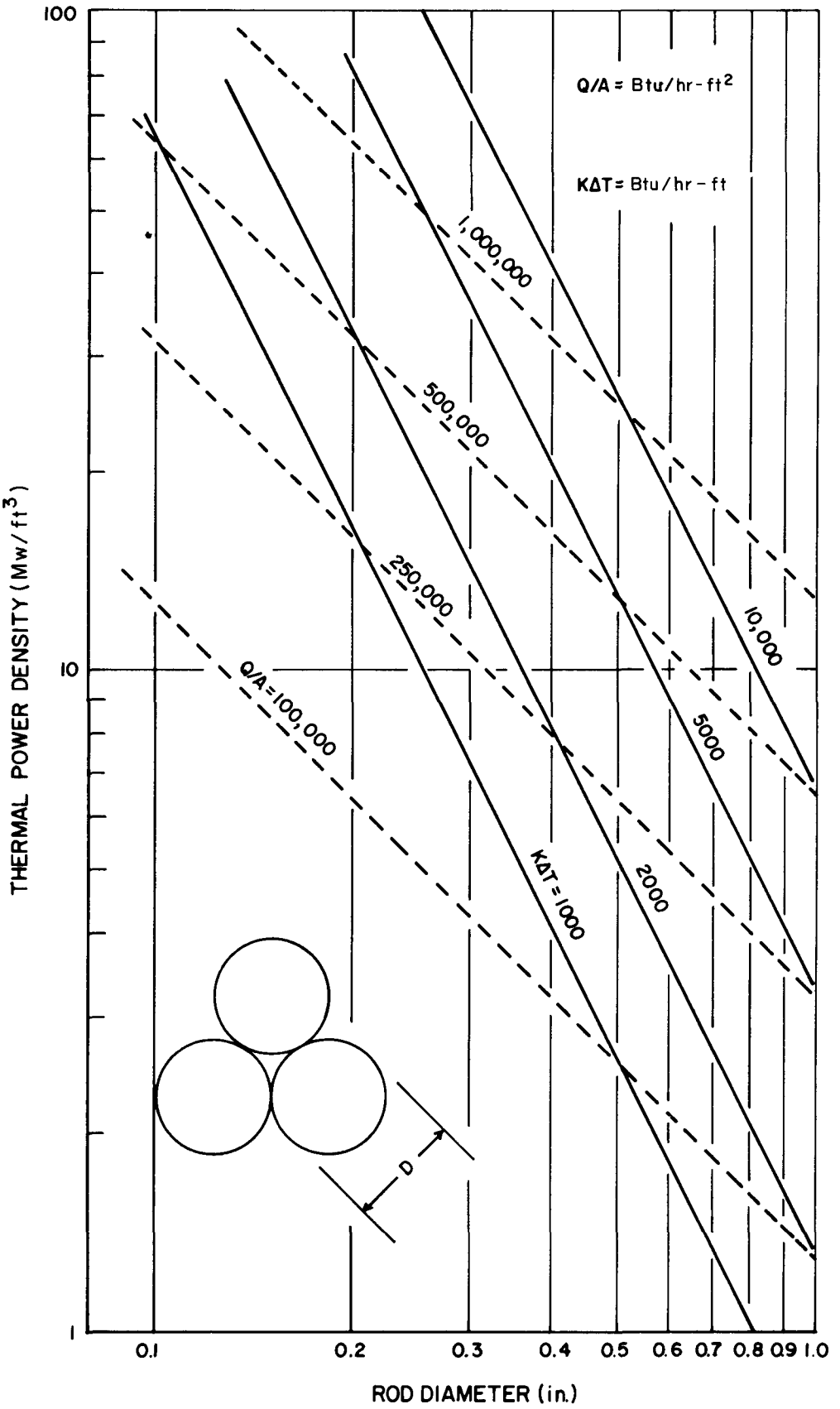

7-19-62 7561-0005A

Figure 21. Reactor Power Density as a Function of Fuel Element Diameter and as a Function of Surface and Volumetric Heat Transfer Limits

though the fissioning of 1 gm of uranium per day releases 1 Mw of power, we have seen that reactor criticality demands anywhere from a few to a hundred kilograms in order to utilize the energy of fission. Furthermore, only a few percent of the uranium inventory or critical mass of the reactor can be utilized because of radiation damage.

Fission results in the replacement of each fissioned uranium atom with two fission products. Thus, as the fissioning of uranium metal, for example, proceeds the metal lattice is being stuffed with one extra atom for each fission. These extra atoms plus the fact that the fission product may not comfortably fill a uranium site result in internal strains in the material. In addition, the energetic particles and fission products collide with the atoms of the parent lattice and disrupt it which causes further strain. The parent lattice can only accommodate so much of this strain until it must yield or distort in order to relieve the fission induced strains. This resulting material distortion and expansion is radiation damage. It can be argued on intuitive grounds that a given material can accommodate some maximum fractional increase in the normal atom density before unacceptable damage results. In other words, some fraction of the total number of atoms per unit volume can be fissioned. Experience shows that radiation damage is indeed well correlated on a total atom percent burnup basis. However, the amount of physical distortion or swelling is a function primarily of the parent lattice or material that is absorbing the fission damage and the temperature at which the material is operating during fission. The above is a gross simplification, however, sufficient data and experience for a quantitative description of the radiation damage limits for all materials do not exist. In fact, it is an extremely difficult, costly, and time consuming task to establish such limits. Figure 22 shows the results of many years of investigation of the UO_2 stainless steel system. This system is of no interest for space reactors but the data illustrate the kind of burnup vs temperature limitations that exist for all materials. Such detailed information is not yet available for the materials and temperatures of interest for space reactors. However, past experience has shown that few materials can absorb more than 1 to 2 at.% burnup without loss of fuel element physical integrity.

If we assume that a material contains 5×10^{22} atoms/cc, which is about the atom density of U metal and we further assume that 1% of the atoms can be fissioned with acceptable radiation damage, then the material can sustain the

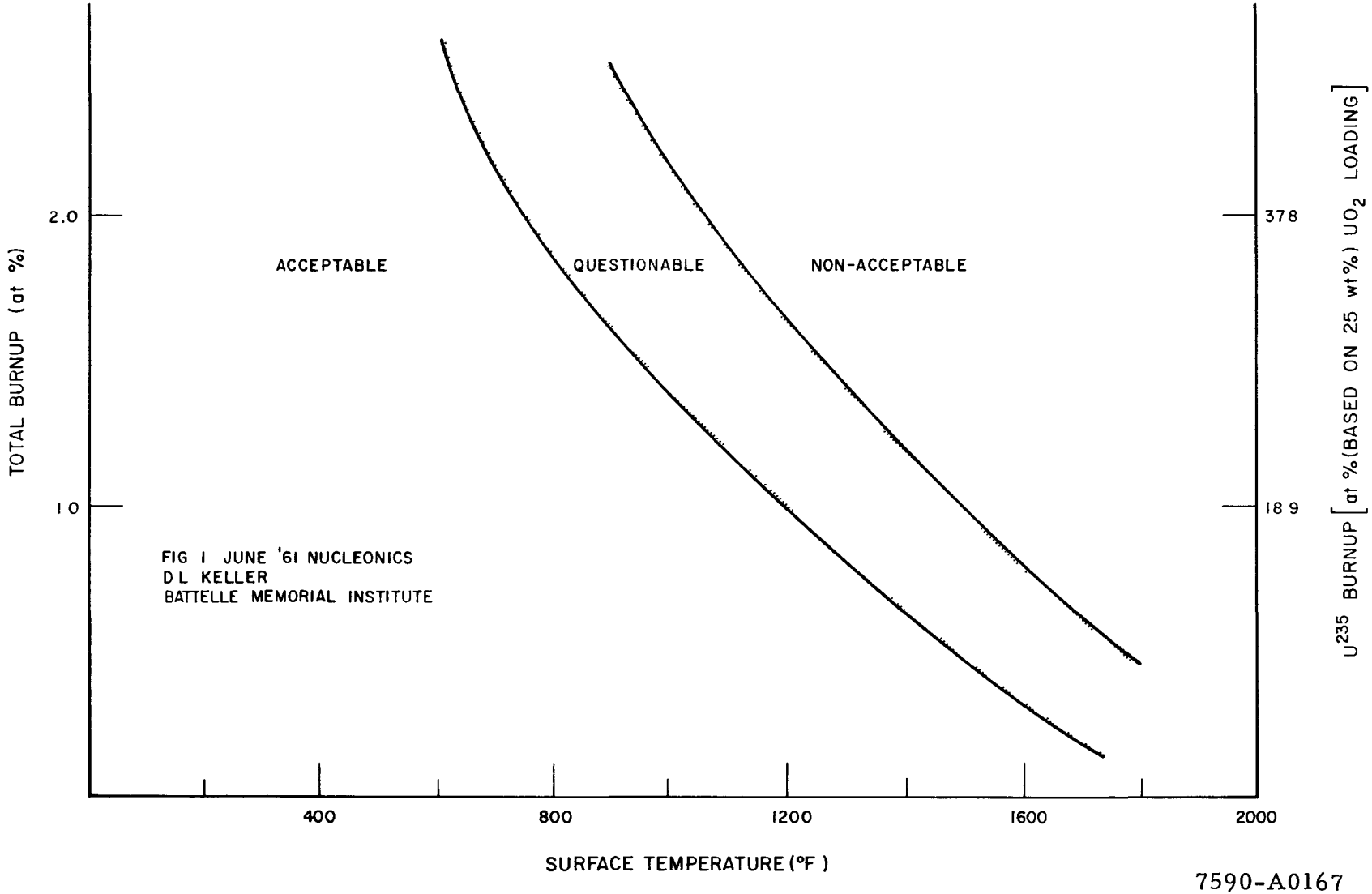

Figure 22. Burnup Performance of Stainless Steel-UO_2 Cermet Fuel Specimens

fissioning of 5×10^{20} atoms/cc. The fissioning of 5×10^{20} atoms/cc results in the release of

$$1 \text{ at.}\% \cong \frac{5 \times 10^{20}}{6 \times 10^{23}} \times 5.3 \times 10^{6} \text{ kwh/mole} = 4.4 \text{ Mwh/cc.}$$

Therefore, the fissioning of 1 at.% releases about 15 Mw-years per cubic foot of reactor core material. Since the atom density of most materials is near the above assumption, this figure is a reasonable approximation.

The temperature-dependence of the burnup limit is of extreme importance when maximum temperatures are desired as is the case for space systems. Even in the case of terrestrial reactor systems where low temperature heat sinks are available there is a tendency to strive for high temperatures in order to maximize Carnot. If, however, one wants maximum net energy output per core either for economic reasons or for endurance reasons, the significant parameter is the product of allowable burnup times Carnot efficiency. This quantity is proportional to the net available energy that can be delivered by one core. Since burnup capability decreases with temperature and Carnot increases with source temperature (for a fixed sink temperature), there is an optimum temperature for maximum system endurance. Figure 23 illustrates this point for a system having the burnup limits of Figure 22 and having a fixed sink temperature of 100°F. The UO_2 stainless steel cermet is generally considered a good "high-temperature" fuel. However, it can be readily seen from Figure 23 that the optimum temperature for maximum endurance is quite low in comparison to the normally considered temperature limits of such a material.

F. SUMMARY EXAMPLE

The relative importance of the various reactor size limitations above can be shown by an example. Assume the following conditions:

1) Reactor critical volume = 0.4 ft^3

2) Heat flux limit = 400,000 Btu/hr-ft^2

3) Fuel thermal conductivity = 15 Btu/hr-ft-°F

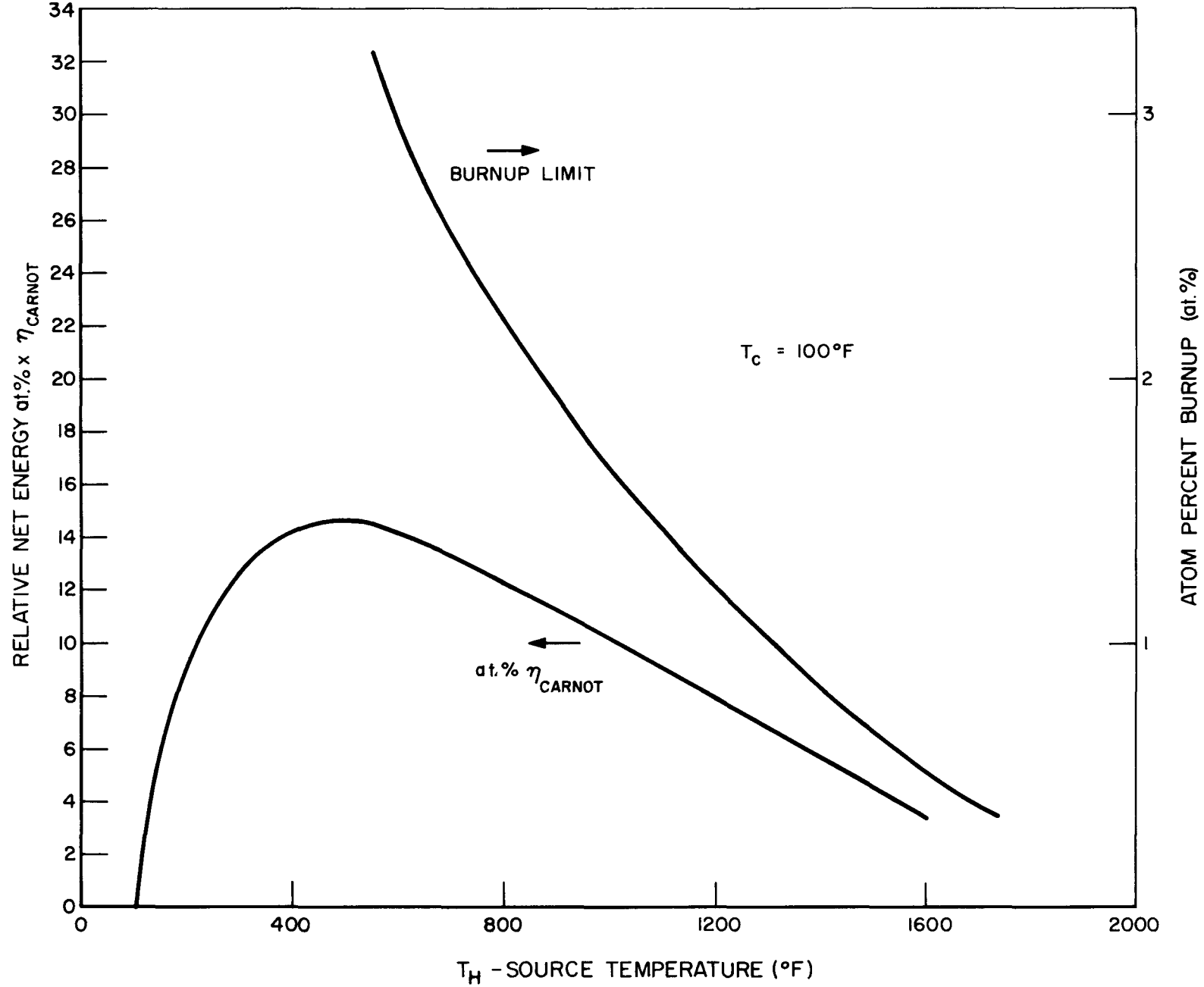

7-19-62

Figure 23. Burnup vs Temperature

7561-0020A

4) Fuel ΔT_{max} = 200°F

5) Fuel burnup limit = 1 at.%

6) Fuel element minimum diameter = 0.15 in.

7) Reactor power = 10 Mwt

8) Lifetime = 1 year

Figure 24 shows the reactor volume as a function of fuel element diameter for the various limits. If fuel element cladding thickness had been included, the void fraction would increase with decreasing rod diameter and the criticality limit and the burnup limit would not be independent of rod diameter.

A probable design point for this example would lie on the burnup limit in order to minimize reactor volume and weight and would also lie on the heat flux limit in order to minimize the number of fuel elements and thus the manufacturing cost.

It should be noted that the above treatment has been high qualitative for illustrative purposes. Throughout, the power distribution in the reactor and the temperature distribution details have been completely neglected. The quantities used have been average values. In general, reactor power varies as a chopped cosine function in all directions. In small reactors this leads to a power distribution with a peak to average value in the range of 1.5 to 2. In a rigorous design analysis, all limits are placed on the maximum temperature, heat flux, power density, or burnup.

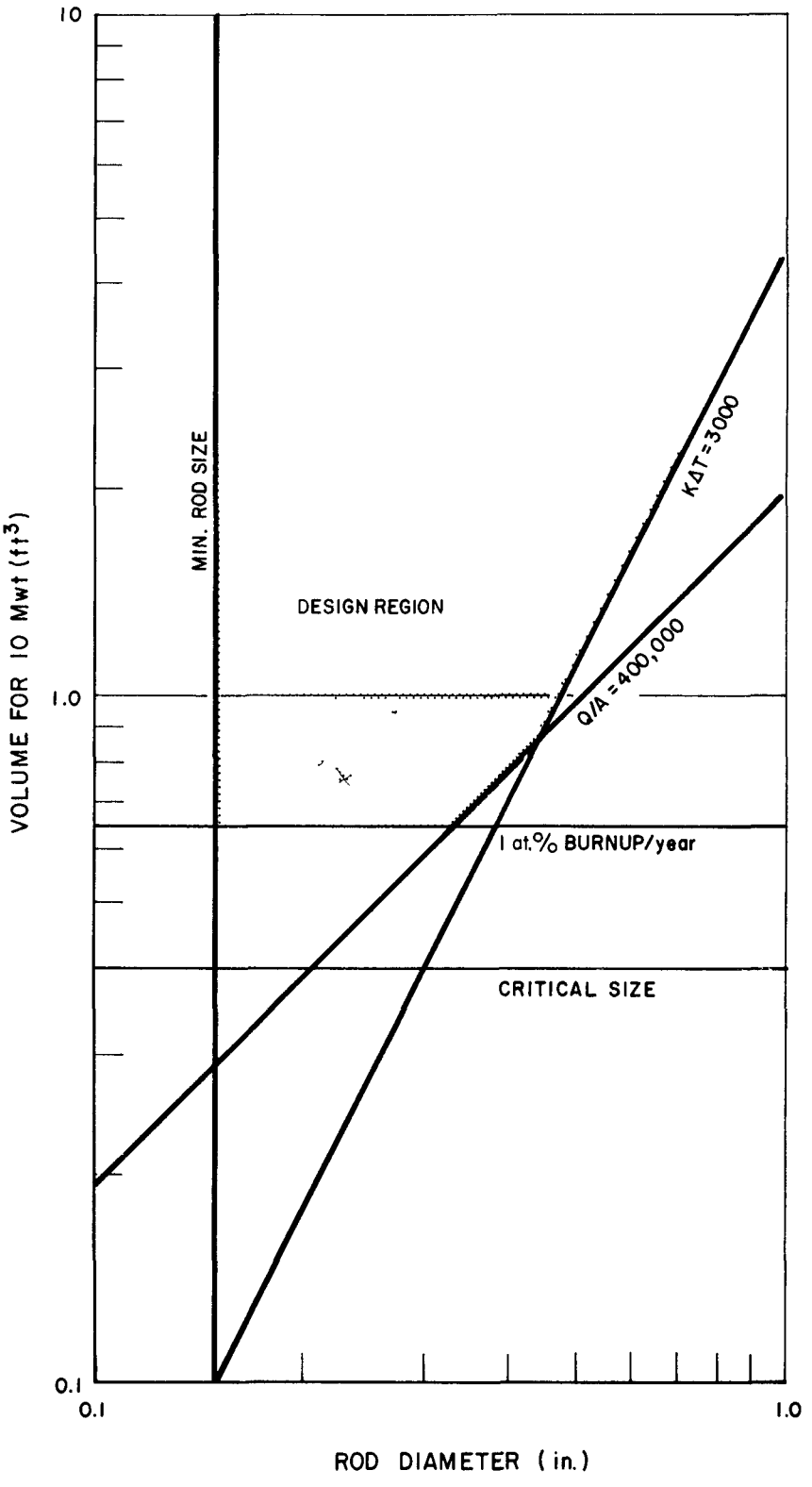

7590-A0168

Figure 24. Reactor Volume Requirements as a Function of Rod Diameter, Criticality, Heat-transfer Limit, and Burnup Limit

Thus far we have considered the requirements and limitations of reactors. In order to establish the specific reactor requirements for a space power application and to select a reactor-power conversion combination, we must consider the mutual interactions of the three major subsystems for nuclear space power plants. These include (1) the reactor heat source, (2) the power conversion cycle, and (3) the waste heat radiator. The power conversion cycle determines the operating temperature of the other two and its weight is relatively insensitive to temperature. The details of the cycle, for example the working fluid, are a function of the operating temperature. The radiator area and weight are, of course, a strong function of the cycle cold temperature. The reactor size, weight, and concept are a function of temperature because of the operating temperature limitations of the applicable core materials. In order to minimize the weight of the heat rejection system, it is necessary that the conversion system operate at a high sink temperature and recover a maximum fraction of Carnot efficiency. Since the waste heat of a cycle must be radiated to space, the area requirement and hence the weight associated with the heat rejection system is, for a given power level, proportioned to the fourth power of the cycle cold temperature and inversely proportional to the cycle conversion efficiency. At low powers, the reactor size is independent of power because of the minimum critical size requirements. Therefore, the conversion efficiency affects only the size of the radiator and the conversion equipment. Since the reactor and shield are the dominant weight of nuclear power systems at low power, the conversion efficiency of the cycle cold temperature is not so important at low powers as it is at higher powers. At higher power levels, however, the radiator becomes the dominant weight item of the system. Consequently, for the higher power systems there is a great incentive to achieve high efficiency and high heat rejection temperatures to minimize the weight of the radiator. This point is illustrated in Figure 25 which shows the relative weight contribution of the different system components as the power level is increased at constant radiator temperature.

A. TURBOELECTRIC SYSTEMS

A turboelectric nuclear space power system will probably utilize a Rankine cycle because it offers a high conversion efficiency, operates at relatively low

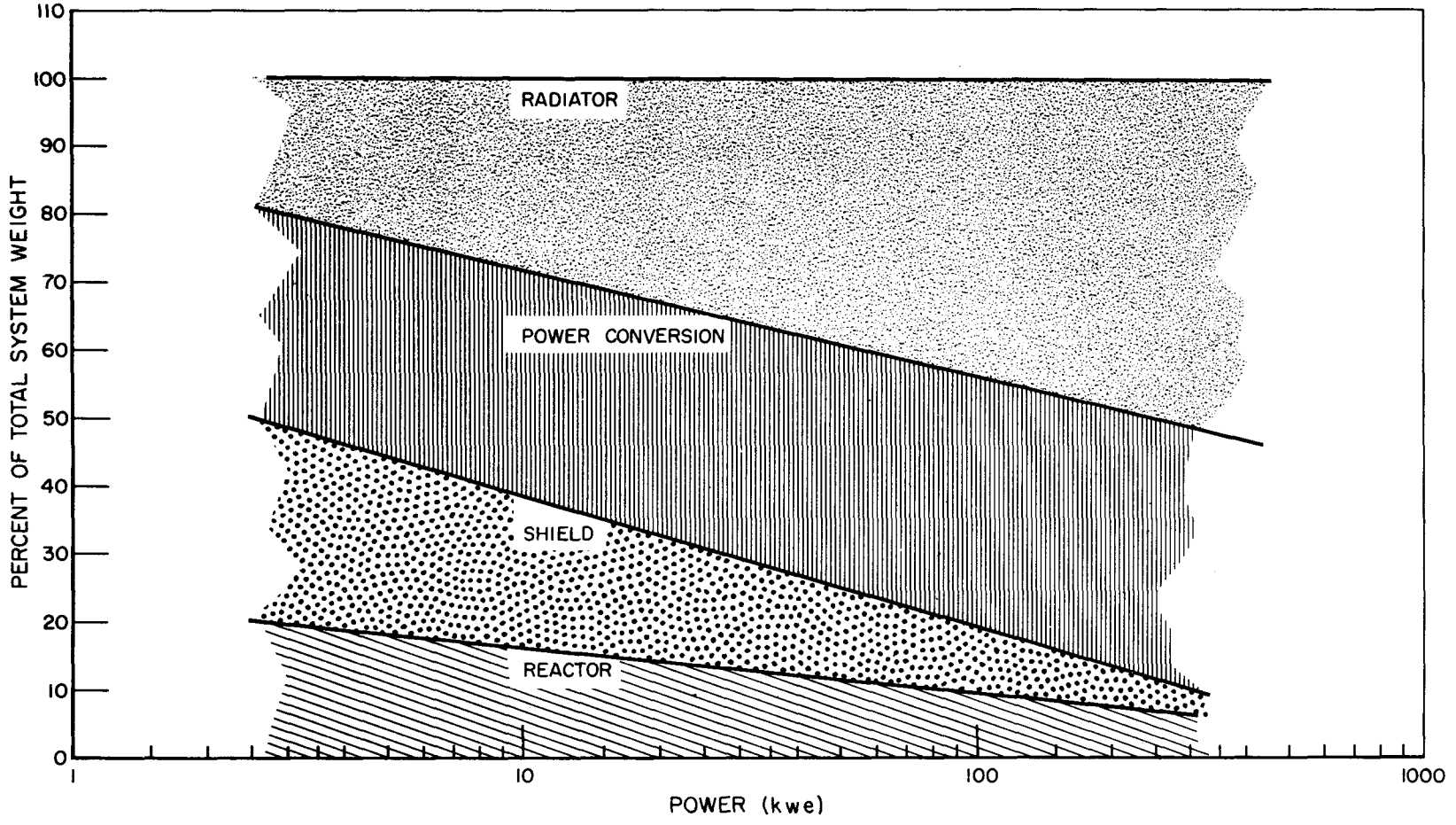

7-19-62

7561-0019

Figure 25. Weight Distribution for Nuclear Turboelectric Systems

source temperatures, and rejects the waste cycle heat at relatively high temperatures. The Brayton cycle appears unattractive for space application because of its lower fraction of Carnot efficiency, higher reactor temperature requirements, and larger radiator area demands.

The optimum heat rejection temperature for a Rankine cycle is determined by the working fluid selected. As a result of balancing Carnot efficiency against the T^4 law of radiation, the optimum radiator of condensing temperature is about 3/4 of the absolute boiling temperature. The relationship between boiling temperature, radiator area, and cycle working fluid is shown in Figure 26. The radiator area per kilowatt of output is calculated on the basis of an optimum Carnot of 25% and a conversion efficiency of 40% of Carnot which results in an overall system efficiency of 10%.

The approximate range of interest for the various working fluids is indicated as falling between a boiling pressure of 50 and 300 psia. This choice is arbitrary; however, a lower boiling pressure limit results from consideration of pressure ratio across the turbine and vapor specific volume. An upper pressure limit results from consideration of system weight. Another point of concern in cycle temperature selection is the condensing pressure. The 5 psia condensing pressure points for the various fluids are shown in Figure 26. The condensing pressure must be high enough to allow for condensing pressure drop while maintaining an adequate boiler feed pump inlet pressure to prevent cavitation.

Figure 26 defines the area of interest or heat source temperature requirements for various Rankine cycle working fluids. The reactor heat source thermal power and temperature requirements for Rankine cycle systems are shown in Figure 27 as a function of electrical power output and available radiator area. This survey assumed a constant fraction (50%) of Carnot conversion efficiency and a constant Carnot efficiency of 25% for minimum radiator area. This latter assumption should not be confused with minimum system weight which can occur at a different value of Carnot. It should be remembered that the actual heat-source temperature requirement is probably several hundred degrees higher than the boiling temperature in order to provide superheat and to allow for temperature drops throughout the system, especially the boiler. This problem can be eliminated by the use of a direct cycle which boils directly in the reactor core to provide saturated vapor. This approach is also attractive

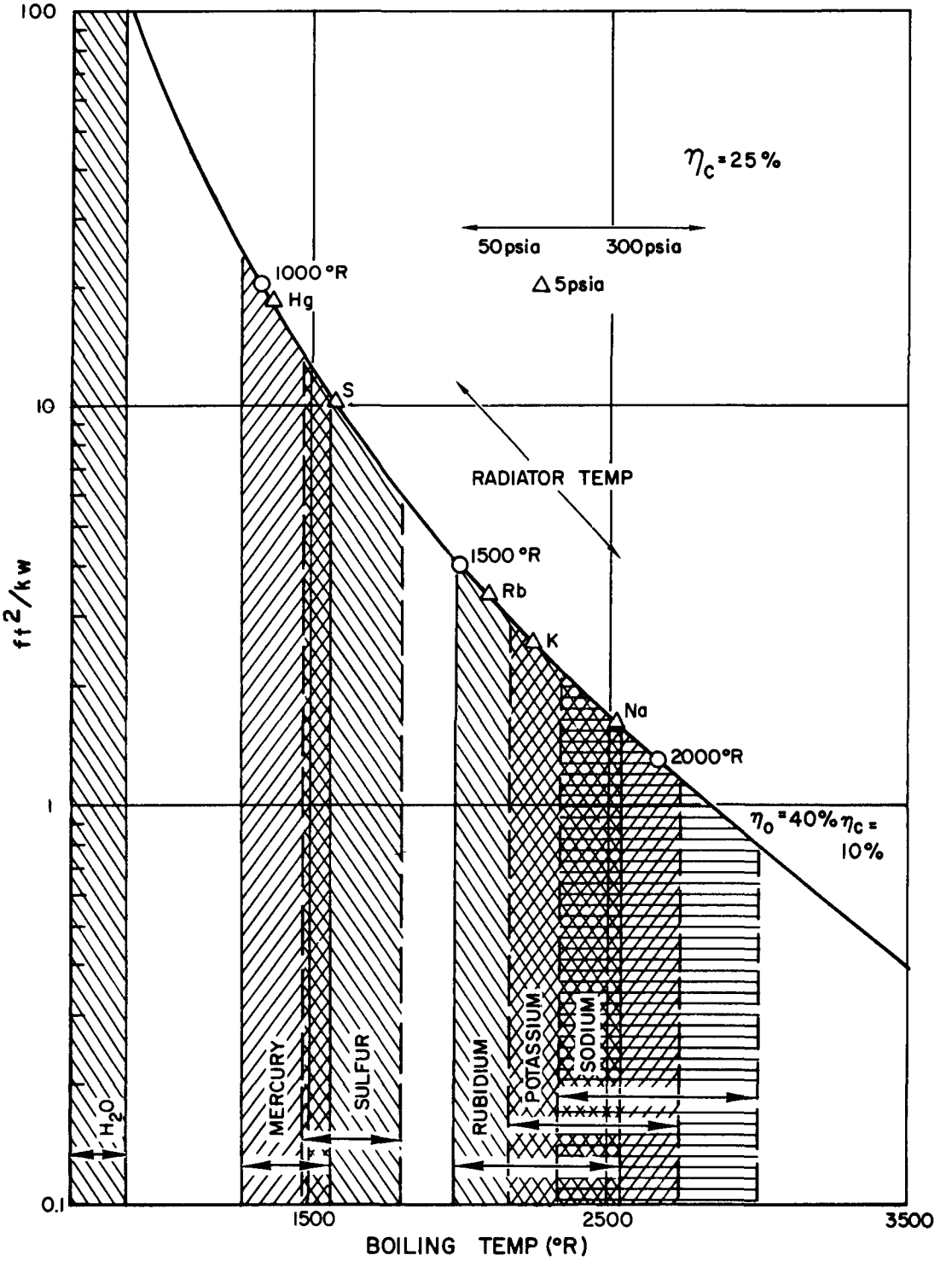

7561-0018

Figure 26. Radiator Area per Kilowatt as a Function of Boiling Temperature for Rankine Cycle Working Fluids

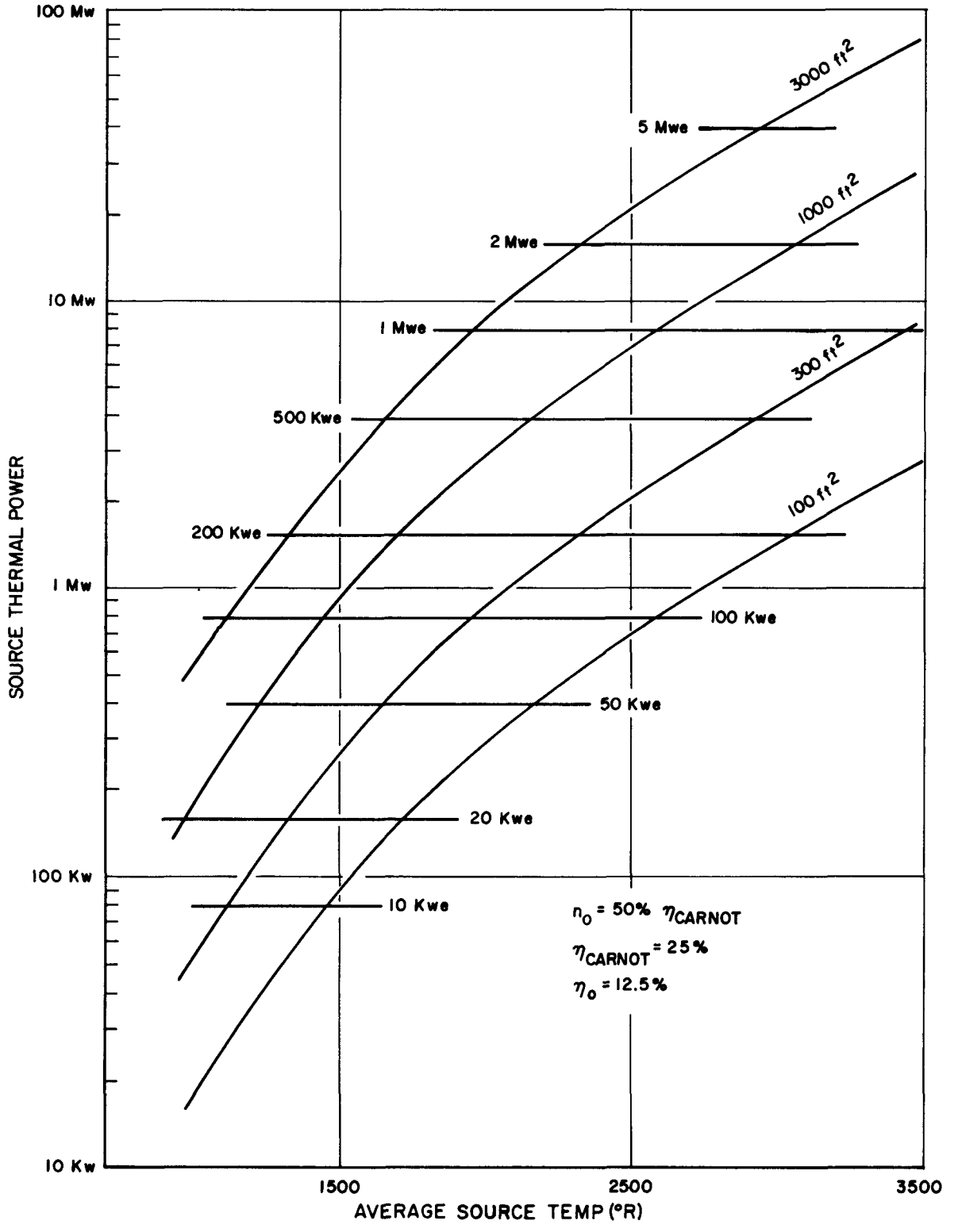

Figure 27. Reactor Thermal-power and Source-temperature Requirements as a Function of Electrical Power Output and Available Radiator Area for Rankine Turboelectric Systems

from the point of view of eliminating system components and weight. However, direct boiling in the reactor can introduce reactor control problems and a saturated cycle probably demands the complication of moisture separation in the turbine.

Since the reactor weight and the cycle selection are a function of temperature and since the radiator weight is a function of temperature and power, the choice of a reactor-cycle combination is a function of system power level. This point can be illustrated by means of an example which compares the weight of the reactor and radiator for a water reactor-water cycle, for a hydride reactor-mercury cycle, and for a carbide reactor-rubidium cycle (see Figure 28). The uranium metal fast reactor is too marginal in its temperature capability. The UC reactor can be ruled out for low powers because the extreme cost of the uranium inventory alone is prohibitive for low power systems which will be used in quantity in the future. The cost of fully enriched uranium is about $15,000 per kg. Thus, a UC reactor will cost a minimum of $1-1/2 million for the uranium inventory alone. This can be compared with a uranium cost of about $60,000 for the U-$ZrH_x$ thermal system. The example shown in Figure 28 assumed a reactor weight increased by 50% over that shown in Figure 20 in order to provide for coolant void and cylindrical geometry. Reactor weights are for this purpose considered independent of power, and radiator area is assumed at 1/2 to 1 lb/ft^2. Figure 28 indicates that:

1) The water system is too limited in its applicable range,

2) The hydride-mercury system has the lower weight below about 20 kwe, and

3) The carbide-rubidium system is better about 20 kwe.

However, this example does not consider the state-of-the-art difference between a 1500°R system and a 2400°R system (see Figures 18 and 19). In effect, lower radiator weight is achieved in the higher temperature system at the expense of not only increased reactor weight but, more importantly, increased materials problems such as strength, corrosion, sublimation, self-welding, etc. In general, increased temperature is rarely an easy solution to a problem. However, there is no denying that high-power systems will demand increased temperature and that the necessary technology will be developed. One cannot rule out a system because of temperature except on the basis of development time. As

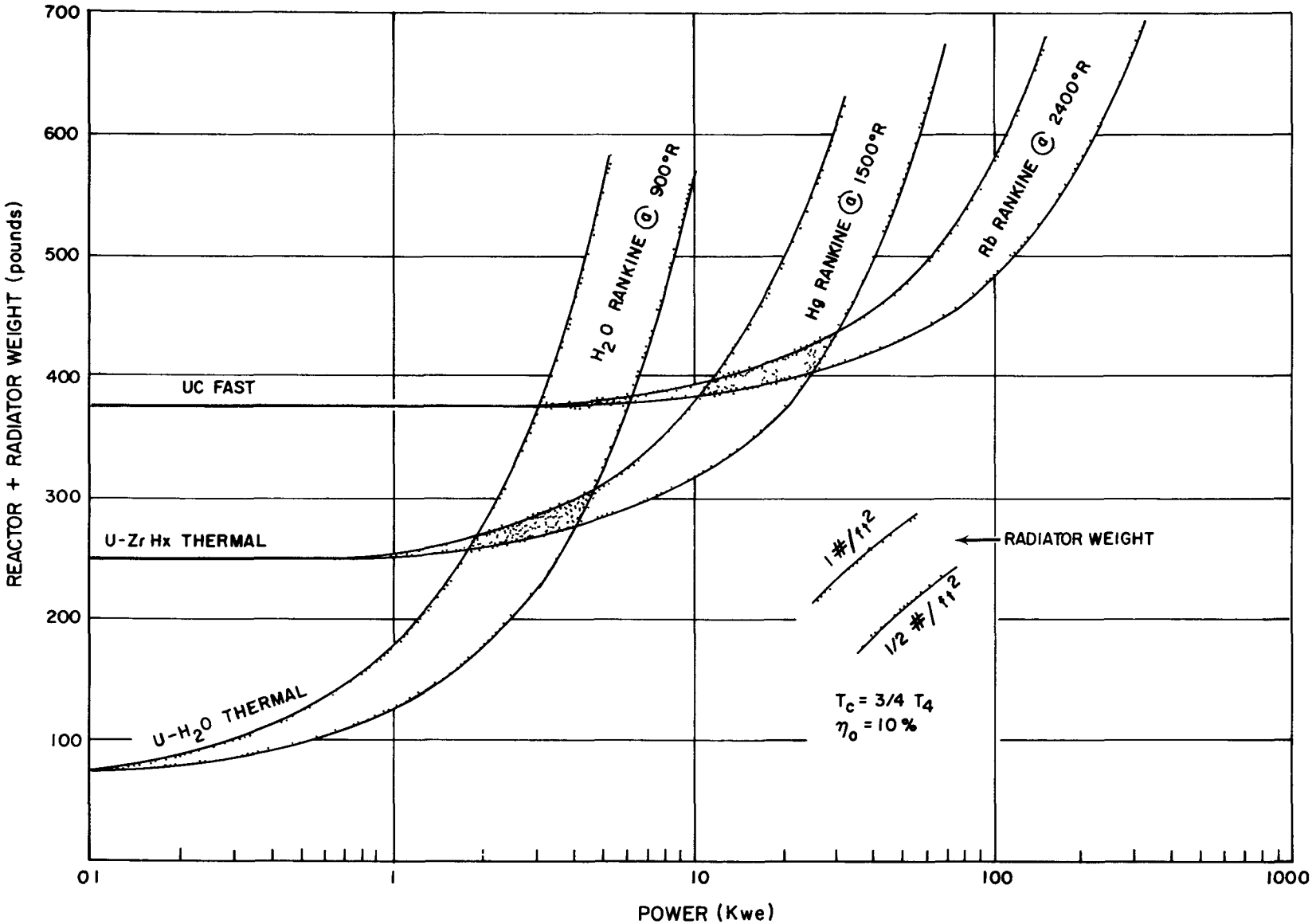

7-19-62 7561-0015

Figure 28. Reactor Plus Radiator Weight as a Function of Power for Various Reactor-cycle Combinations. (Reactor weights have been increased by 50% over Figure 20 to provide for coolant void and cylindrical geometry.)

temperatures increase, greatly increased development times must be allotted. Availability will then in effect move the crossover point to a higher temperature system to much higher power levels until the technology exists to make the simple weight consideration independent of state-of-the-art differences. Thus, for example, the hydride-mercury system may well be extended into the 100 kwe range because of technological availability even though it does not have the lightest weight potential at that power. It is, however, clear that the high-temperature systems must ultimately be developed in order to achieve the minimum specific weight (lb/kwe) required for future missions and especially for electric propulsion. As illustrated in Figure 25, at very high powers the reactor weight per kilowatt becomes small and the radiator weight per kilowatt becomes dominant. Radiator area and weight can only be reduced by increased source temperature. The significance of increased source temperatures for minimum radiator area is even further increased when the weight penalty for meteorite protection is considered.

The influence of operating temperature on the reactor fuel burnup limit should not be forgotten. In the example of Figure 23 the effect of temperature on the useful energy from a UO_2-stainless steel cermet core was illustrated. In the case of a space system the reward for higher temperature is lower radiator area and weight and the penalty is decreased core endurance or a larger core for a given endurance requirement. Thus, if temperature is increased radiator weight will decrease and the reactor weight will increase if the reactor size is determined by a burnup limit. The following example will illustrate this situation. Assume:

1) The reactor core material has the same burnup dependence on temperature as shown in Figure 22.
2) 1 at.% = 10 Mw-yr.
3) Reactor weight = 750 lb/ft^3 of core.
4) Power = 1 Mwe.
5) Efficiency = 10%.
6) System life = 1 yr.
7) Radiator weight = 1 lb/ft^2.

Figure 29 shows the reactor and the radiator weight for these assumptions as a function of operating source temperature. The results indicate a minimum reactor plus radiator weight at a source temperature of about 1700°F. This result should not be taken literally since the reference fuel material, UO_2 stainless steel cermet, is not a useful fuel for space systems. However, it could be considered representative of a very stable high-temperature fuel. A significant optimization must await complete burnup versus temperature data for applicable high temperature fuels like UC.

The SNAP 2 system at 3 kwe and the SNAP 8 system at 30 kwe use the mercury Rankine cycle power conversion coupled to a U-ZrH_x thermal reactor. These two systems are currently being developed under AEC and NASA sponsorship.

B. THERMOELECTRIC SYSTEMS

Direct conversion of heat to electricity by means of the Seebeck (thermoelectric) effect offers advantages of static operation and high reliability potential. However, the temperature limits and the conversion efficiency of current "state-of-the-art" converter materials limit the usefulness of thermoelectric conversion systems to relatively low power levels. The only materials that can be currently considered for space are PbTe, Pb-Sn-Te, and the Ge-Si alloys. The basic PbTe material has a theoretical conversion efficiency of about 15% of Carnot and is limited to a peak hot-junction temperature of about 800°F by sublimation. Through converter design the upper temperature limit can be extended by use of an encapsulant to suppress sublimation. The Ge-Si alloys have a lower conversion efficiency, about 11% of Carnot, but are not as limited in operating temperature. However, other practical engineering considerations such as thermal impedances and electrical contact resistance limit the net efficiency of practical devices to about 10% of Carnot. In a reactor-powered space system, efficiency and thus Z is not of prime importance.

$$Z = \frac{S^2}{\rho K} \ (^\circ C^{-1})$$

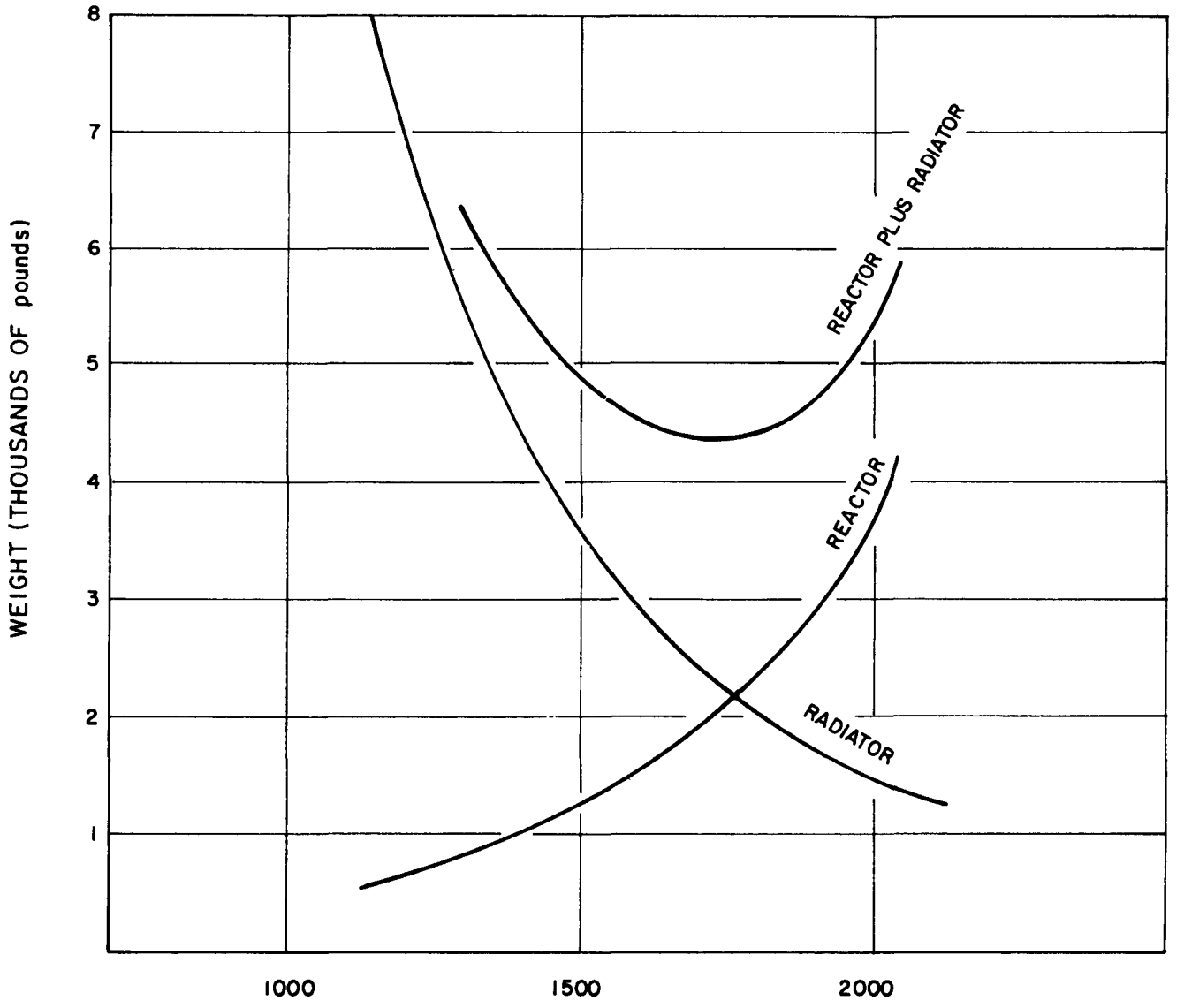

7-24-62 7561-0037

Figure 29. Trade-off Between Reactor Weight and Radiator Weight as a Function of Operating Temperature. (This illustration applies to a reactor which has the burnup limit of Figure 22.)

where

S = Seebeck coefficient (volts/°C)

ρ = electrical resistivity (Ω-cm)

K = thermal conductivity (watts/cm-°C)

The theoretical efficiency of a thermoelectric device is about

$$\eta = \frac{1}{4} Z \Delta T \quad ,$$

and the power output of a space system

$$P_o = \eta Q_R = \left(\frac{1}{4} Z \Delta T\right)\left(\sigma \epsilon A T_c^4\right) \quad ,$$

since minimum radiator area occurs at $T_c / T_H = 4/5$ for a low efficiency system

$$P_o = \left(\frac{1}{4} Z \frac{T_H}{5}\right)\left[\sigma \epsilon A \left(\frac{4}{5} T_H\right)^4\right] \quad ,$$

$$P_o = \left(\frac{1}{20}\right)\left(\frac{4}{5}\right)^4 \sigma \epsilon A Z T_H^5 \quad ,$$

or

$$P_o \sim A Z T_H^5 \quad ,$$

where

P_o = electrical power output

ΔT = temperature difference ($T_H - T_c$)

σ = Stefan-Boltzman constant

A = radiator area

T_H = source temperature

ϵ = emissivity

Q_R = heat rejected

It is therefore readily seen that the power of a thermoelectric space system is an extreme function of the allowable source temperature and that small differences in Z can be easily compensated by source temperature if the thermoelectric material is not temperature limiting. There is, however, a serious lack of conversion materials or devices experience of significance above 1000°F. Because of the upper limit on current thermoelectric material operating temperature, the U-ZrH_x SNAP reactor is more than adequate as a heat source for current thermoelectric-conversion systems. In fact, there is room for a 200 to 300°F improvement in the materials capability.

The principal weight of a thermoelectric system is the reactor weight. In general, the converter weight is small. In theory the converter weight could be made quite small: however, in practice the device inefficiency resulting from thermal and electrical losses increase with decreasing converter weight. The reactor weight is fixed by criticality limits of the reactor concept necessary to provide the source temperature. The radiator area per unit electrical output is large because of the hot temperature limit and the low conversion efficiency. The optimum Carnot for a low-efficiency system is 20%. Therefore, the thermoelectric systems will have a net efficiency of about 2%. Figure 30 shows the radiator area per kilowatt for thermoelectric systems as a function of hot-junction temperature and conversion efficiency.

For low-power systems (less than a few kilowatts) the simplicity and reliability advantages of a thermoelectric system can outweight the disadvantage of large radiator area. However, at large powers radiator weight and size or awkwardness limit the attractiveness of these systems until such time as better materials have been developed and reduced to practice. The reactor heat-source temperature and power requirements of thermoelectric systems are shown in Figure 31 as a function of electrical power out and available radiator area.

The SNAP 10A system at 500 watts uses Ge-Si conversion materials and the U-ZrH_x SNAP reactor. It is under development by the AEC.

C. THERMIONIC SYSTEMS

The thermionic converter is particularly suited for consideration for use in a nuclear space power system. It has a potentially high thermal conversion efficiency, it can operate at a very high heat sink temperature, is capable of high power density, and is a static operating device.

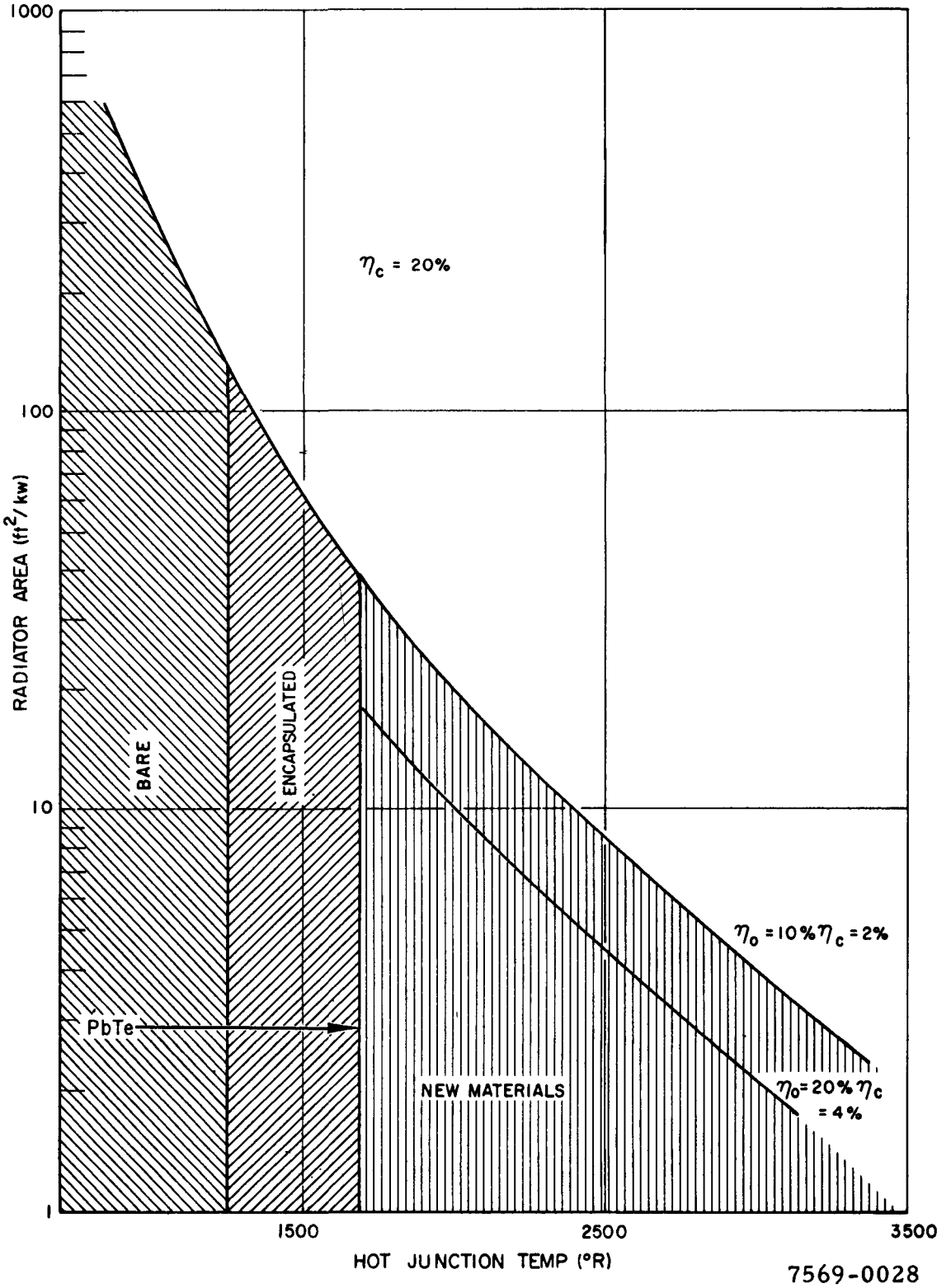

Figure 30. Radiator Area per Kilowatt as a Function of Hot Junction Temperature for Currently Available PbTe and Future Materials

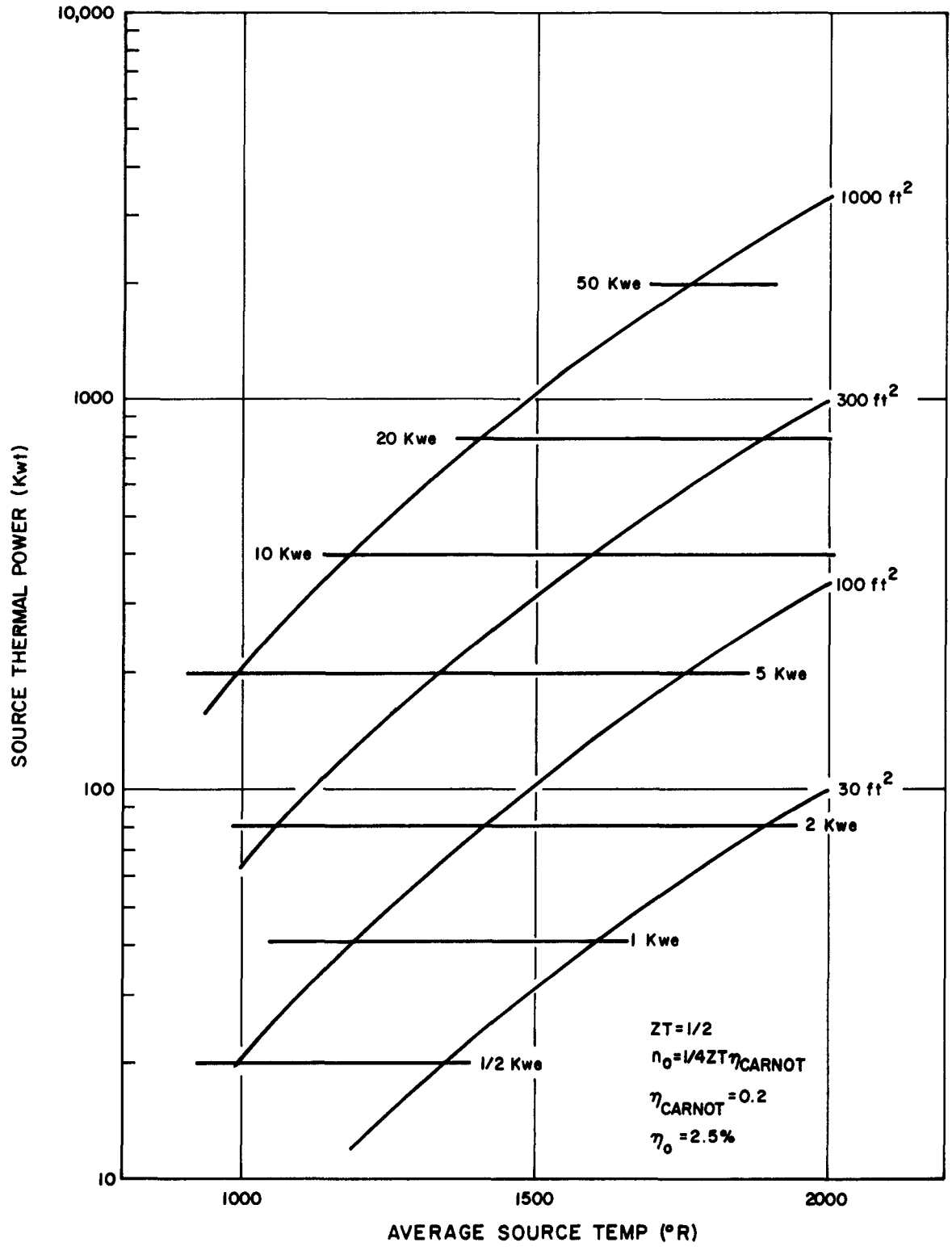

7-19-62 7561-0017

Figure 31. Reactor Thermal Power and Source Temperature Requirements for Thermoelectric Systems as a Function of Electrical Power and Radiator Area.

The thermionic converter may be pictured as an "electron-boiler." It consists of an emitter, a collector, electrical leads, and suitable structure. The emitter is heated to a temperature at which it can emit a large current of electrons. These electrons pass across an interelectrode space and are collected on a second electrode, the collector. The electrons leaving the collector deliver power to an external load as they return through leads to the emitter.

Two types of thermionic converters are possible. Each is characterized by its means of neutralizing the interelectrode space charge. In the vacuum diode the electrode spacing is made of the order of a few thousandths of an inch or less in order to limit the negative charge buildup between the electrodes. In the cesium diode, space charge neutralization is accomplished by injecting positive cesium ions into the space between the electrodes, and the spacing requirements become far less stringent. The required temperatures and actual measured efficiencies for these diodes are listed in Table XIII.

TABLE XIII
THERMIONIC CONVERTER OPERATING CONDITIONS

Type	Typical Emitter Temperature	Typical Collector Temperature	Actual Observed Efficiencies
Vacuum diode	1600 to 1900°F	700 to 1100°F	2 to 6%
Cesium diode	2600 to 3500°F	1100 to 1400°F	12 to 14%

For reactor application the cesium diode appears most practical for the following reasons: (1) the efficiencies of the cesium diode are considerably greater than those for the vacuum diode; (2) very close electrode spacings are not require; and (3) choice of materials is larger, since cesium vapor helps establish electrode surface characteristics.

Because of the extremely high cathode (emitter) temperature the system requires the cathode to be loaded with fissionable fuel to attain the necessary temperature. Inspection of Figure 20 reveals that the most applicable reactor concept for thermionic systems is the UC fast reactor. Only UC and UO_2 have the necessary temperature capability. UC has the advantage of higher uranium density and thus smaller reactor size and weight. Low power systems could consist of a solid reactor core with heat conducted to converters on the outer

surface. For high power levels, however, large emission surface areas are required so that reactors of this type would be comprised of an array of converter-fuel-elements. Hence, the reactor and power conversion system become one and the same.

One method of employing the thermionic converter is to integrate it in a nuclear reactor core in such a manner that the fuel material also serves as the cathode of the converter. A typical thermionic conversion fuel element is illustrated in Figure 32, where a number of thermionic converter cells are shown connected in series. Since each cell is capable of producing a potential of approximately 1 volt, many cells must be connected in series to produce useful high voltage. Each cell consists of a cathode, an anode, an interelectrode space containing cesium vapor, insulation to provide the proper electrical configuration, and an outer sleeve to isolate the entire element from its external surroundings and provide the structural integrity for the assembly.

The cathodes are solid cylinders of fuel material which are held in place by the insulation separators and the electrical leads in the manner of a filament in a light bulb. Nuclear heat supplies the thermal energy to "lift" free electrons at the cathode surface to an energy level at which they are emitted into the interelectrode space. This electron removal of heat from the cathode is accompanied by other cooling processes including radiation to the anode, and conduction of heat through the electrical leads connecting the anodes to the cathodes. These latter two processes are heat losses and must be accounted for in cell optimizations. It may be that the cathodes will have to be clad to prevent deleterious effects caused by the release of the fission products from the fuel.

The anode is a thin cylindrical shell of metallic conductor surrounding the cathode. The electrons which travel to the anode from the cathode are absorbed with the conversion of their kinetic energy into sensible heat. This heat must be removed from the anode to maintain the electrode temperature difference. For good heat transfer the anode must be in thermal contact with the outer metallic sleeve, which is cooled by a liquid metal. In order that the anode of the adjacent cells are not electrically shorted, a layer of electrical insulation must be interposed. The annular space between the electrodes contains cesium vapor which is ionized by the high-temperature environment and serves to neutralize the space charge which is produced by the high electron flux in the interelectrode space. The thermionic fuel elements are assembled into a close spaced hexagonal lattice to form a cylindrical reactor core.

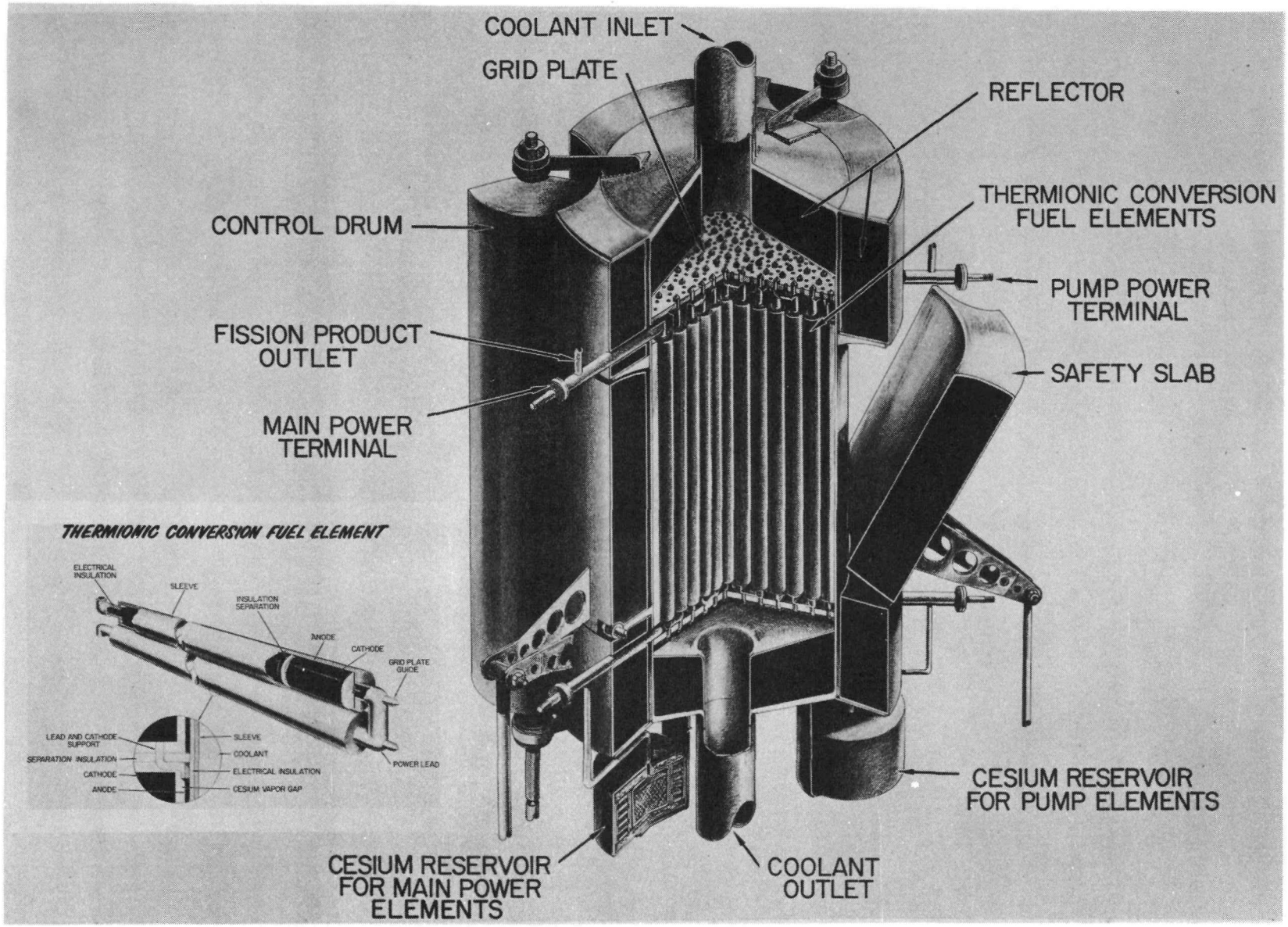

7590-A067A

Figure 32. Thermionic Fuel Element

The characteristics of a thermionic conversion system can be explored through an evaluation of the ideal converter, i.e., one that is emission-limited only. An ideal converter is limited by the surface emission process. Transport effects which inhibit the interelectrode flow of electrons are assumed not to be present. Thus, the performance of an ideal converter defines an upper limit on performance for all types of thermionic converters. The maximum obtainable efficiency is uniquely determined in the ideal converter by T_e, the emitter temperature; ϕ, the collector work function; ϵ, the emissivity; and K_G, the gas conductivity. If one inserts reasonable values for the independent variables, the ideal or ultimate converter performance can be established. Such results with ϕ = 1.7 ev and K_G = 0 are shown in Figure 33. The significant feature is that both optimum efficiency and power density increase with increasing temperature. The output power of a combined reactor-thermionic converter will then be a function of the reactor fuel element (cathode) surface area and the operating temperature. The required reactor volume as a function of cathode temperature is shown in Figure 34 for 1 Mwe and 10 Mwe. The values for ϵ = 0.1 in Figure 33 were used and the cathode surface area was taken as 3/4 of the maximum for cylindrical fuel-converter cells of 1/4 in. and 1/2 in. diameter. It can be seen from Figure 33 that both reactor volume and radiator area are a strong function of cathode or fuel temperature. It should be noted that this survey assumes constant conditions throughout and makes no allowances for reactor power or temperature distributions. The indicated minimum bare core critical volume assumes a UC fuel element that occupies 2/3 of the core volume. The core size could be reduced by the addition of a reflector. It is not clear that the requisite increase in operating temperature is desirable. However, when reactor power distribution is considered in a real case, it is clear that a reflector is mandatory for the purpose of power flattening. From a materials point of view, the minimum operating temperature seems desirable. However, the decreased power density at lower temperatures causes a significant penalty in core volume and weight. From the point of view of minimum system weight, it seems desirable to increase temperature until the core is no longer power-density limited but becomes reactor-criticality-limited. Depending on the burn-up capability of the fuel, it may be necessary to increase core volume for endurance. The very configuration of a thermionic reactor system makes it extremely sensitive to fuel swelling due to fission products. The feasibility of a thermionic reactor system remains to be demonstrated. It is obvious that the potential

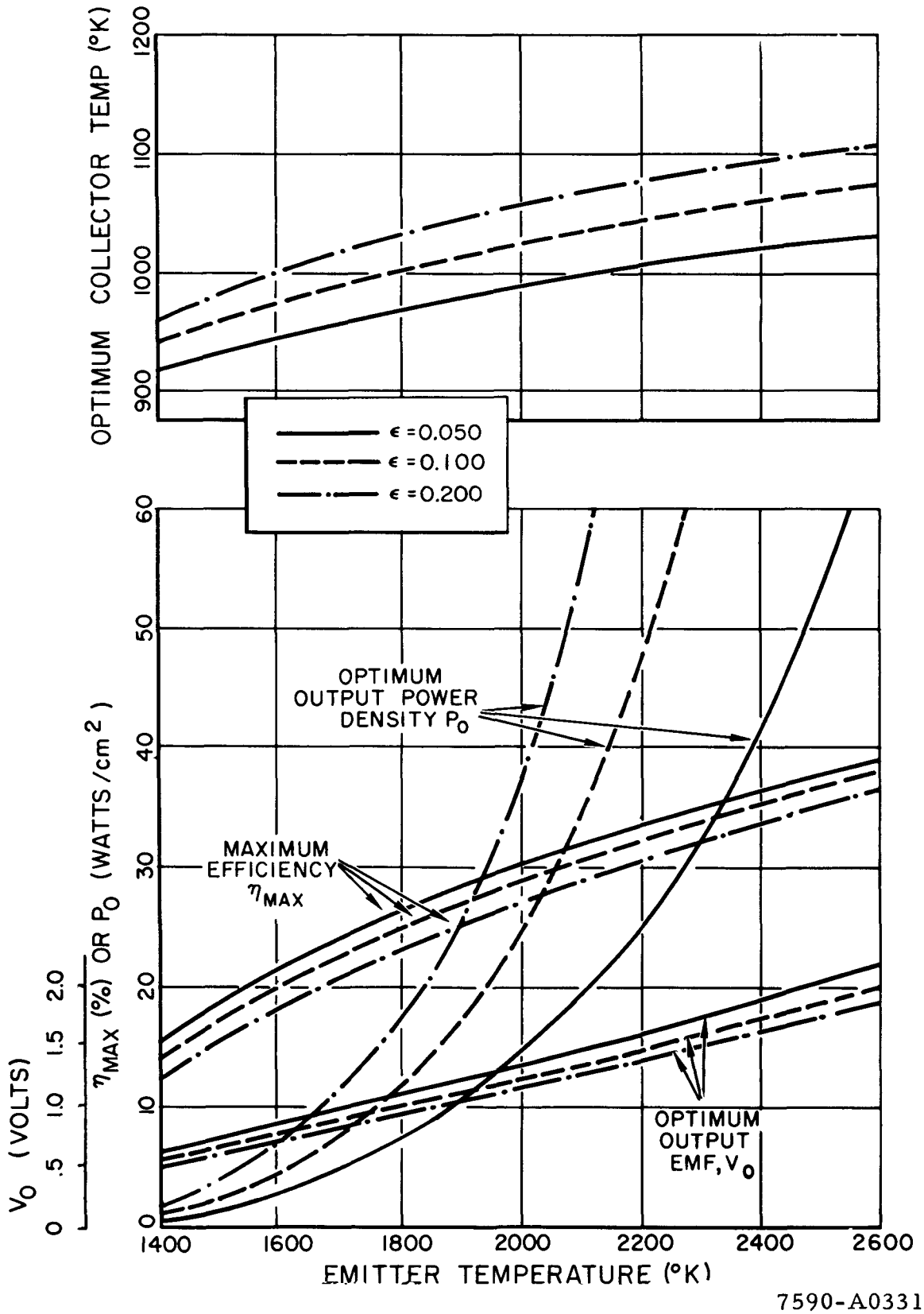

Figure 33. Optimum Parameters for the Ideal Thermionic Converter (φ_{coll} = 1.7 ev, K_{gas} = 0)

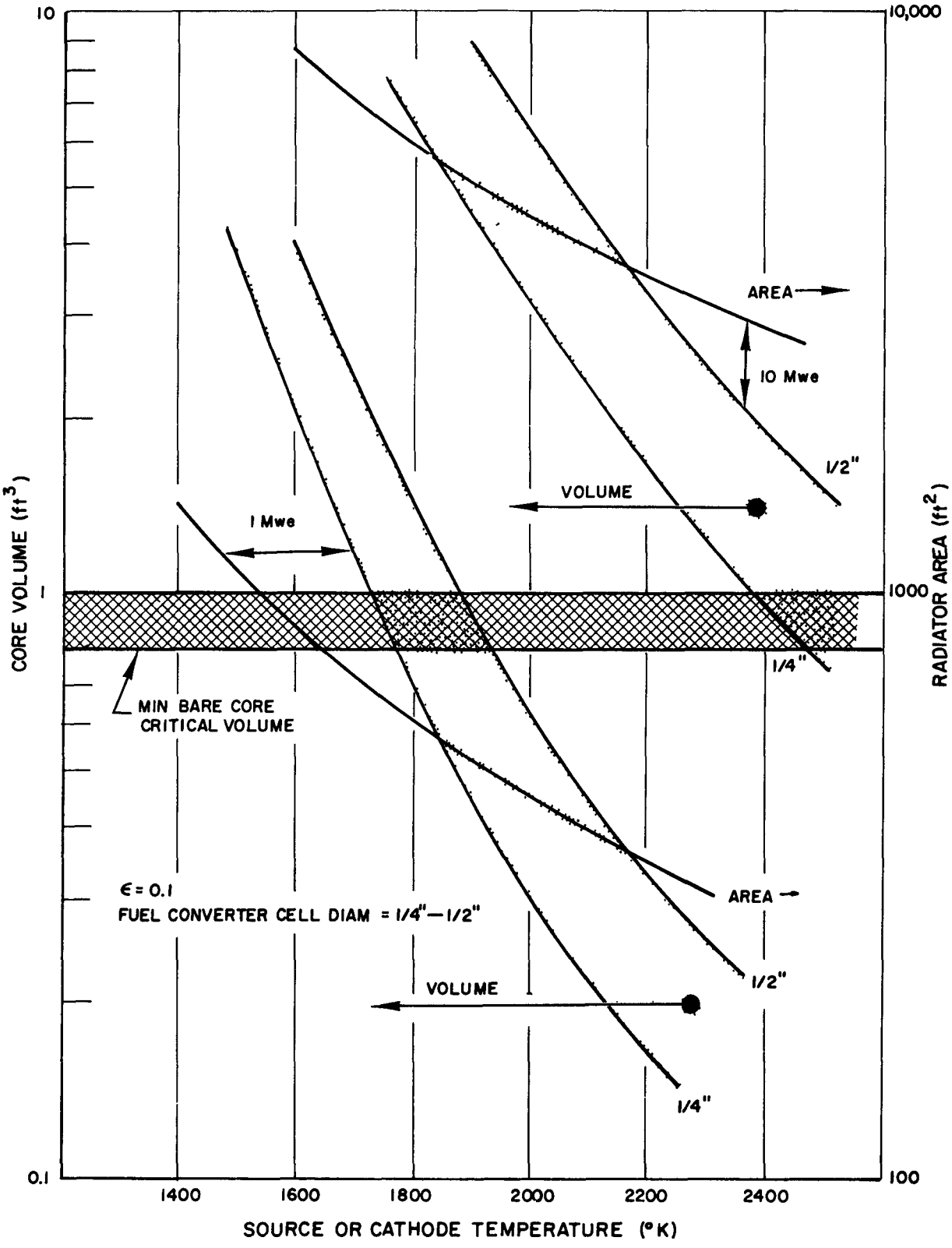

7-24-62 7561-0034

Figure 34. Core Volume and Radiator Area as a Function of Core Temperature for a Thermionic Reactor

limit to feasibility is fuel swelling. The general hope is that the extreme fuel temperatures will contribute to feasibility by allowing fission products to rapidly diffuse out of the fuel material and thus minimize swelling. In the above analysis, the parameters were optimized for maximum efficiency. In general this is not the correct approach for a minimum-weight high-power system. However, if the thermionic reactor concept indeed turns out to be reactor-energy content-limited, the maximum efficiency approach is probably correct. The increased radiator area and weight do not in any way constitute the same kind of feasibility limit. Figure 32 presents a conceptual design of a 300-kwe reactor assembly which consists of the core composed of converter fuel elements located by an upper and lower grid plate, a reflector with movable sections for nuclear control, electrical terminals for power output, and cesium circulation system.

D. SYSTEM COMPARISON

A generalized picture of the performance and applicable power range of the thermoelectric, Rankine turboelectric, and thermionic nuclear space power systems is shown in Figure 35. The most dominant variable in these space power systems is temperature. Each major performance improvement can be characterized by an increase in temperature. Namely,

Thermoelectric	800 - 1200°F
Hg Rankine	1200 - 1400°F
K or Rb Rankine	1800 - 2300°F
Thermionic	3000 - 3500°F

Temperature is not only the key to increased performance, but will in the end, pace the technological advances necessary to achieve these projected goals.

At low power levels (up to a few kilowatts) the reactor and shield are the dominant weight contributors. The immediate relatively low space power requirements will be filled with the most immediate technology. In effect, performance will be sacrificed for low temperature and simple systems. The thermoelectric system fits this description. The reliability advantage of its static operation is very desirable for the low power requirements of early space utilization systems. The lack of orientation requirement, freedom from battery storage, and high resistance to the space environment will make these systems very competitive in the apparent range of solar cells.

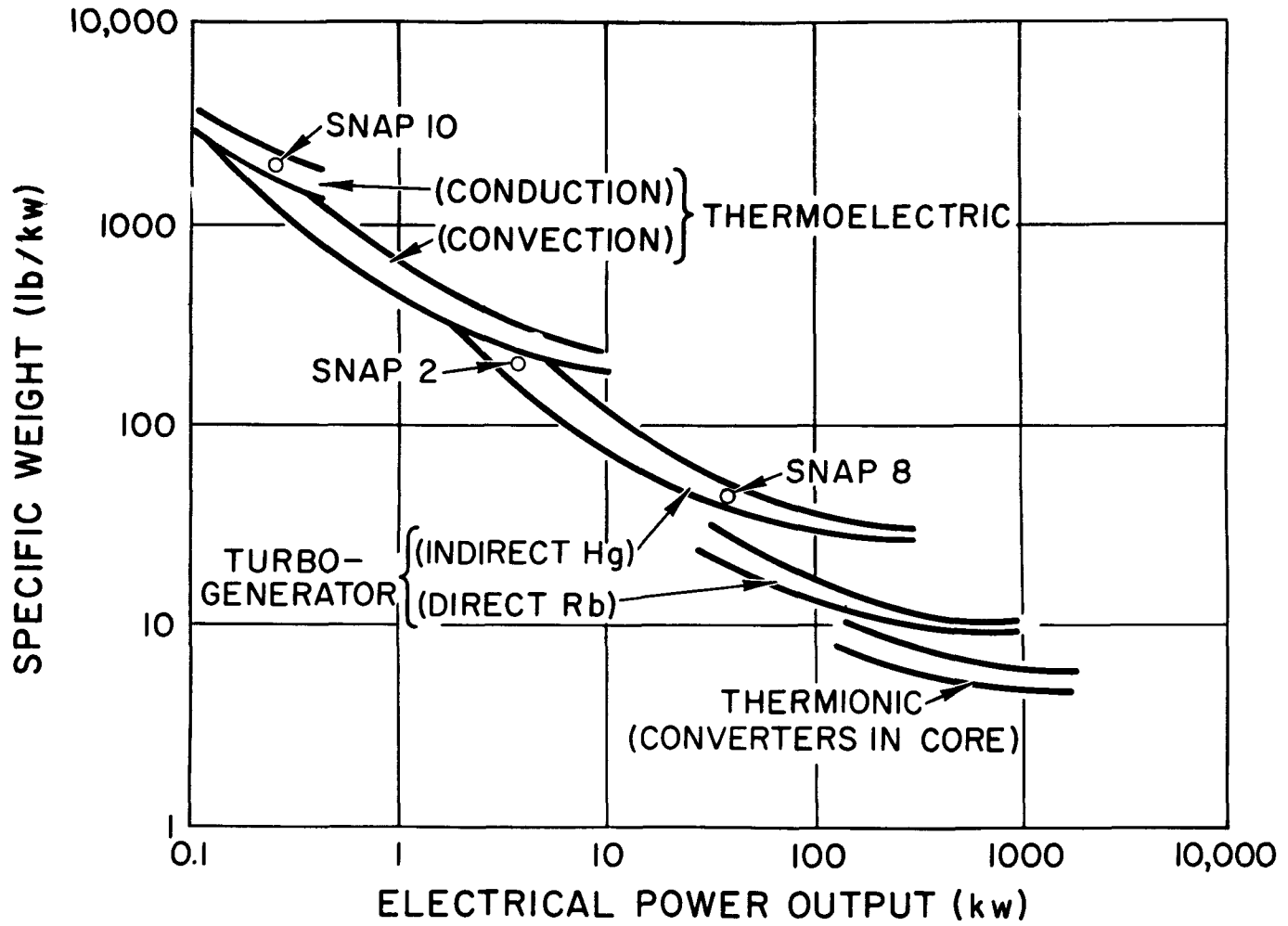

Figure 35. Specific Weight vs Power Output for Nuclear Power Systems

At intermediate power levels (a few to hundreds of kilowatts), increased performance is mandatory. The weight and radiator awkwardness of low-temperature and low-efficiency systems is intolerable. The increased performance brings with it the materials problems of higher temperature, dynamic control, the mechanical perturbations of rotating machinery, and more severe problems in orbital startup and zero-gravity operation. For this power range the ultimate Rankine system will not be selected because of the time scale associated with the required technology. The hydride reactor-mercury Rankine system requires the least extrapolation of the state-of-the-art. It is most probable that this combination will be used at power levels beyond its region of optimum performance because of its availability.

At high powers (hundreds to thousands of kilowatts) the system selection may be more application-dependent. In the case of manned orbital stations or lunar bases the dominant consideration will be reliability. Very probably the increased confidence in and inherent reliability of lower temperature systems will outweigh the performance advantages of a higher temperature and newer system. In the case of electric propulsion, both maximum performance and reliability will be necessary for this form of propulsion to be competitive. The required performance will dictate the highest possible temperature system. The thermionic reactor concept seems very attractive for this application; however, the required temperatures will delay its availability. For these high-power systems the reactors will be fast and probably fueled by UC or a mixture thereof. The availability of extremely high temperature reactor heat sources is totally dependent on currently undemonstrated fuel burnup capability.

A summary of the immediate and the future space nuclear power systems is shown in Figure 36.

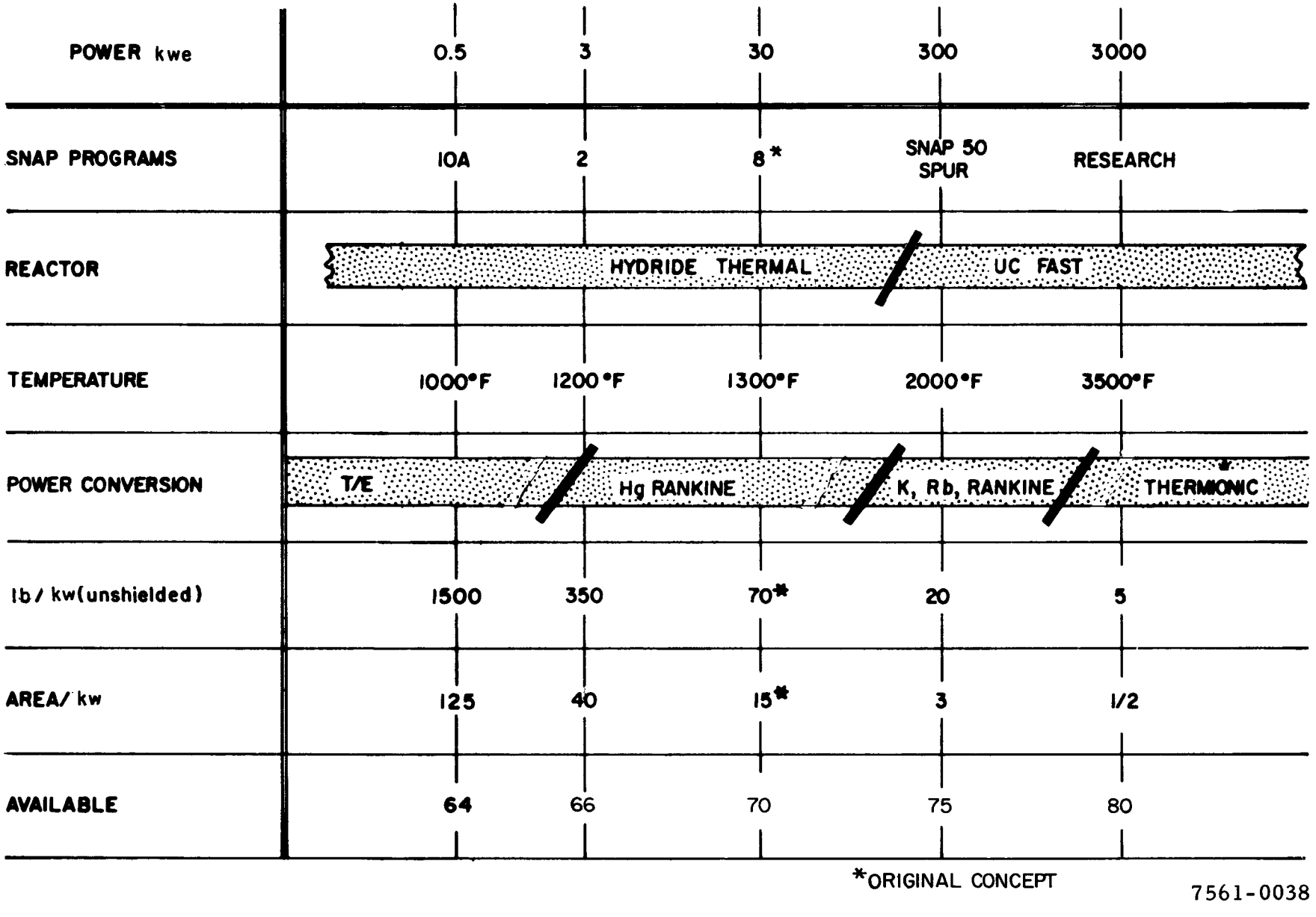

Figure 36. Space Nuclear Power Summary

PART III
SNAP SYSTEMS

1. SNAP HYDRIDE REACTOR

SNAP 2, 8, and 10A all use the same reactor concept as a heat source, see Table XIV. The reactor concept employs a homogeneous fuel moderator of zirconium hydride containing U^{235}. For minimum weight, the reactor is reflected by beryllium and controlled by variation of the effective reflector thickness by means of angular rotation of eight semicylindrical beryllium drums. The core is composed of a bundle of cylindrical fuel-moderator elements, see Figure 37. Each fuel element is clad in a thin wall steel tube for liquid metal exclusion. The fuel elements are contained in a steel core vessel, with the beryllium radial reflector outside the vessel. The reflector is completely separable from the core for safe reactor shutdown during handling (Figures 38 and 39). The thermal output is removed by the flow of NaK-78 axially through the core within the interstitial passages between the fuel elements.

The first SNAP reactor critical assembly was performed in October 1957. The SNAP Experimental Reactor (SER), Figure 40, was designed and constructed during 1959. It went critical in September 1959 and operated until the completion of the test program in December 1960. During this operating period the SER logged a total of 222,000 kwt-hr. The reactor demonstrated the necessary SNAP 2 performance requirements of 50 kwt with a core inlet of 1000°F and an outlet of 1200°F. The maximum fuel temperature in the SER was about 1300°F. Out of the above total, the SER operated continuously with no interruptions for 1000 hr at SNAP 2 temperature and power conditions.

A second generation reactor, the SNAP Development Reactor (SDR) went critical in April 1961 and was under test continuously until December 1962. During this period the reactor produced a total of 270,000 kwt-hr. Both reactor tests operated for approximately the energy requirement of SNAP 10A for one year. There has never been a reactor failure in the program.

Even though the reactor has been successfully operated at its design conditions of 50 kwt and 1200°F outlet temperature, the reactor has been derated for SNAP 10A in order to utilize passive control and to ease power

TABLE XIV

SNAP REACTOR PARAMETERS

Parameter	SNAP 10A	SNAP 2	SNAP 8
Output, kwe	0.5	3	35
Thermal, kw	30	50	600
Efficiency, %	1.6	6	8
Converter	thermoelectric	Hg Rankine	Hg Rankine
Reactor coolant	NaK-78	NaK-78	NaK-78
Temp out, °F	1000	1200	1300
Temp in, °F	900	1000	1100
Reactor size, in.	16 x 14 diameter	16 x 14 diameter	19 x 15 diameter
Core volume, ft^3	0.3	0.3	0.6
Power density, Mwt/ft^3	0.099	0.165	1.0
Reactor wt, lb	250	250	500
Fuel-moderator	Zr-Hydride	Zr-Hydride	Zr-Hydride
Rods, number	37	37	211
U^{235}, kg	4.3	4.3	7.0
N_H, Hatoms/cm^3	6.5×10^{22}	6.5×10^{22}	6.0×10^{22}
Max. temp, °F	1050	1300	1450
OD, in.	1.25	1.25	0.56
Heat flux, $Btu/hr\text{-}ft^2$	10,200	17,000	40,000
Neutron flux, $n/cm^2\text{-}sec$	1.8×10^{11}	3.1×10^{11}	2×10^{12}
Radial reflector, in.	2.3 Be	2.3 Be	3 Be
Be control drums	4	4	6

conversion development. The SNAP 10A reactor weighs about 250 lb and is shown in Figure 41. This reactor has undergone component level qualification in a thermal and vacuum environment (Figure 42) and under simulated launch mechanical conditions (Figure 43). For SNAP 10A, the reactor produces about 30 kwt at an outlet temperature of 990°F and an inlet temperature of 882°F. For SNAP 2, the reactor produces about 50 kwt at 1200°F outlet temperature. The SNAP 2 reactor is shown in Figure 44 and differs only in minor mechanical details from the SNAP 10A reactor.

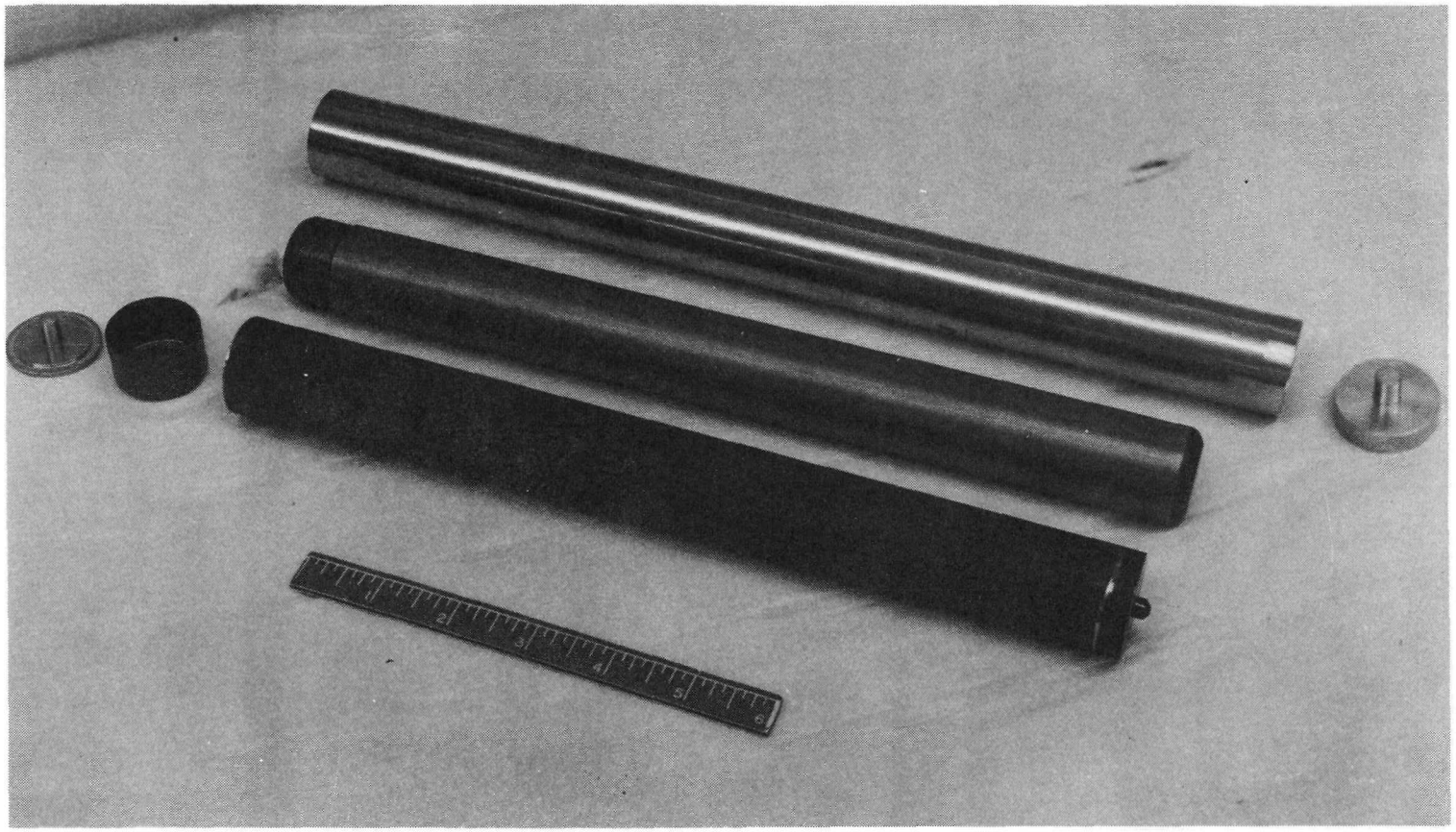

8-27-62

7550-51569A

Figure 37. SNAP 2 Fuel Element

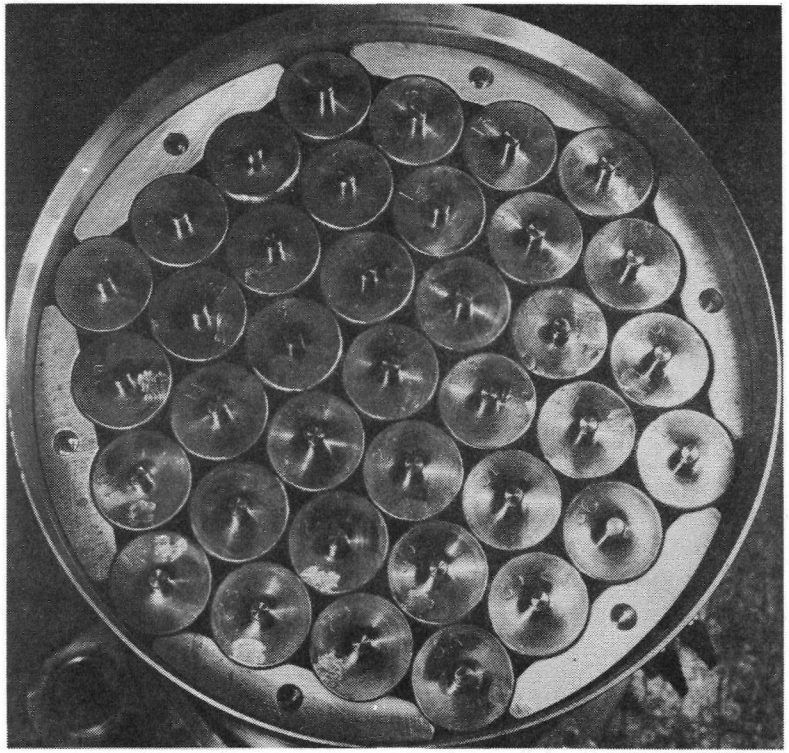

7-5-63

a. Internal View of the SNAP 10A/2 Core

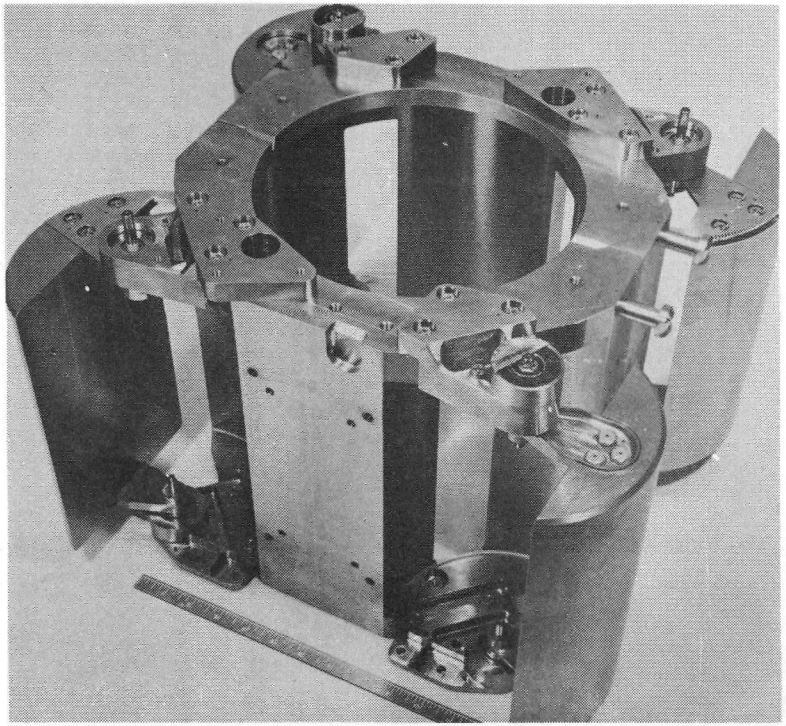

7561-0516

b. SNAP 10A/2 Reactor Beryllium Control Subassembly

Figure 38. SNAP Reactor

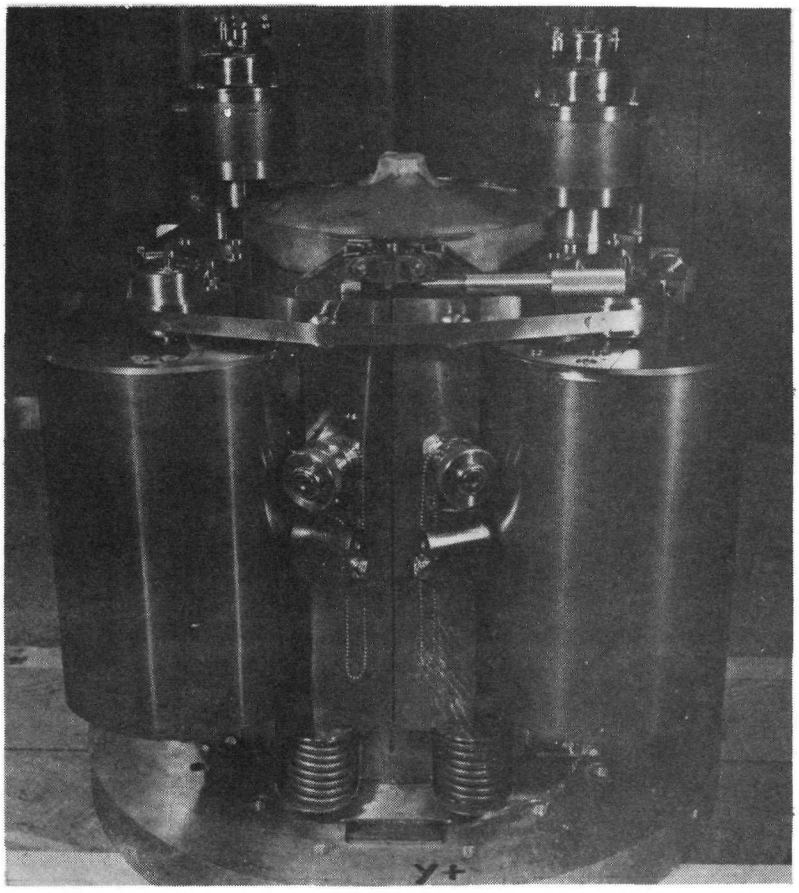

Side View

7-5-63 7561-0517

Top View

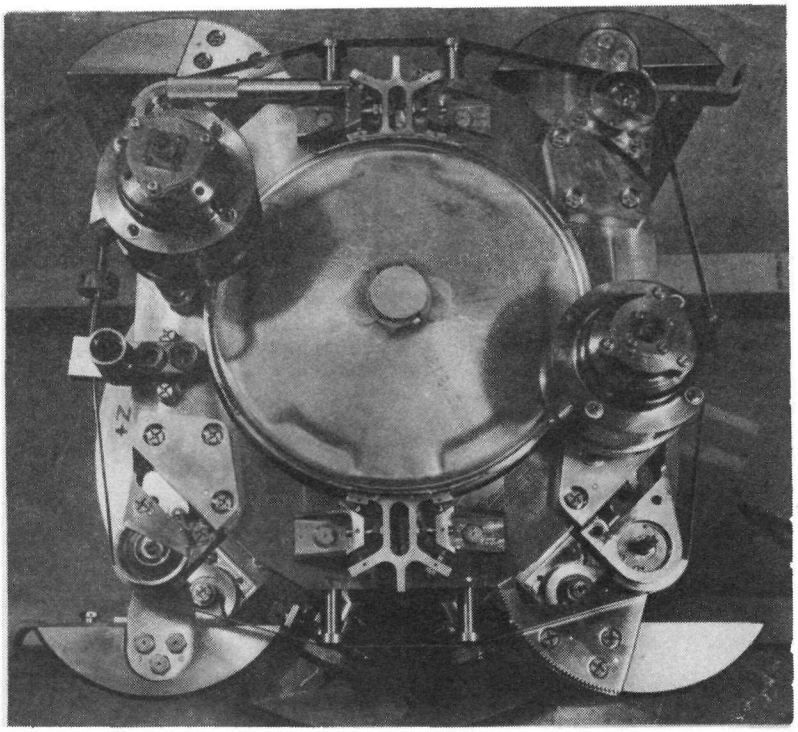

7-5-63 7561-0517

Figure 39. SNAP 10A/2 Reactor

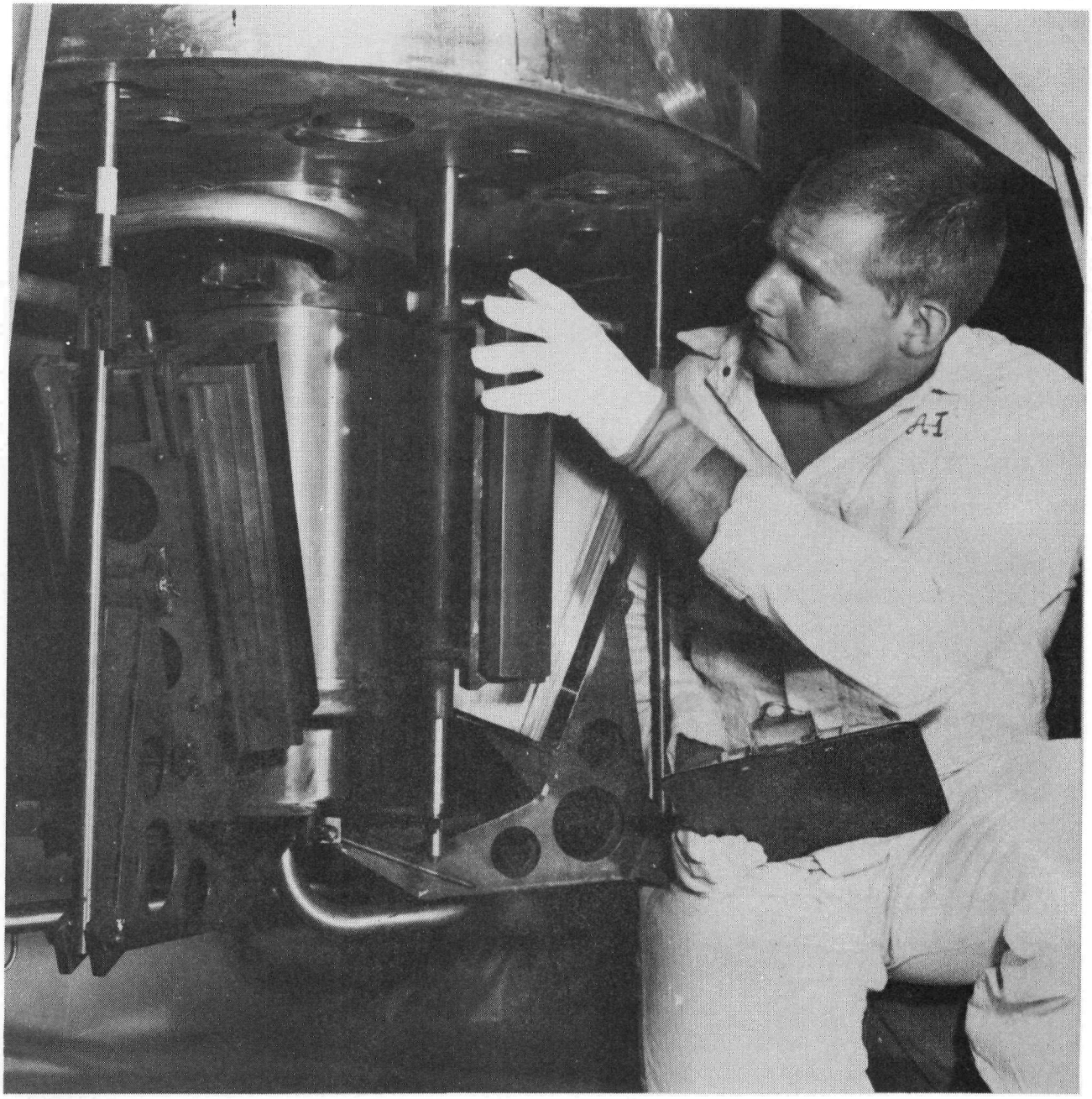

8-8-60 7550-2047

Figure 40. SNAP 10A/2 Experimental Reactor

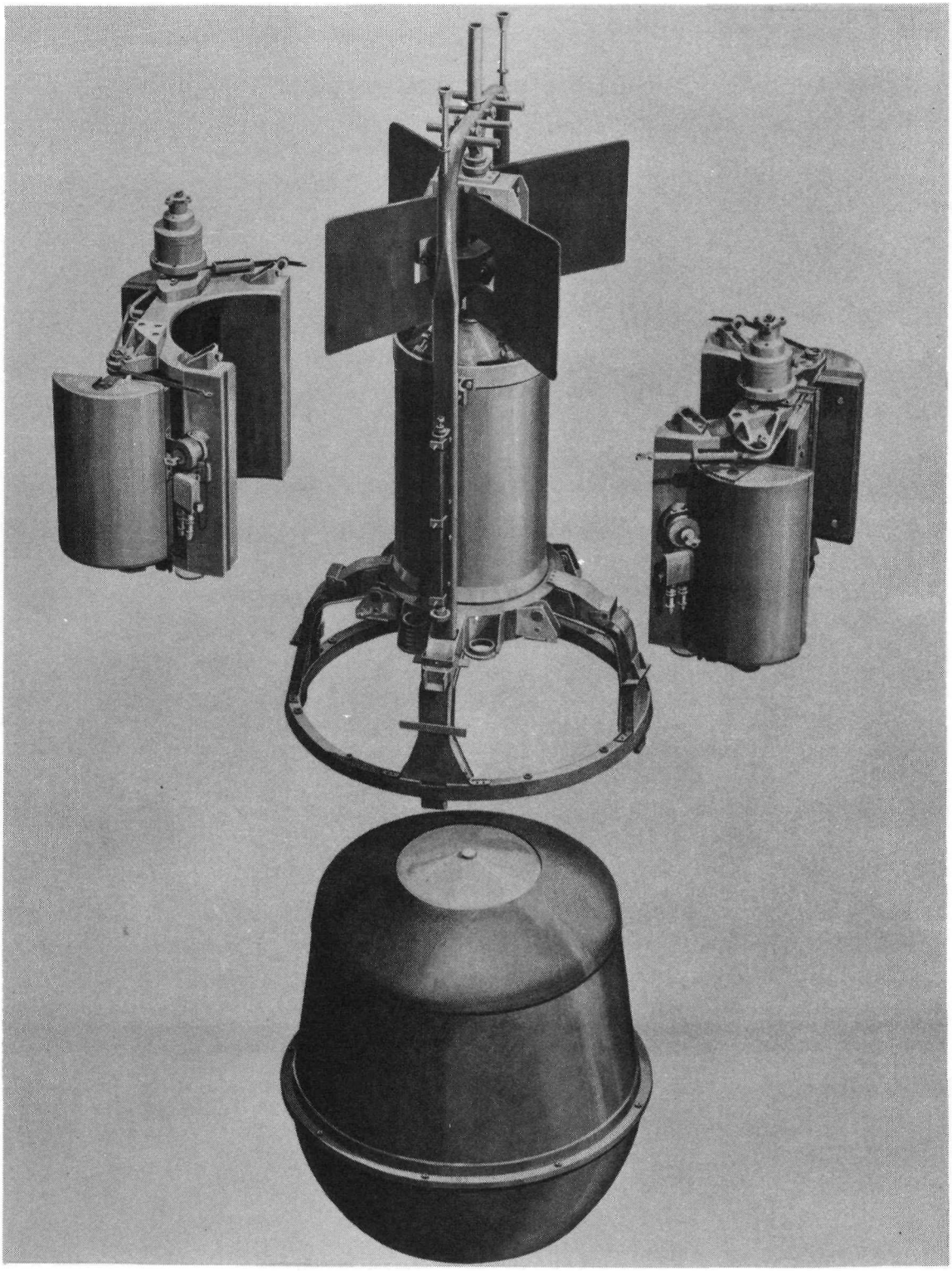

8-2-63 7623-0019

Figure 41. Exploded View of SNAP 10A/2 Reactor and Shield

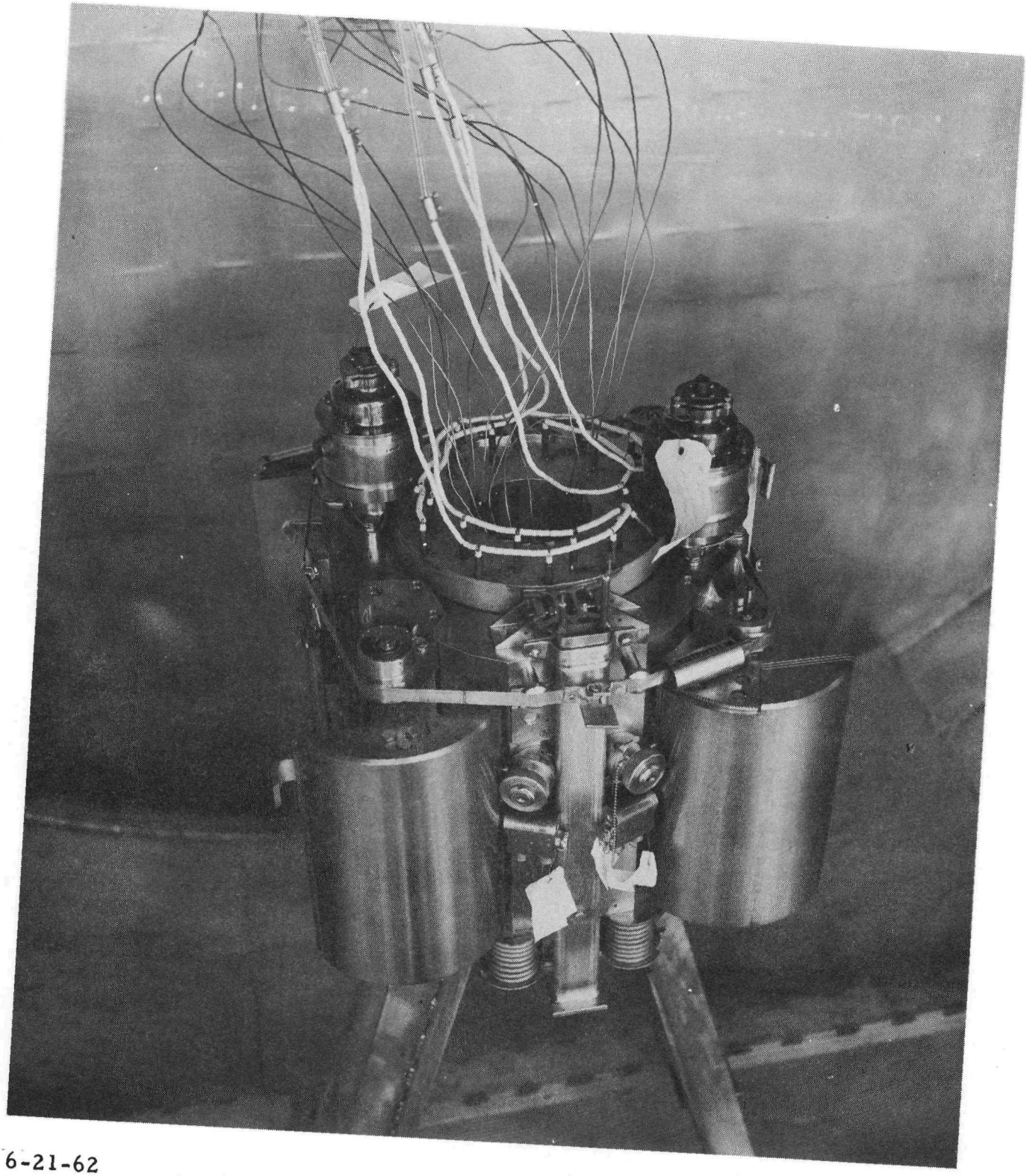

6-21-62

7580-5275

Figure 42. Thermal and Vacuum Environment Qualification Test of the SNAP 10A Reactor

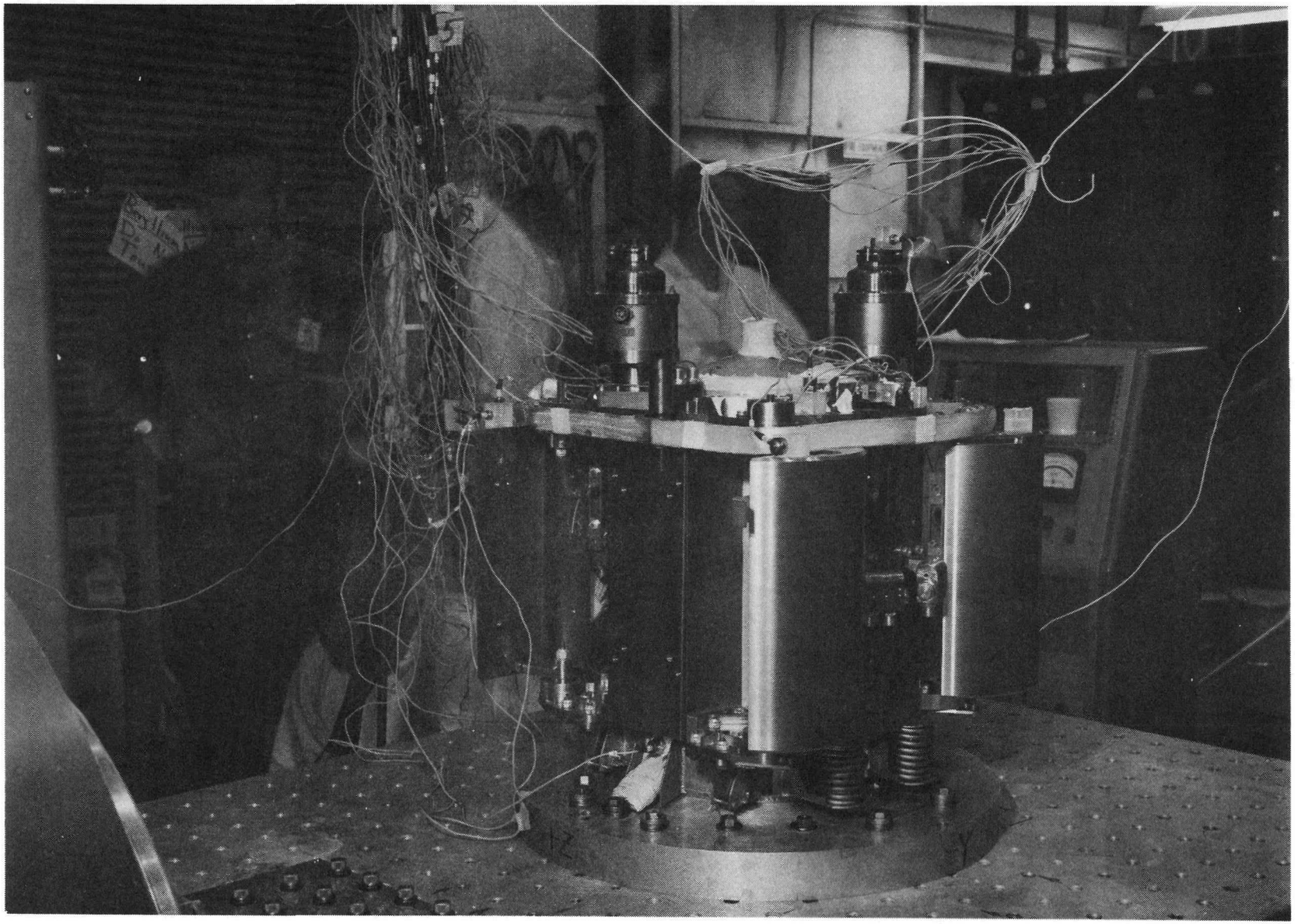

5-15-62

7580-5259C

Figure 43. Launch Shock and Vibration Environment Qualification of the SNAP 10A Reactor

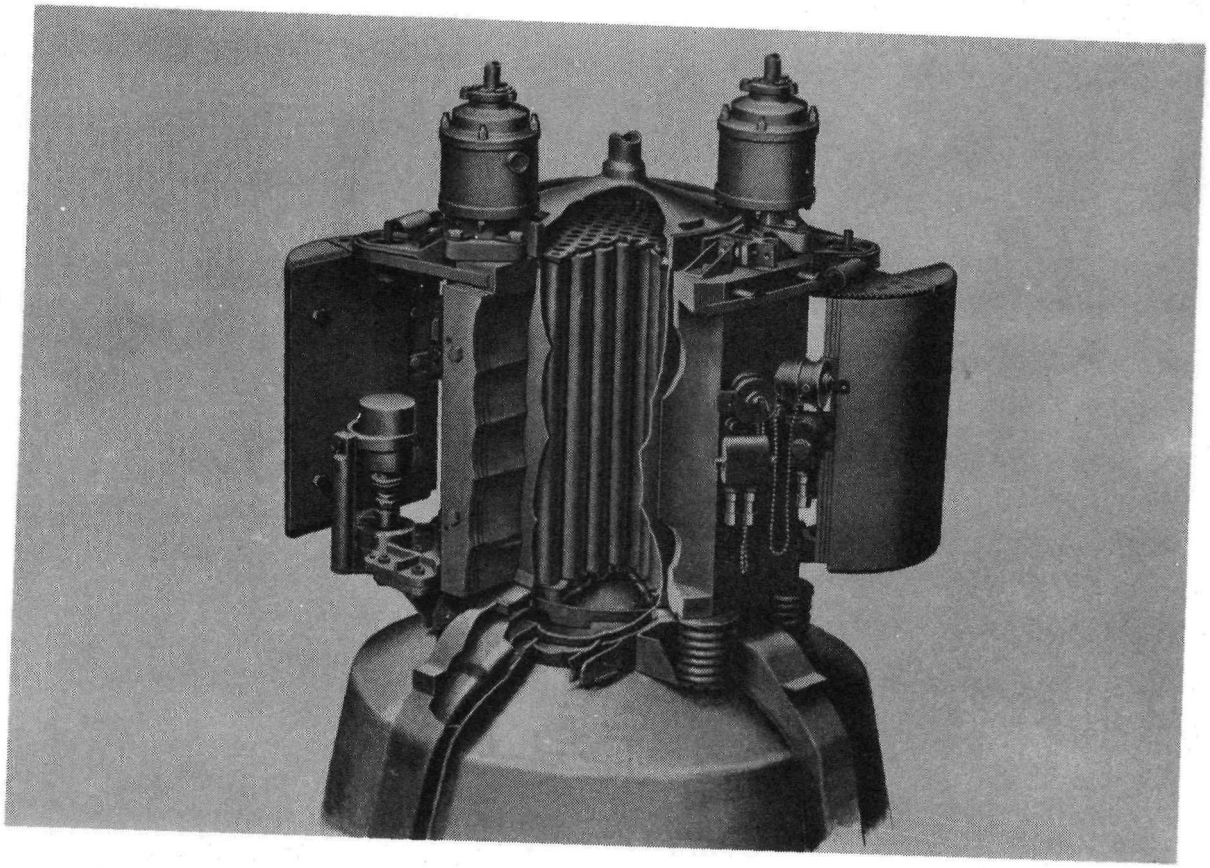

5-1-62

7550-20265

Figure 44. SNAP 2 Reactor

The SNAP 8 reactor, see Figure 45, which produces 600 kwt at 1300°F, is a sealed-up version of the SNAP 10A/2 reactor. The core, see Figure 46, has been enlarged and the fuel elements are smaller in diameter. The first power demonstration test of the SNAP 8 core design has been initiated. A view of the ground test configuration during final installation is shown in Figure 47.

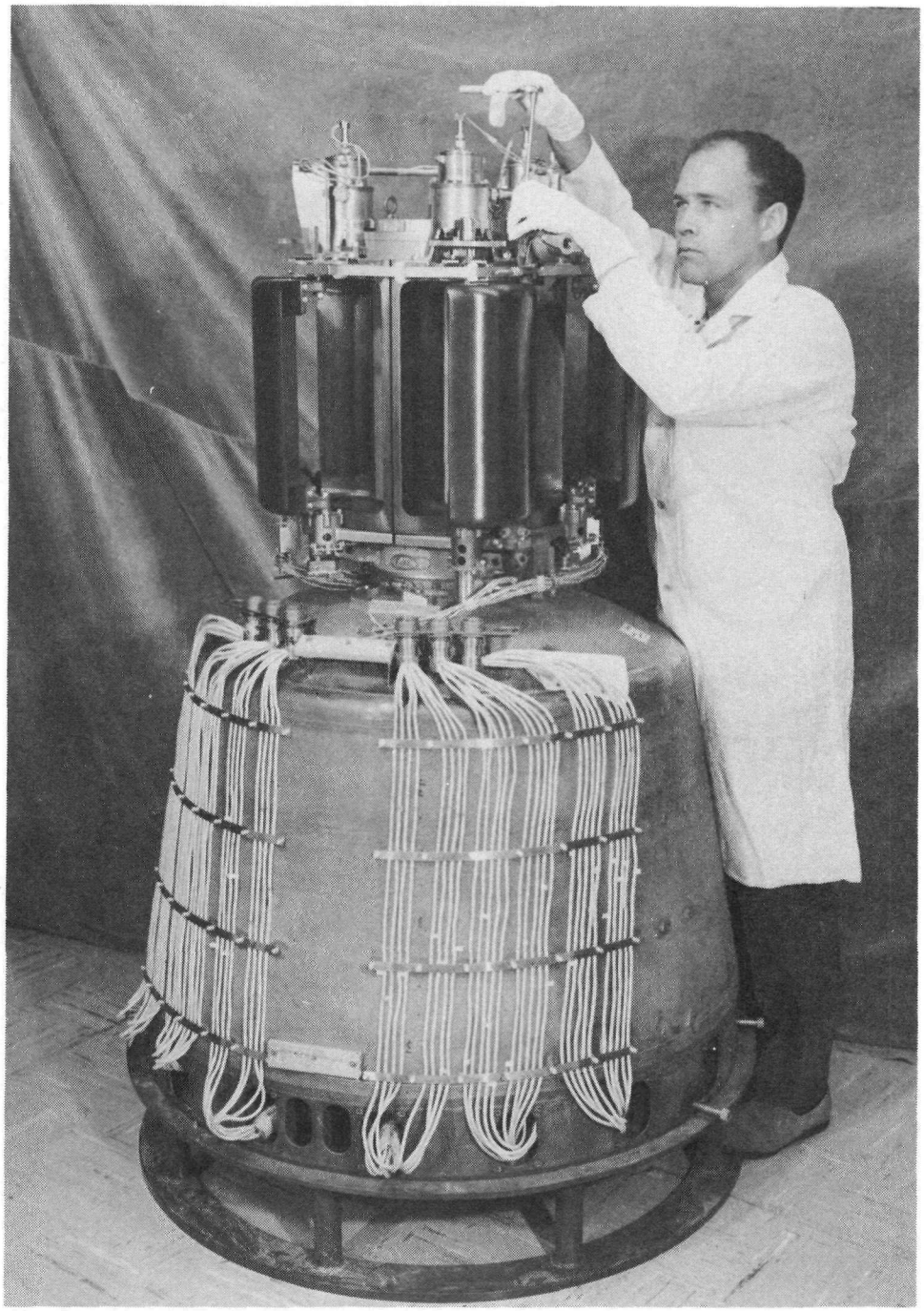

7-22-63 7568-1215

Figure 45. SNAP 8 Reactor and Shield

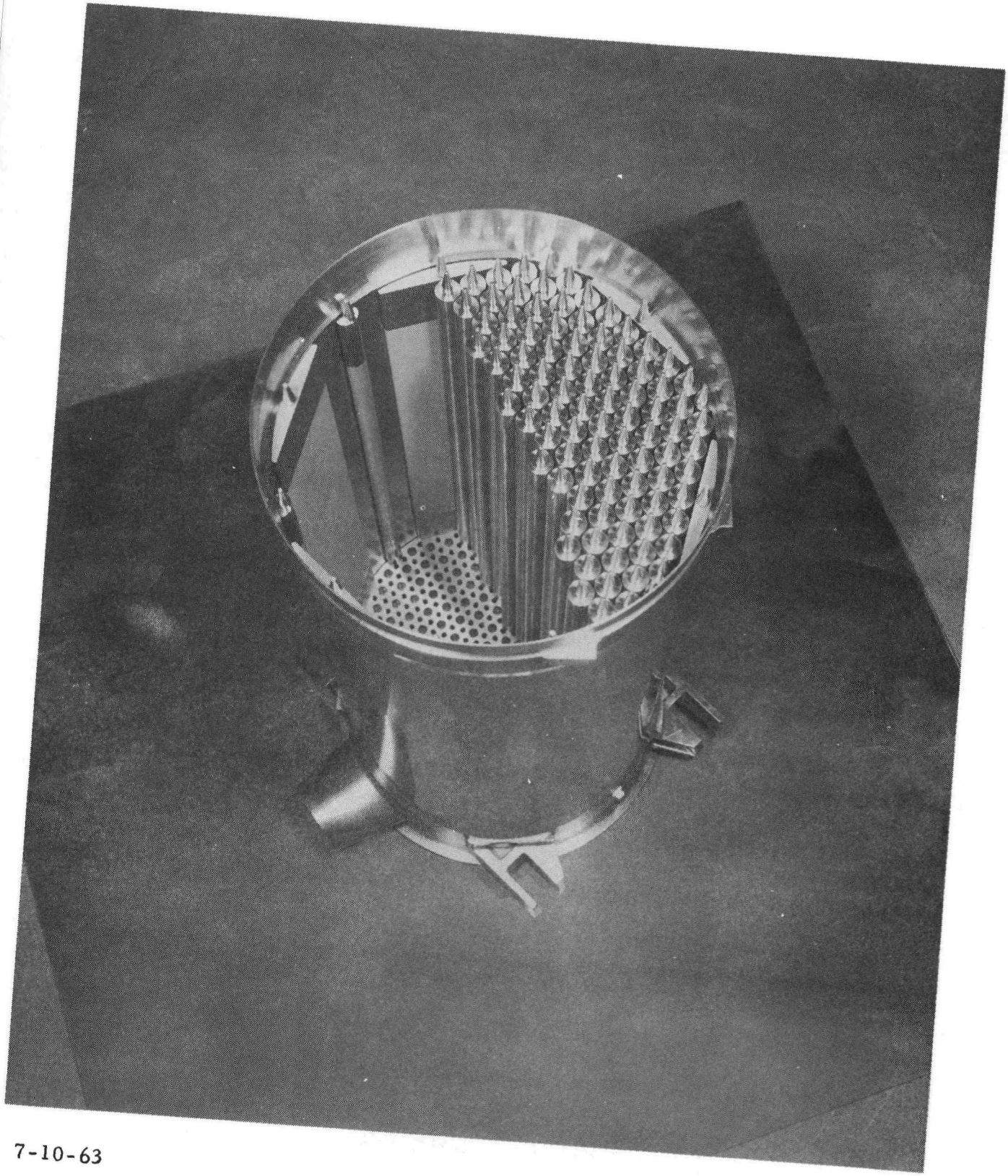

7-10-63

Figure 46. Internal View of the SNAP 8 Core

7568-1128A

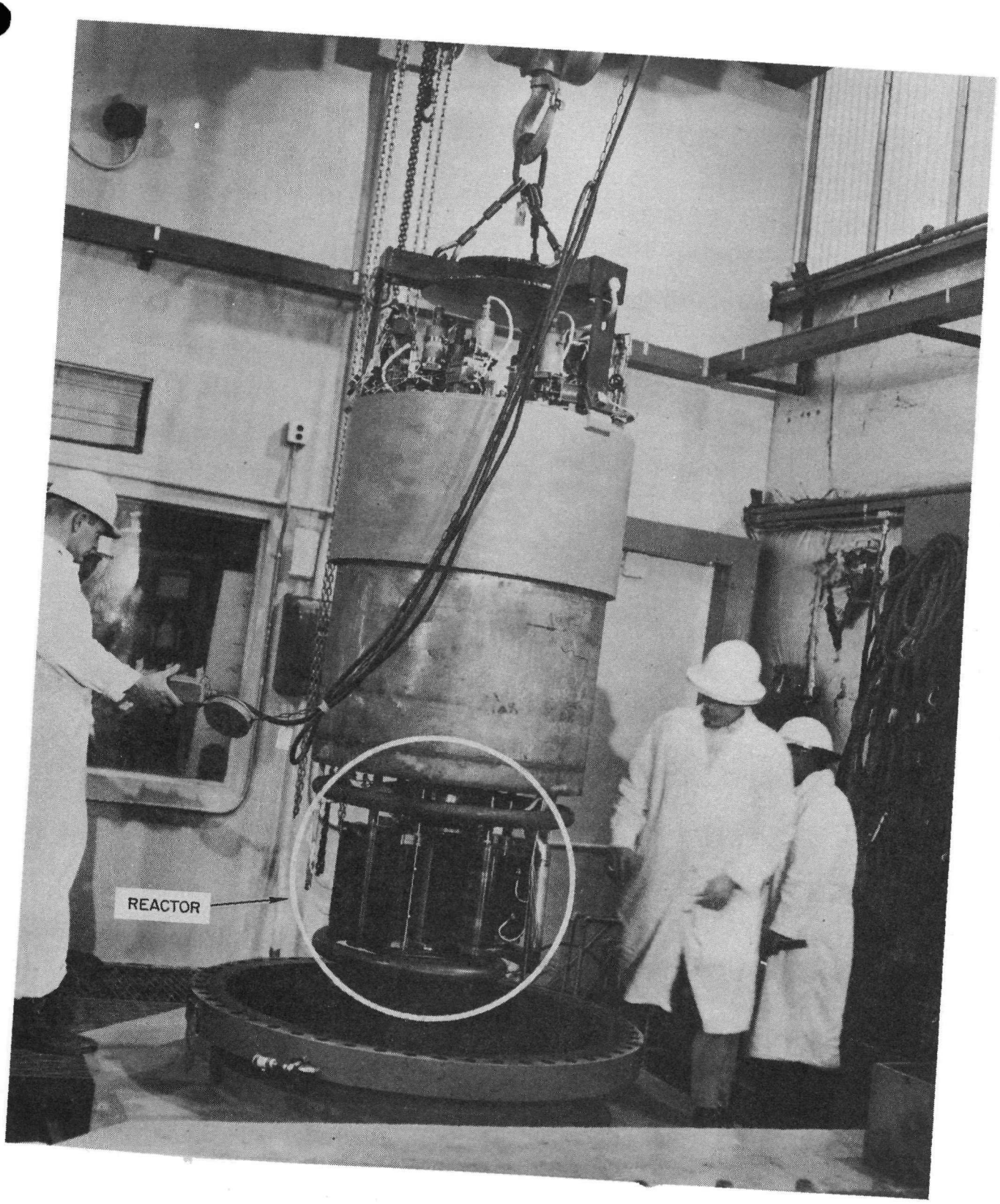

Figure 47. SNAP 8 Experimental Reactor Test Assembly Being Lowered into the Test Facility

7568-56110 CN

2. SNAP 10A

The objective of the SNAP 10A Program is to develop a nuclear reactor power unit capable of producing a minimum of 500 electrical watts for a period of one year in a space environment. As presently scheduled, SNAP 10A will be the first reactor powered electrical system to be flight tested in earth orbit. The SNAP 10A system is shown in Figure 48.

SNAP 10A employs a (ZrH) thermal reactor coupled to an integral Si-Ge thermoelectric converter-radiator which converts NaK-transported fission heat to electrical power. The unit is approximately conical in configuration with a base diameter of ~5 ft and an overall height of ~11 ft. The first flight system will have a shielded weight of 950 lb. The 225-lb shield will restrict the radiation dose at the base to about 4×10^{12} nvt of fast neutrons and 1×10^{7} r of gammas during the one-year lifetime. After orbital startup on ground command, the unit operates without the need for active control, without moving parts, and without attitude orientation requirements. Because of the negligible heat rejection variation during the orbital sun-shade transient, SNAP 10A provides a continuous source of at least 500 watts without the limitations of secondary battery-solar cell combinations. On a production basis, the SNAP 10A unit should cost about one million dollars.

The SNAP 10A system, shown schematically in Figure 49 derives its thermal energy from a temperature and power-derated SNAP 2 reactor.

The fission heat is transferred from the reactor to the thermoelectric power converter by means of a liquid metal (NaK-78) coolant loop. The liquid metal is circulated by a d-c Faraday conduction pump which derives its current from a shorted PbTe thermocouple operating between the NaK outlet temperature and a cold junction determined by a small pump radiator. The pump magnetic field is supplied by a permanent magnet. A photograph of the flight design pump is shown in Figure 50. The NaK flow is divided among 40 parallel tubes arranged axially along the unit's conical surface.

Each NaK tube is a series fluid connection of three thermoelectric modules. Thus, the full 500-watt converter is made up of 120 modules of about 4 to 5 watts each. A detailed drawing of a module is shown in Figure 51 and an actual module photograph is shown in Figure 52. Seventy-two cylindrical pellets of

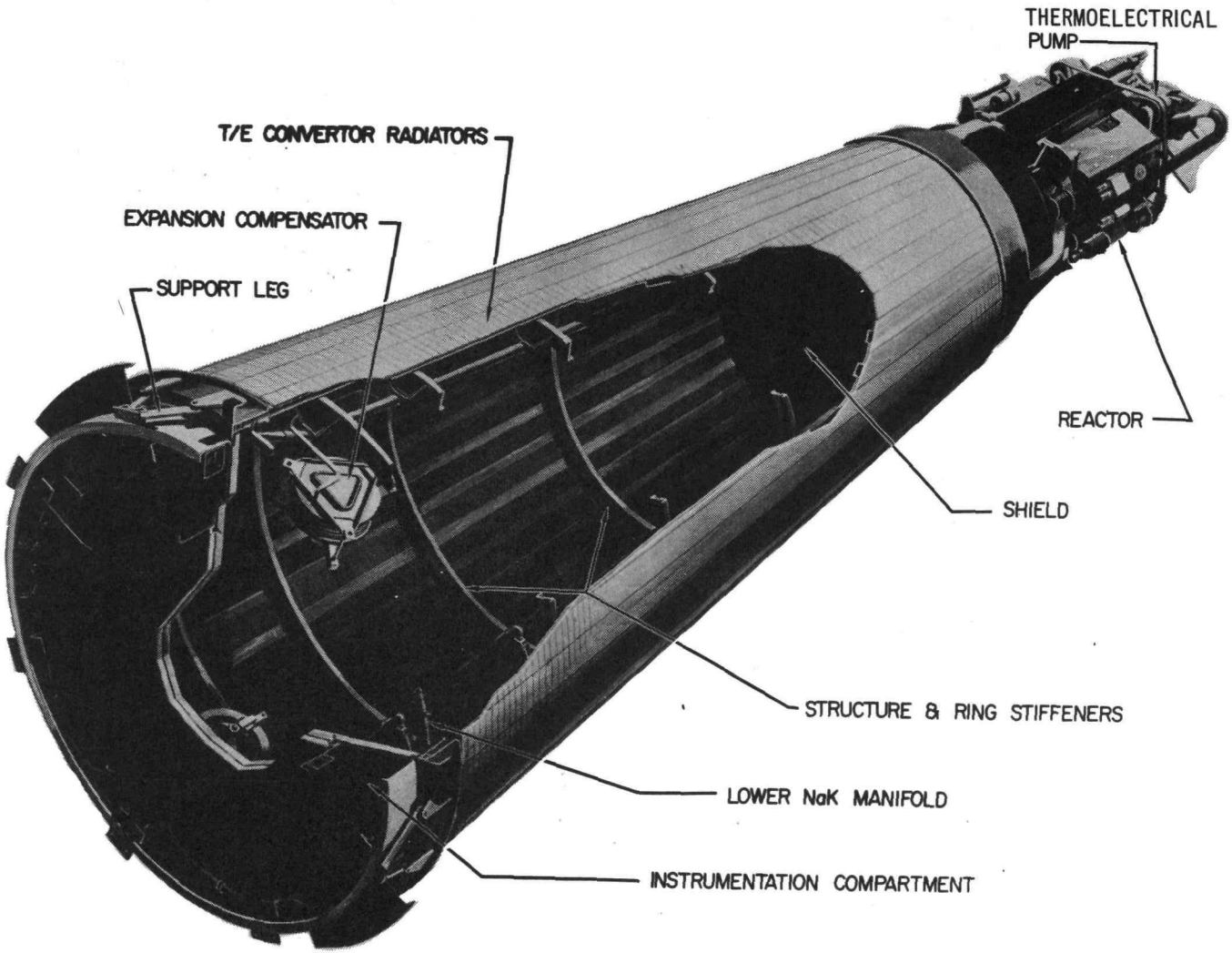

3-5-63

7561-0033D

Figure 48. SNAP 10A System

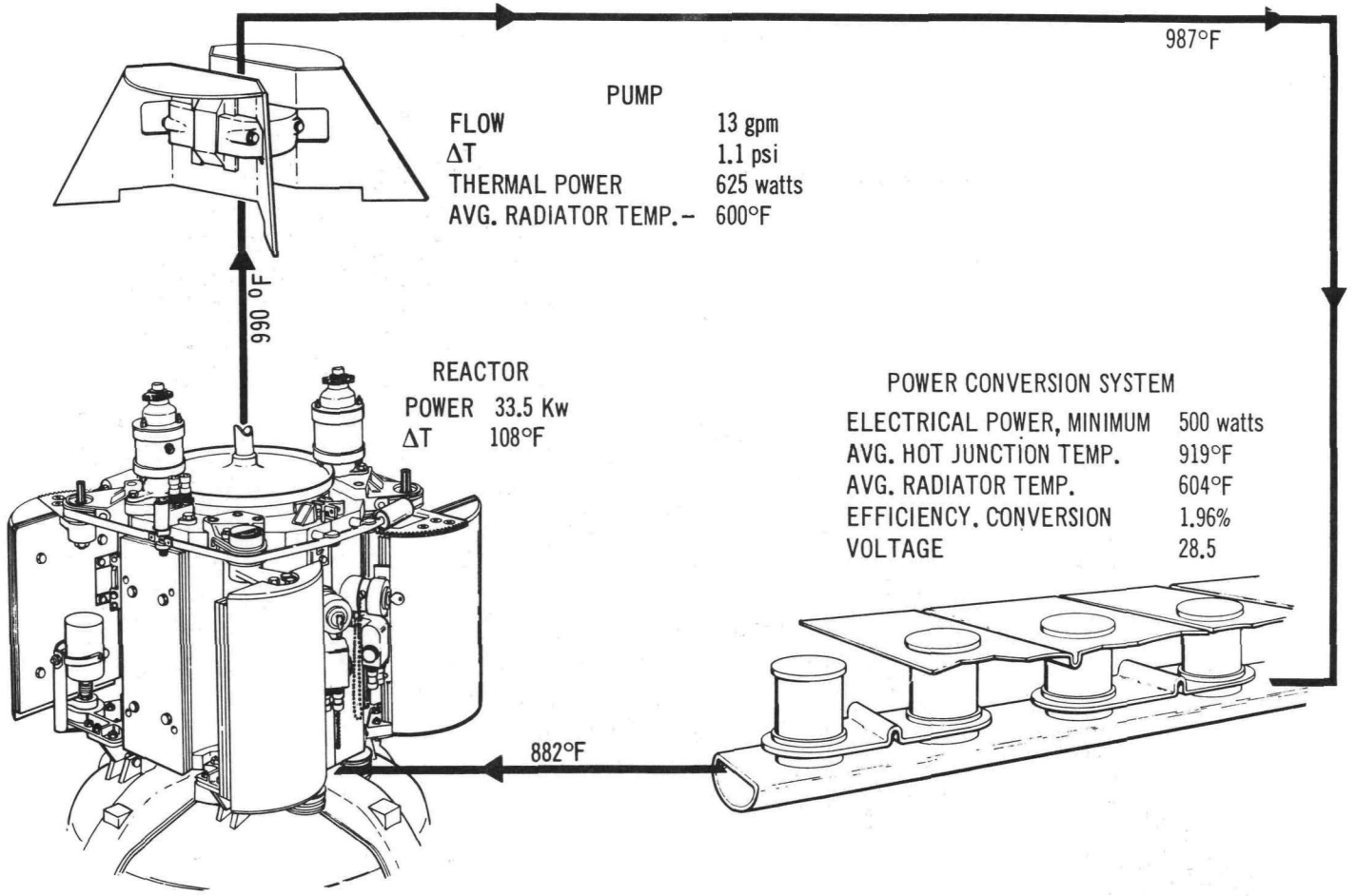

3-5-63

7561-0032A

Figure 49. SNAP 10A Schematic Diagram

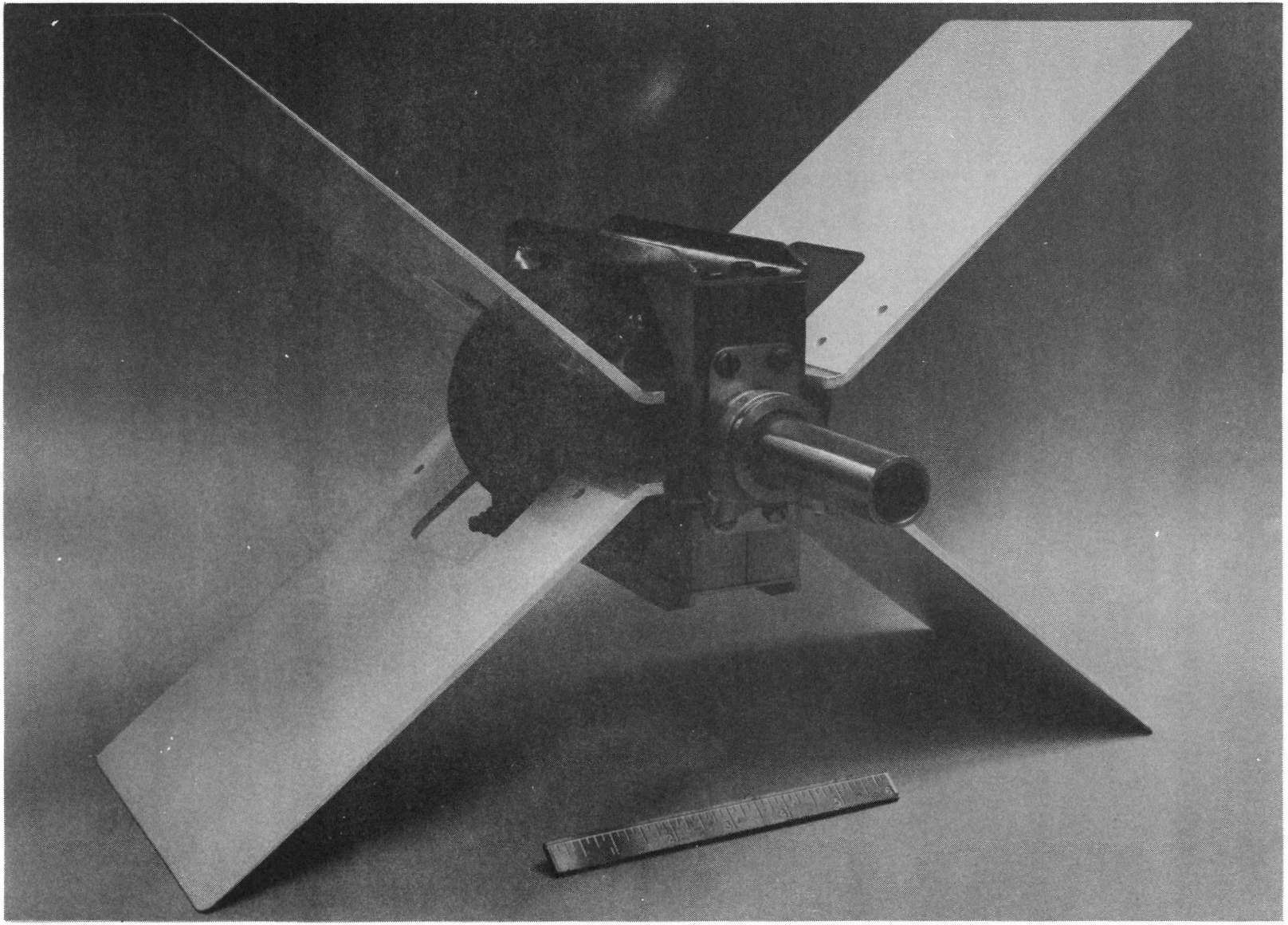

10-26-62

7561-5469

Figure 50. SNAP 10A Thermoelectric Powered NaK Pump

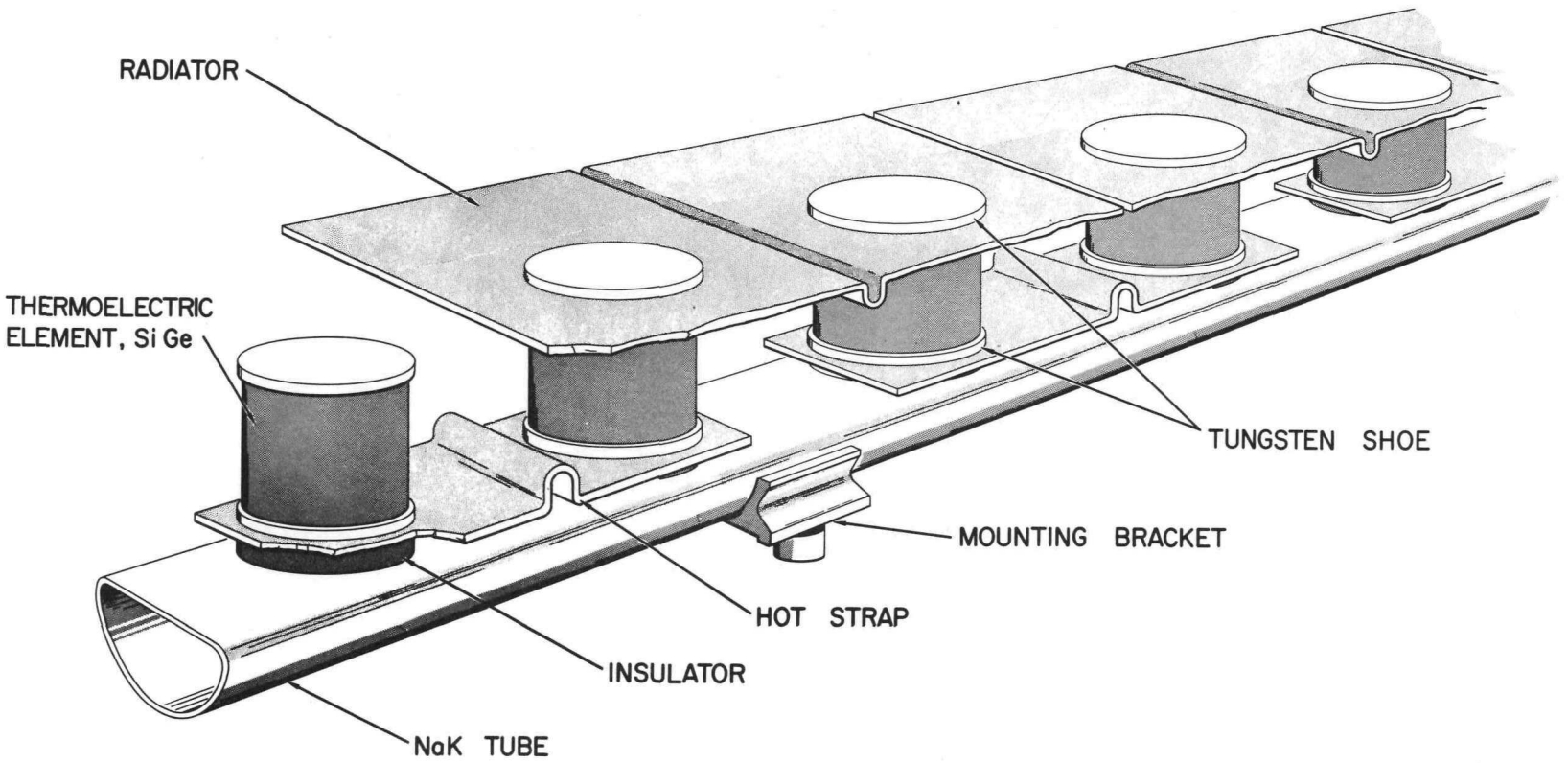

2-23-62

7580-1032 C

Figure 51. SNAP 10A Thermoelectric Converter Module

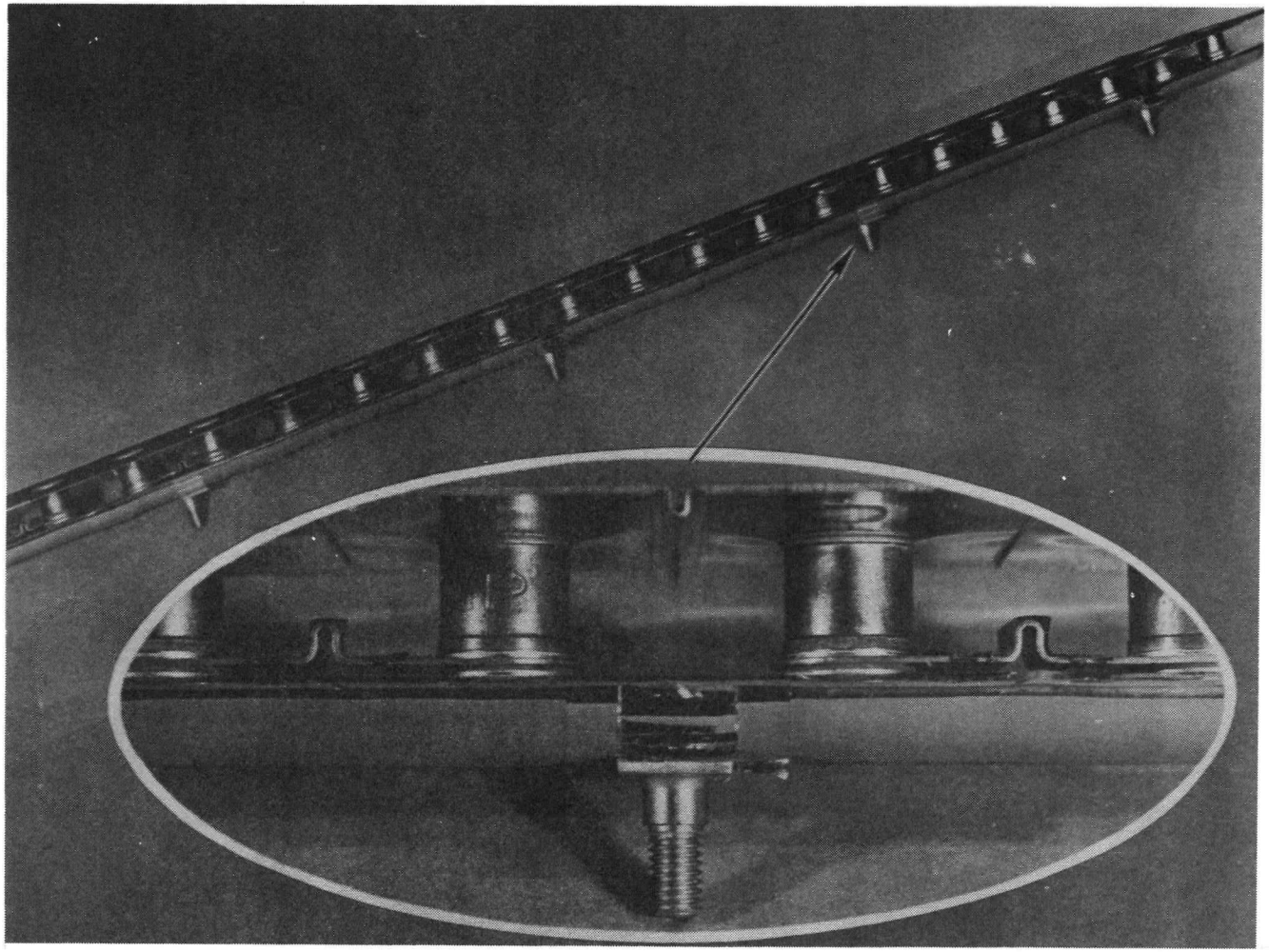

7-16-62

7561-5102 Ba

Figure 52. SNAP 10A Thermoelectric Converter Module

n- and p-doped Ge-Si alloy thermoelectric material are alternately spaced along the length of each NaK tube. The pellets are electrically insulated from the NaK tube by means of thin alumina disks. The pellets are electrically connected in series with copper straps at the hot end and aluminum combination strap-radiators at the cold end. Each aluminum radiator platelet is electrically insulated from adjacent platelets by a clearance gap. All material interfaces from the NaK tube through the aluminum radiator are either metallurgically bonded or brazed. Each material stack from NaK tube to radiator is capable of supporting 200 to 300 lb in tension. The radiator platelets have an emissivity of about 0.89 and are sized to maintain the thermocouple cold junction at an average temperature of 604°F. The total radiator area (including gaps) is approximately 65 ft^2. Thus far in the program a total of about 500 modules or 4 equivalent 500-watt converters have been fabricated.

The series string of couples on each NaK tube is mated with an adjacent string by an electrical cross connection at each radiator platelet along the length of the NaK tube. These adjacent pairs of series-parallel-connected couples are then connected in series. This connection has eliminated the possibility of one open couple causing a system failure. The open circuit failure rate during launch will be less than 1 to 2 opens per thousand elements. The converter reliability should be in excess of 99%. The SNAP 10A thermoelectric generator has an open circuit voltage of about 60 volts and a generator resistance of about 1.6 ohms.

A conical corrugated titanium structure supports the reactor shield mass and forms a mounting bed for the thermoelectric modules. A photo of this structure is shown in Figure 53. The structural adequacy of the SNAP 10A system has been demonstrated by subjecting structural and mass mockup systems to the simulated launch environment. A structural qualification test is shown in Figure 54.

A prototype system has successfully undergone thermal performance testing in a vacuum chamber. The test employed electrical heat to simulate the reactor output. The test setup is shown in Figure 55. This test verified overall thermal compatibility of the system.

The electrical interface to the Agena flight test vehicle is being verified by means of a combined electrical mockup test at LMSC. The SNAP 10A mockup

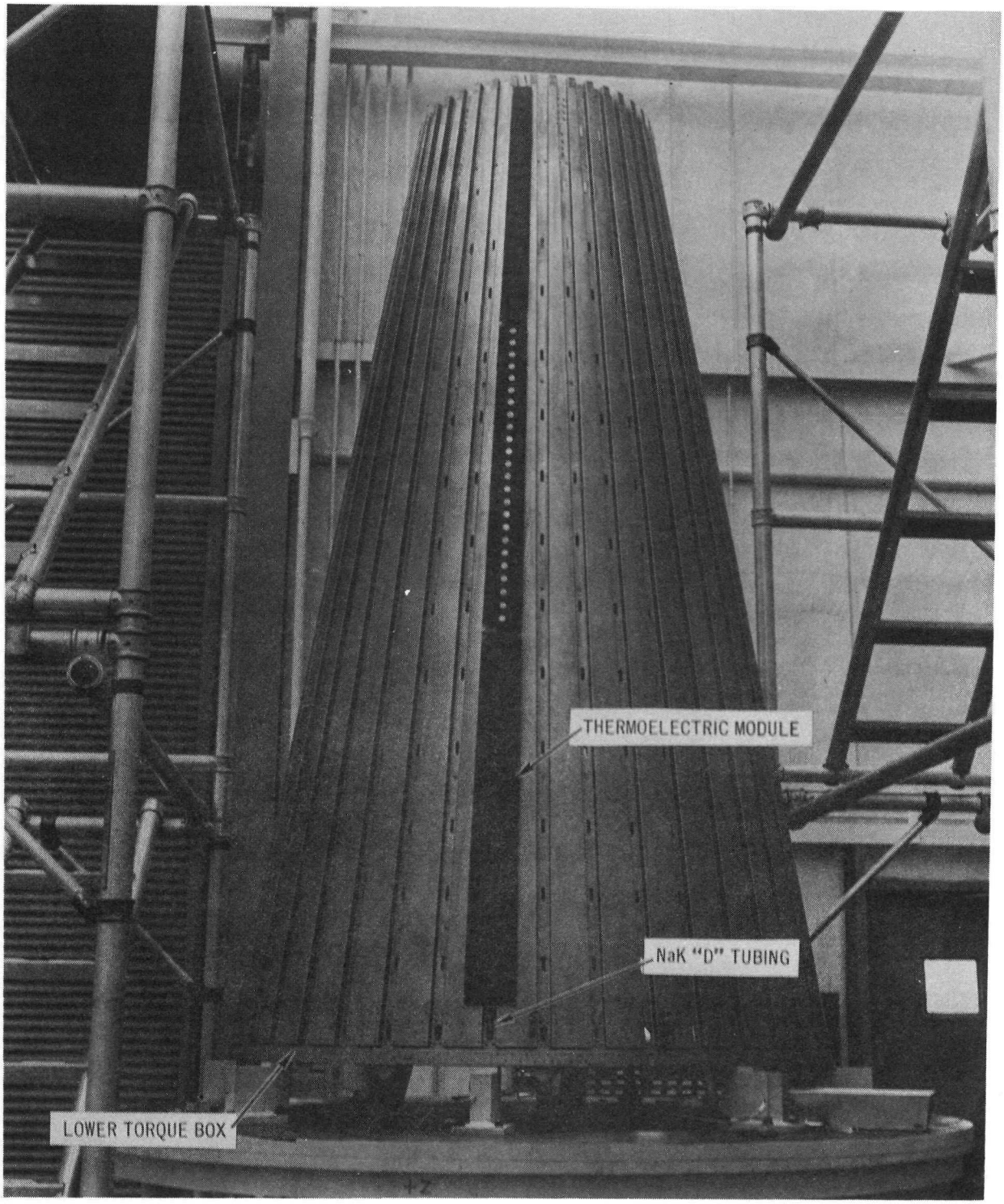

3-5-63 7561-5429A

Figure 53. SNAP 10A Titanium Structure

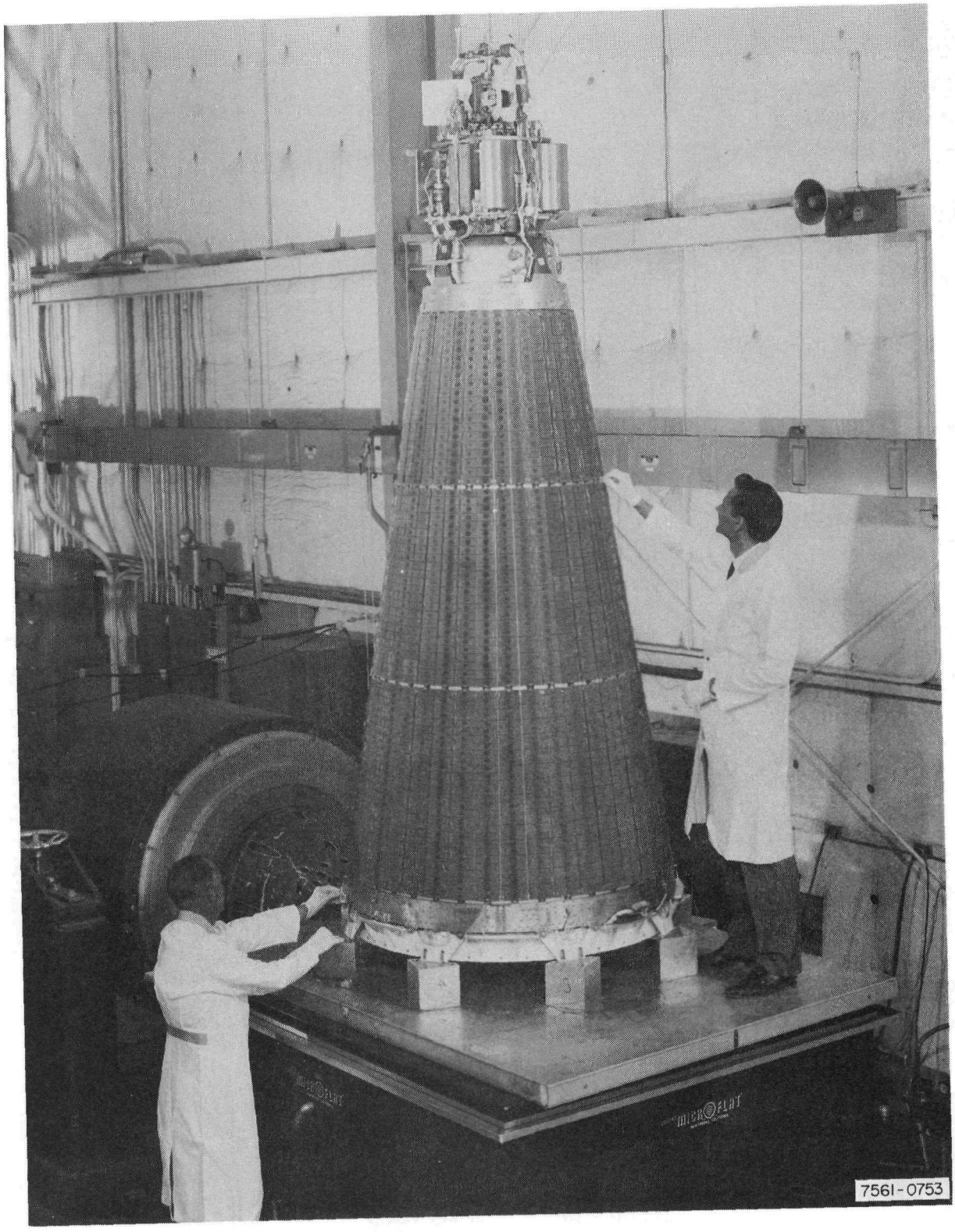

Figure 54. SNAP 10A System Preflight Qualification Test-
Shock and Vibration

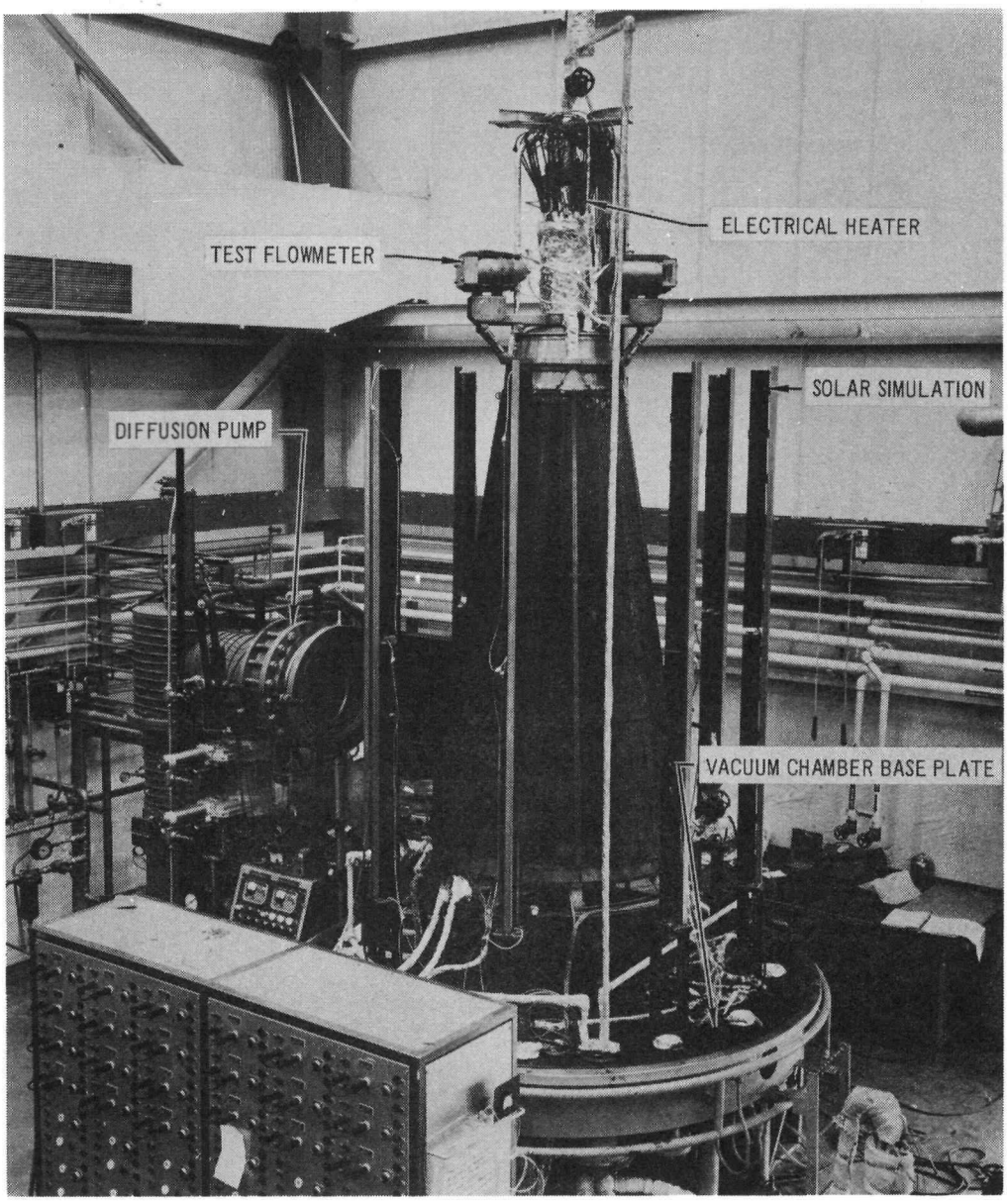

2-29-63 7580-18229B@

Figure 55. SNAP 10A System Thermal Performance Test

mated to an Agena mockup is shown in Figure 56. The SNAP 10A/Agena interface and the instrument compartment are shown in Figure 57. The fabrication of two flight-design systems for preflight qualification testing has been recently completed. A photo of one of these units is shown in Figure 58. This specific unit will be tested with an electrical heater simulating the reactor. The second unit will be tested with a live reactor.

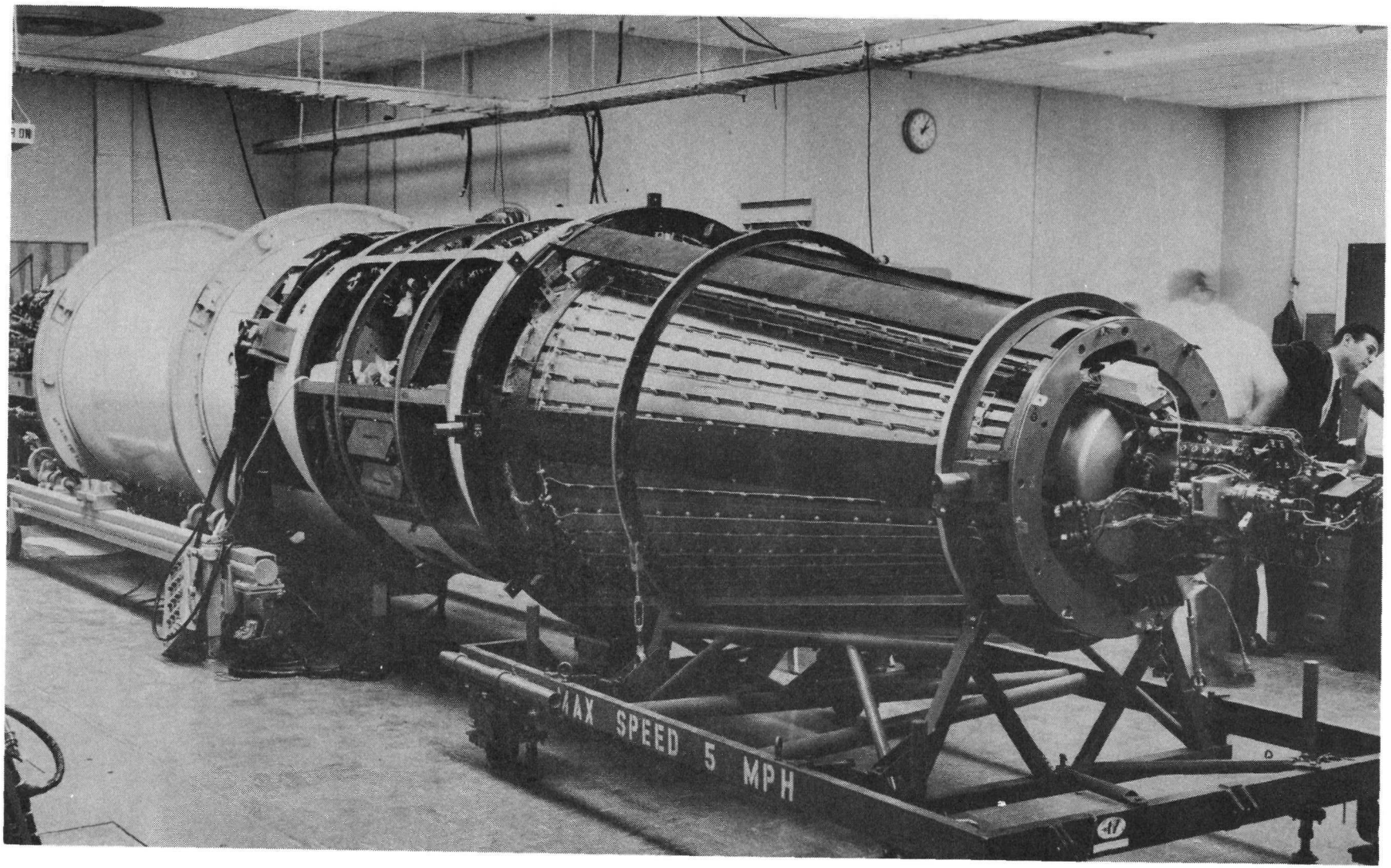

2-20-63

7561-5038

Figure 56. SNAP 10A System Electrical Simulator Compatibility Test with an Agena Mockup

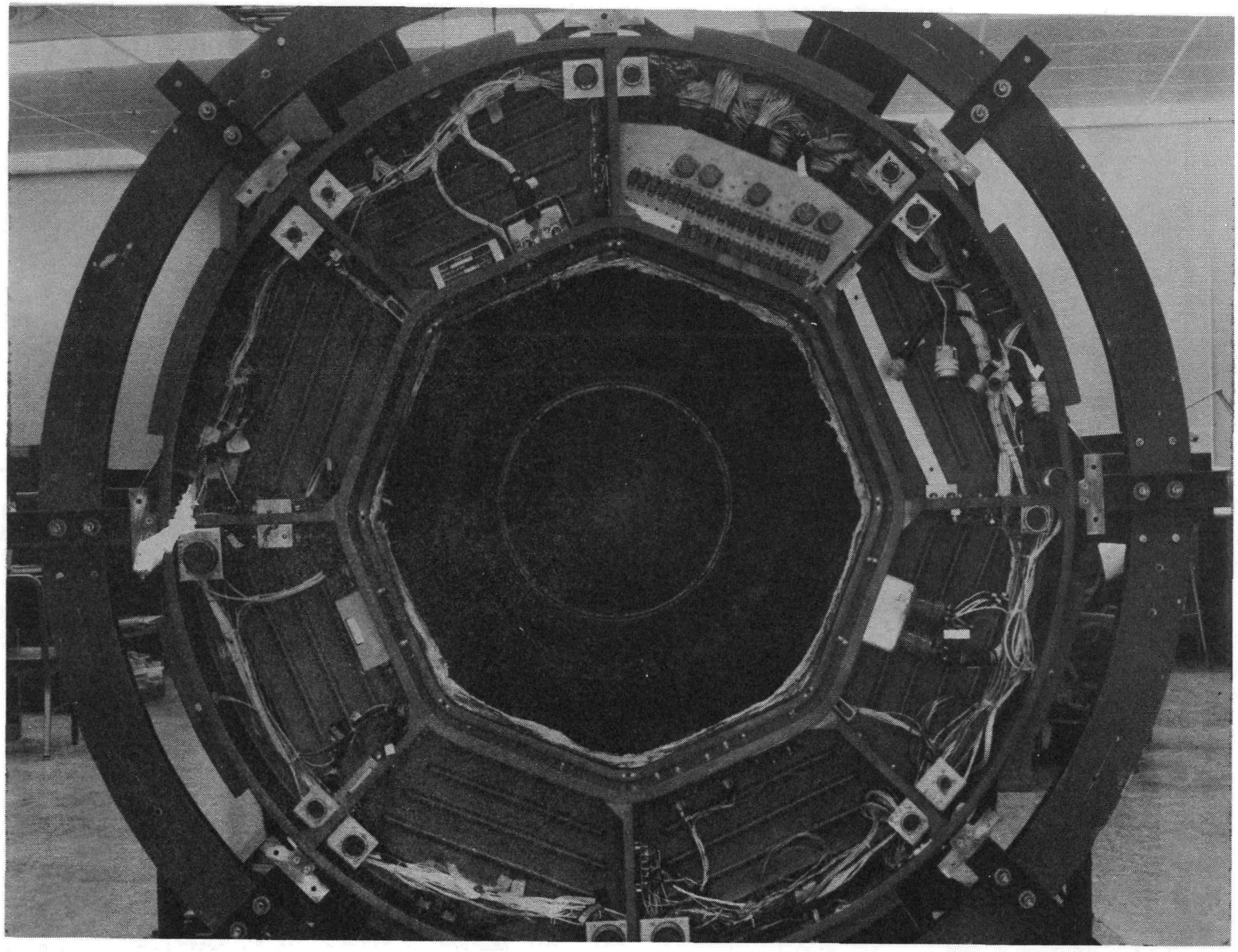

7561-18122

Figure 57. SNAP 10A Instrument Compartment

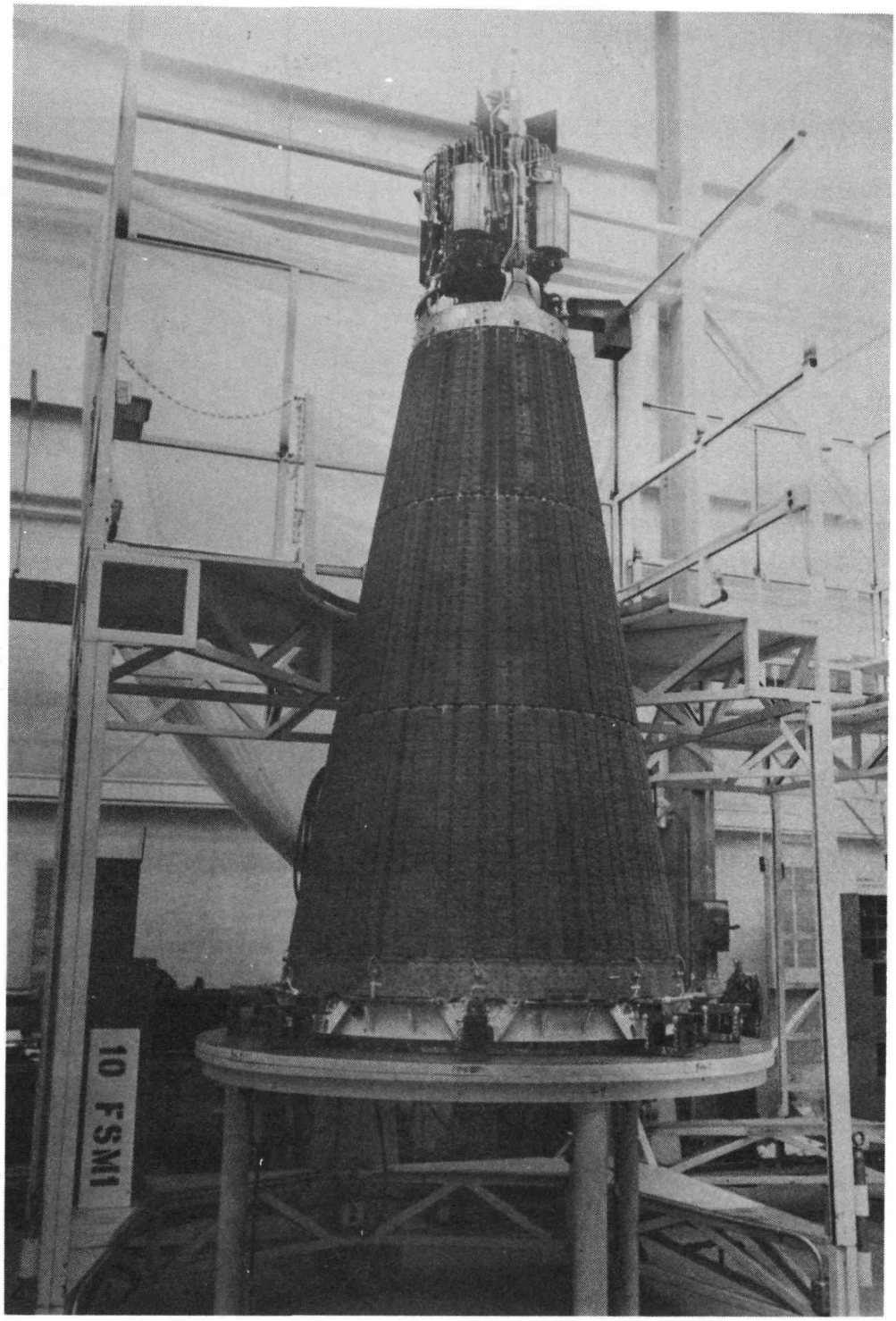

4-16-63 7561-51207

Figure 58. SNAP 10A Preflight Qualification System

3. SNAP 2

The objective of the SNAP 2 program is to develop, test, and qualify a 3-kwe nuclear auxiliary power unit for space utilization. The SNAP 2 concept is the result of a 1956 preliminary study which evaluated the state-of-the-art of reactor and power conversion technology, as well as projected space vehicle and mission requirements. The following development objectives for SNAP 2 have evolved:

1) 3 kwe net output

2) One year unattended automatic operation

3) System weight: 1200 lb (unshielded)

4) Cycle heat rejection area: 120 ft^2

A system schematic is shown in Figure 59. Energy is produced in the nuclear reactor by the fissioning of U^{235}. A liquid metal (NaK-78) heat transfer fluid is circulated through the reactor core and the mercury boiler superheater by a rotating permanent magnet pump. In the boiler superheater the reactor heat is transferred from the primary reactor coolant to the mercury working fluid of the Rankine power conversion cycle. The reactor heat converts liquid mercury into superheated vapor which is expanded through a turbine. The resulting mechanical power output of the turbine is converted to electrical power by the alternator. The mercury vapor exhaust from the turbine is condensed in the radiator-condenser which is part of the outer skin of the space vehicle. The mercury condensate is returned to the boiler by a boiler feedpump.

All the power conversion system rotating components are mounted on a single common shaft component which is called the combined rotating unit (CRU). Thus, the entire SNAP 2 power conversion system has only one moving part which is supported on liquid mercury lubricated bearings. The entire assembly of rotating machinery is enclosed within a hermetic housing which prevents the loss of the mercury working fluid during the system life. The CRU is shown schematically in Figure 60. The individual components of the rotating shaft include: (1) the rotating permanent magnet NaK (pump) whose operation is similar to that of a conventional E-M pump with the exception that the moving magnetic field is provided by a rotating magnet; (2) the mercury turbine which is a two-stage axial flow impulse machine; (3) the alternator which is a permanent

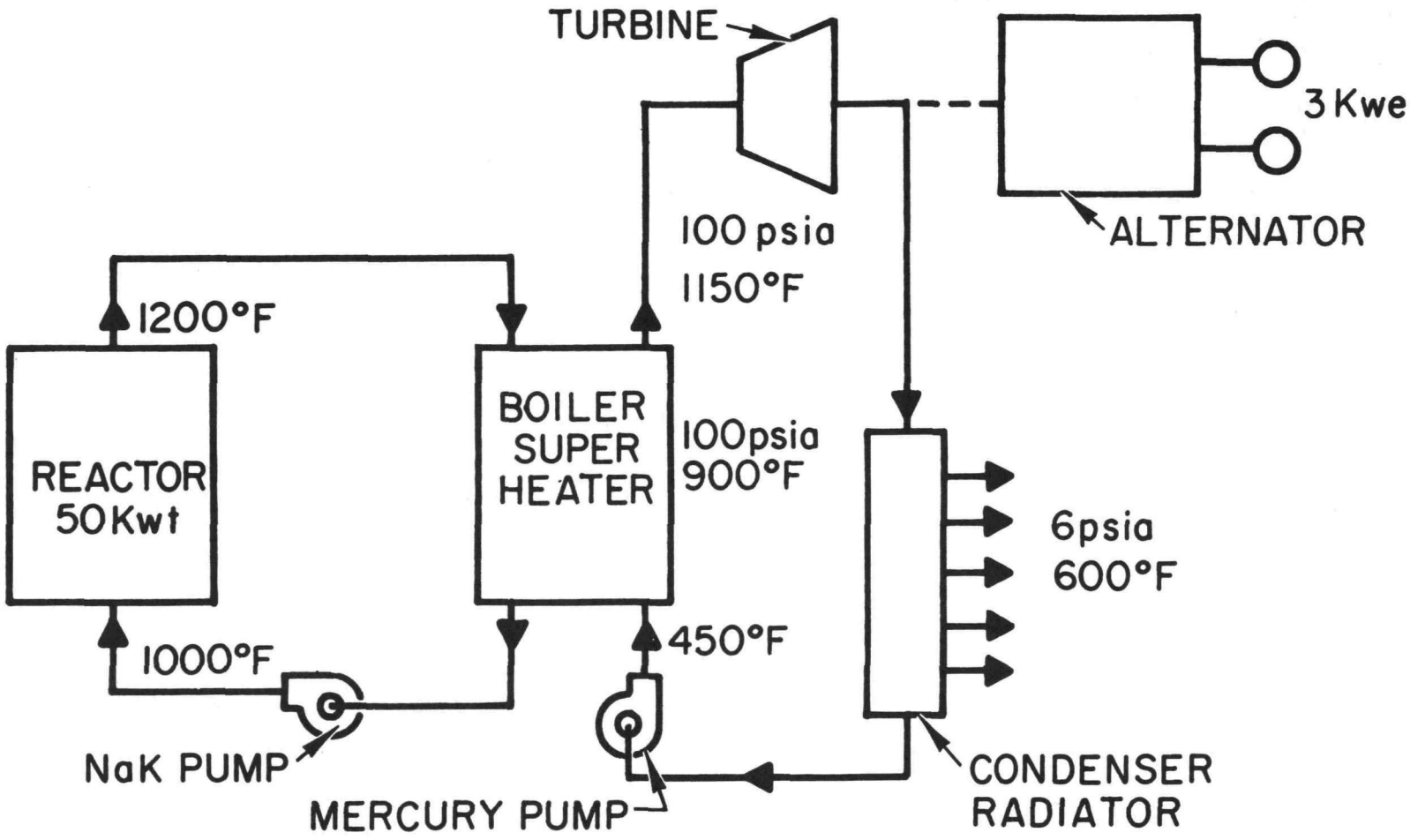

Figure 59 SNAP 2 System Schematic

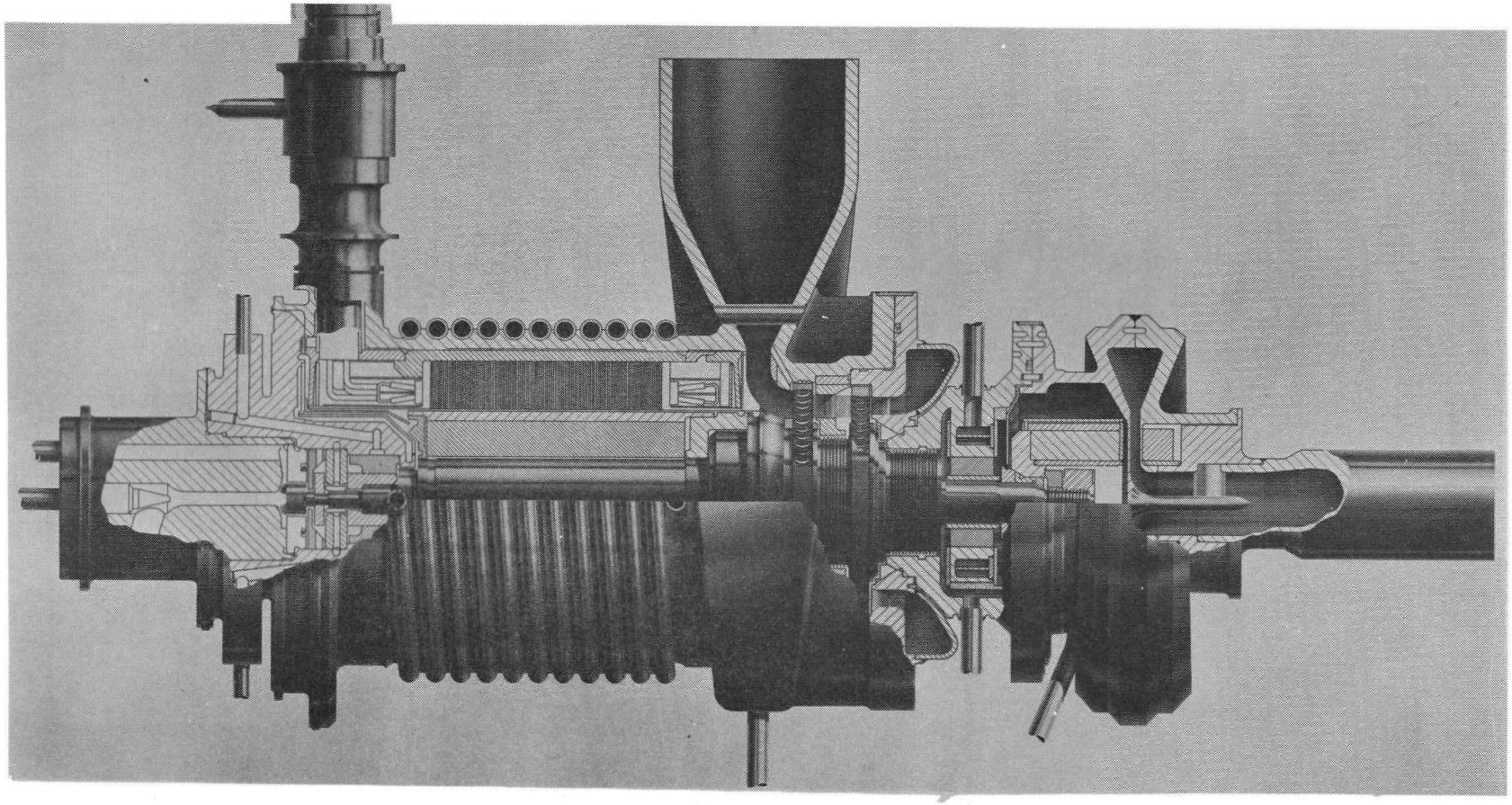

7550-20287

Figure 60. SNAP 2 Combined Rotating Unit - CRU IVM

magnet machine with a sealed stator and delivers 3.5 kw at 1800 cps; and (4) the mercury pump which is a conventional but miniature centrifugal pump supplying pressurized mercury to the boiler and to the bearings.

The mercury boiler-superheater is a tube and shell, counterflow, once-through boiler with NaK in the shell and mercury in the tubes. The boiler is in a coiled tube configuration which cancels fluid angular moments.

The cycle rejection heat is radiated to space by a combined radiator-condenser which forms part of the outer structural skin of the space vehicle. Mercury condensation takes place at 600°F and 6 psia within a number of small-diameter parallel tubes which are attached to a high thermal conductivity skin which in turn radiates the heat of condensation to space. The total area necessary to radiate 40 kw at 600°F is about 100 ft^2. A developmental radiator-condenser is shown in Figure 61.

The first Combined Rotating Unit (CRU), Figure 62, for the power-conversion package was successfully tested in September 1959. Similar power packages have accumulated in excess of 2500 hr of successful operation.

The major system components, the reactor heat source and the power-conversion package, have been demonstrated at the required design point. The remaining development effort is concentrating on system integration and vehicle configuration packaging. The SNAP 2 system configuration is shown in Figure 63.

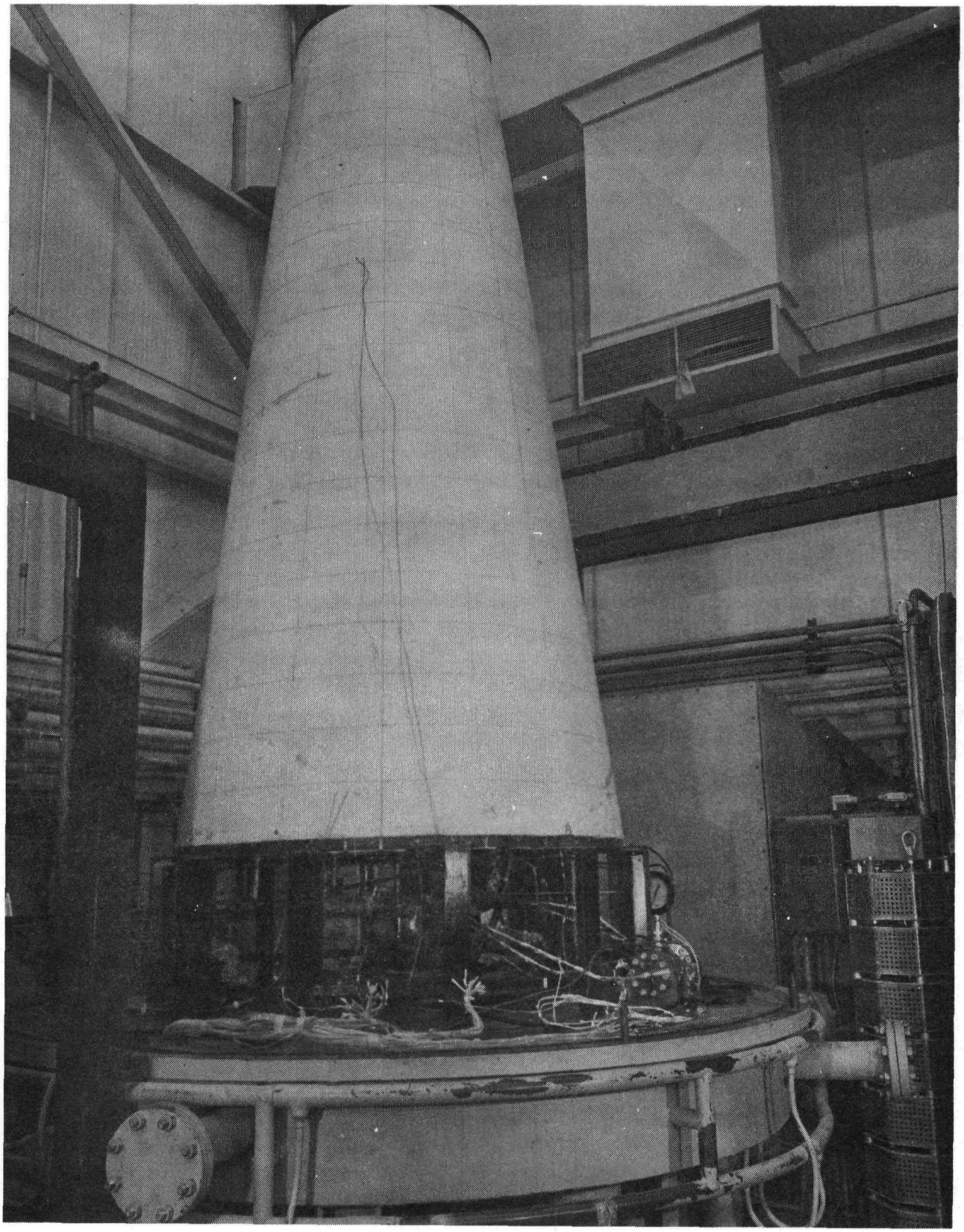

7562-5535

Figure 61. Developmental SNAP 2 Radiator Condenser

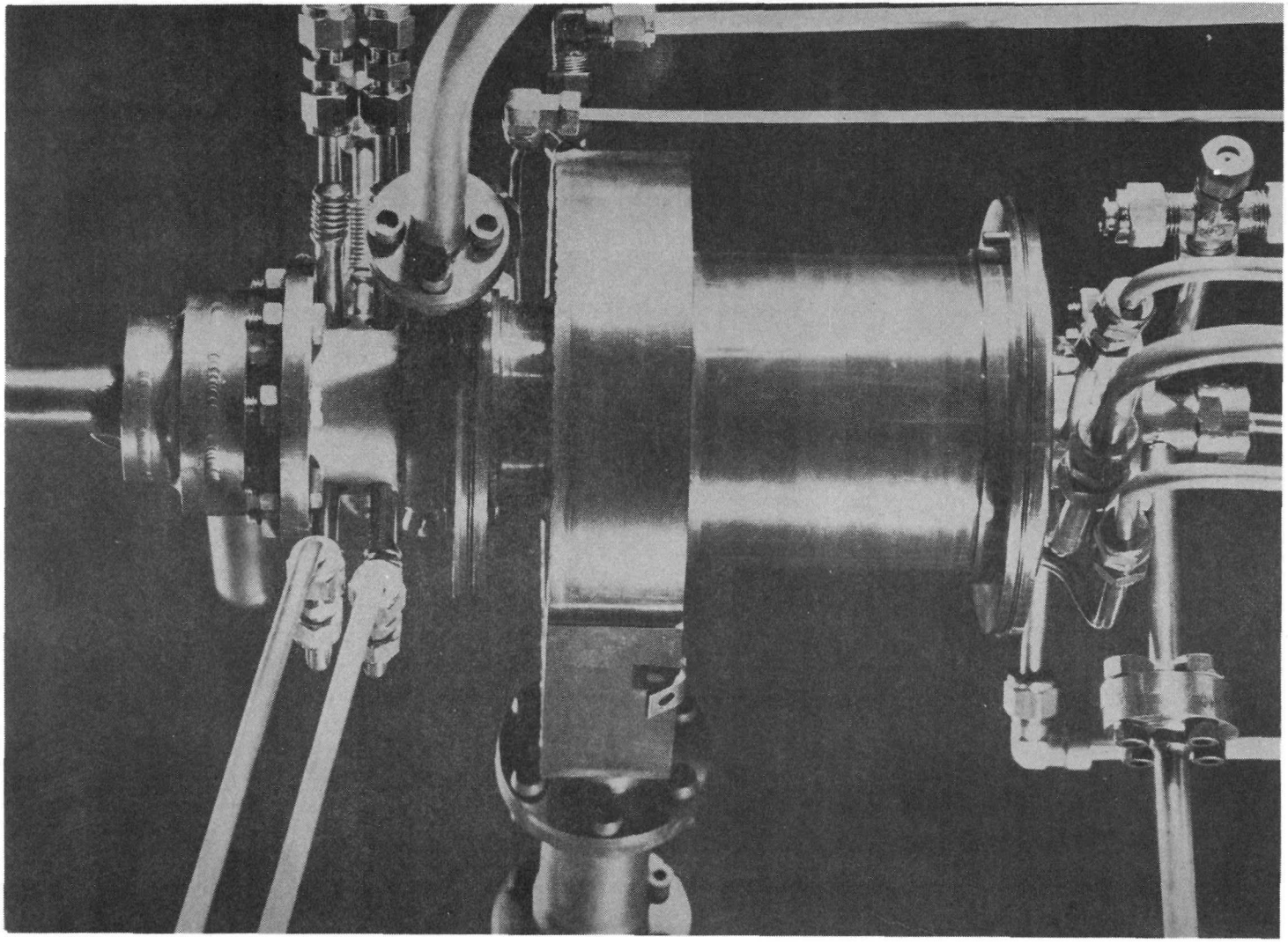

7550-2005

Figure 62. SNAP 2 Combined Rotating Unit (1959)

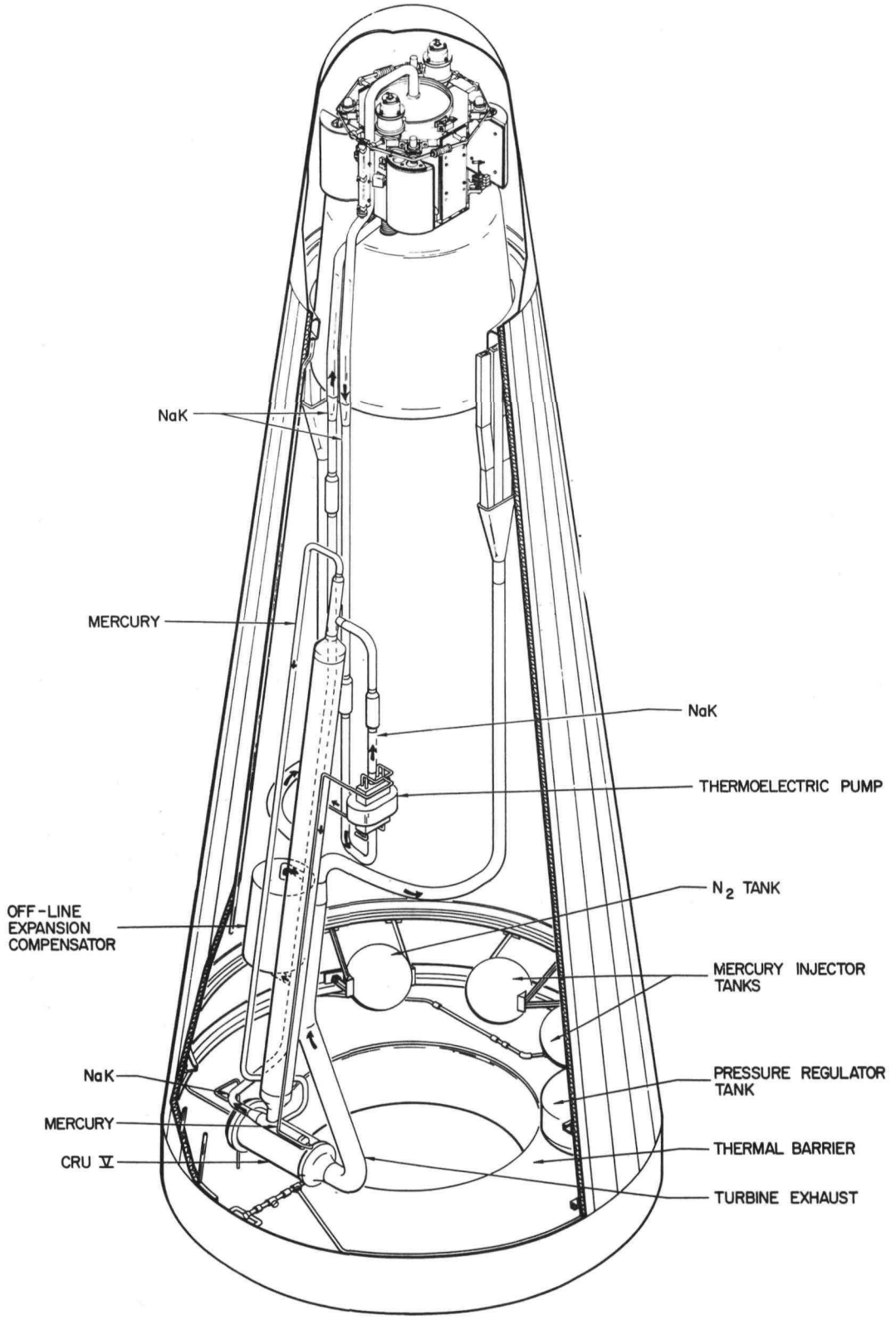

4-22-63

7562-0168A

Figure 63. SNAP 2 System

PART IV
APPLICATION

1. VEHICLE INTEGRATION

A nuclear auxiliary power unit (NAPU) offers many advantages for the longer lived satellite and space probe missions. SNAP 2 for example furnishes 3 kw of well regulated electrical power with a system weight of approximately 1200 lb unshielded or about 1500 lb shielded (this is highly dependent on vehicle design as is shown later). This corresponds to about 2 watts/lb or, on an energy basis, some 20,000 watt-hr/lb. There is no sun-shadow transient and no orientation problem such as is associated with a solar unit. Integration of the nuclear APU into a vehicle is straightforward.

The major problem presented to the designer concerns the APU location with respect to other components of the vehicle system. There are many ramifications to this choice of location that must be considered before an optimum design can be obtained. For example, the reactor-shield combination is the heaviest component in the NAPU and may vary from a minimum of 250 to 400 lb for an optimum vehicle arrangement with a radiation resistant payload; 500 to 600 lb for an optimum vehicle with a conventional transistorized payload; and 1000 to 2000 lb for an inept vehicle-payload arrangement. Vehicle design will be simplified in most cases if this mass is located on the vehicle thrust line, although in some instances other heavy components in a vehicle may be used as counterbalances. This restriction will normally prevent location of the reactor-shield combination in the propulsion section of the vehicle since tanks, pumps, and thrust chambers usually preclude centerline locations. In general, a NAPU nose cone installation with a conical radiator, a payload section which may be initially nestled within the radiator, and a propulsion section is optimum. Figure 64 shows the integration of SNAP 10A with the Atlas-Agena.

Structural scatter of nuclear radiation emitting from the reactor can cause a high payload dose if shielding for the scattered radiation is not used. With the reactor located in the vehicle nose and the nose cone skin jettisoned, and with the payload extended back below the radiator, an optimum system results. The reactor and shield are on the vehicle thrust line and no structural scatter occurs since the entire vehicle-payload complex is within the shadow of the shield. With a conventional transistorized payload of any practical volume, the shield weight will be 250 to 300 lb for SNAP 2

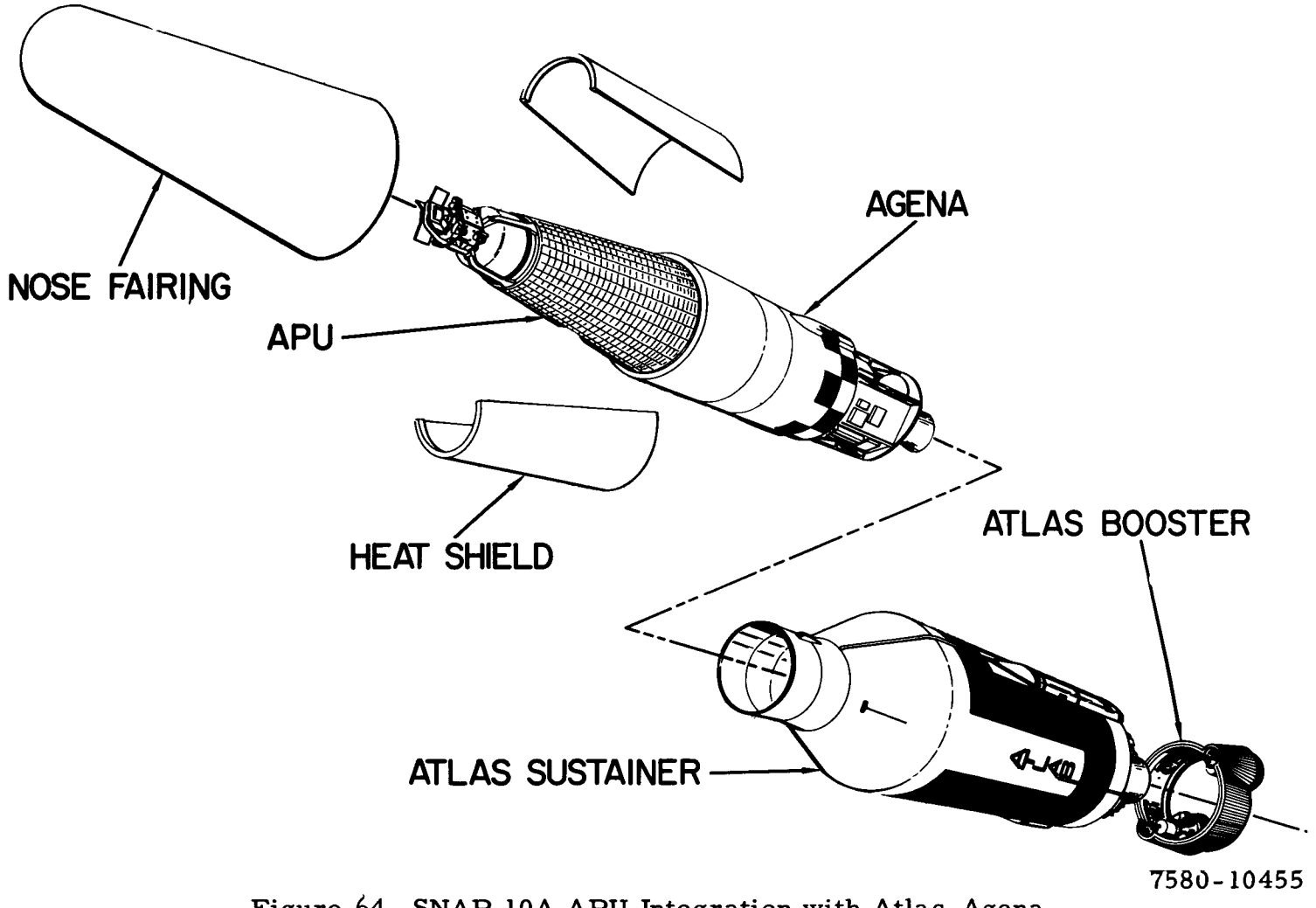

Figure 64. SNAP 10A APU Integration with Atlas-Agena

The SNAP 2 NAPU is about 13 ft long. NAPU access on the launch pad is good with the nose cone location but payload visual access in orbit may be sacrificed unless the propulsion system is jettisoned. Placing the reactor-shield combination at the tip of the vehicle increases gravitational restoring torques for satellite applications but can perturb the vehicle flight stability. Reentry burnup of the reactor is more easily obtained with the exposed nose location.

It was indicated above that the payload tolerance affects the shield weight a great deal. It has been assumed that a conventional payload utilizing transistors can be subjected to 10^7 r of gammas and 10^{12} nvt of fast neutrons. A payload especially designed for NAPU's could utilize hard vacuum tubes and radiation resistant transistors in especially designed circuits which are tolerant of component drifts. Such a payload could be expected to withstand greater than 10^{14} nvt and 10^9 r.

Extremely radiation-sensitive payloads, i.e., photographic film, should be equipped with individual shields so as to raise their tolerances to the payload design value.

Van Allen and cosmic radiation sources are usually no problem for unmanned systems. Exceptions occur in the case of photographic film and a few other very sensitive components. The yearly dose in the inner Van Allen belt (at about 2000 miles) taking into account various geometric factors, fraction of time spent in the maximum dose rate region, etc., is about 10^5 r. That in the outer belt (about 13,000 miles) is somewhat higher but also more easily shielded. In either case, a great deal of attenuation can be obtained by use of the vehicle skin and other structure members as shielding.

The requirements for manned applications depend heavily upon mission and upon the vehicle arrangement. If the mission is to spend most of its time in the Van Allen belts, the crew compartment will have to be well shielded and as a result the reactor shielding need not be significantly different than for electronic missions. If Van Allen radiation is to be avoided, the crew compartment shield will be quite light and other steps must be taken to reduce reactor shield. Normally, a configuration would be used with the crew compartment extended well to the rear of the NAPU. This not only provides the geometric r^{-2} reduction in dose rates but, more important, reduces the cone angle that the shadow shield must cover. The design if optimized when the incremental reduction in shield

weight is offset by the incremental increase in telescope extension members and power conductor weights. The system shield weights for various SNAP units are shown in Table XV.

TABLE XV

MINIMUM SHIELD WEIGHTS

(lb)

	Core to Payload Separation (feet)	Hard Electron Tubes (10^{16} nvt, 10^{11} r)	Special Transistors and Diodes (10^{13} nvt, 10^{8} r)	Present Germanium Transistor (10^{12} nvt, 10^{7} r)	Man (7.6×10^{7} nvt, 2.6 r)
SNAP 10A	6	0	170	250	-
	30	0	70	100	-
SNAP 2	13	0	170	250	2140
	30	0	130	190	1640
SNAP 8	20	35	220	320	2300
	30	0	190	270	1900

A more general survey of shadow shielding requirements is shown in Figure 65.

If an established vehicle is modified for a NAPU, it may be necessary to conceal the radiator within the vehicle until orbit is reached, then ejecting the vehicle skin. If the NAPU is integrated into the vehicle design early in the development, it would be possible to combine many of the functions of vehicle support, space radiation surface, and aerodynamic skin. A substantial weight reduction may be so gained.

The SNAP 2 radiator will operate at 600°F; therefore, it may be undesirable to have any payload components near by. In a configuration such as shown in Figure 63, a payload package may be carried to orbit nestled within the radiator and then extended to the rear prior to NAPU startup. This eliminates temperature interactions and significantly reduces shield weight and minimizes vehicle length at launch.

Since a more reliable NAPU can be developed if it operates at constant electrical load and since induced torques are minimized under this condition, it is usually desirable to provide a dummy load control which insures a constant load to NAPU. It is necessary that payload transients be considered in the design of the dummy load control although serious interactions are not likely.

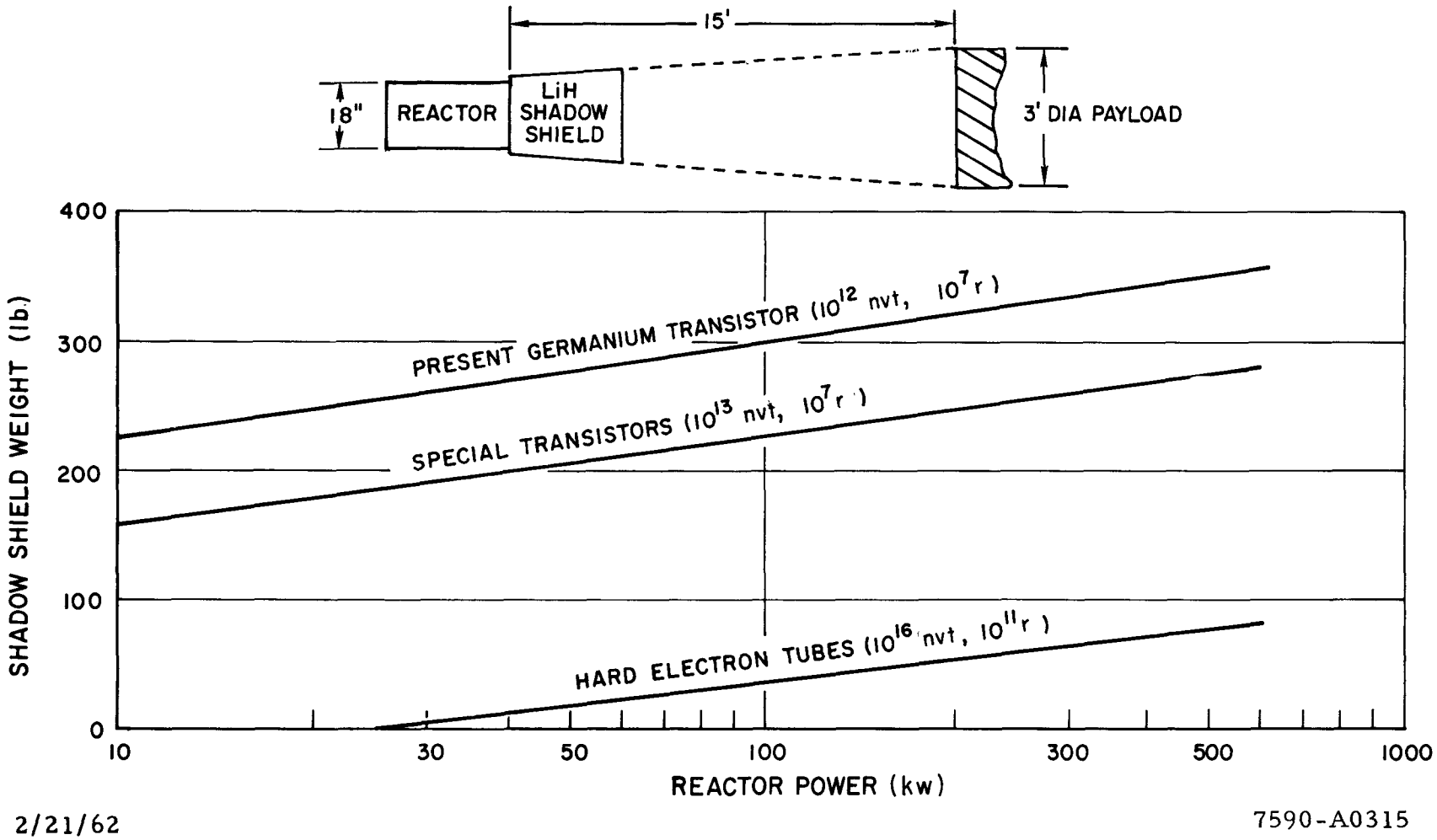

Figure 65. Shield Weight vs Reactor Power for Various Payload Tolerances

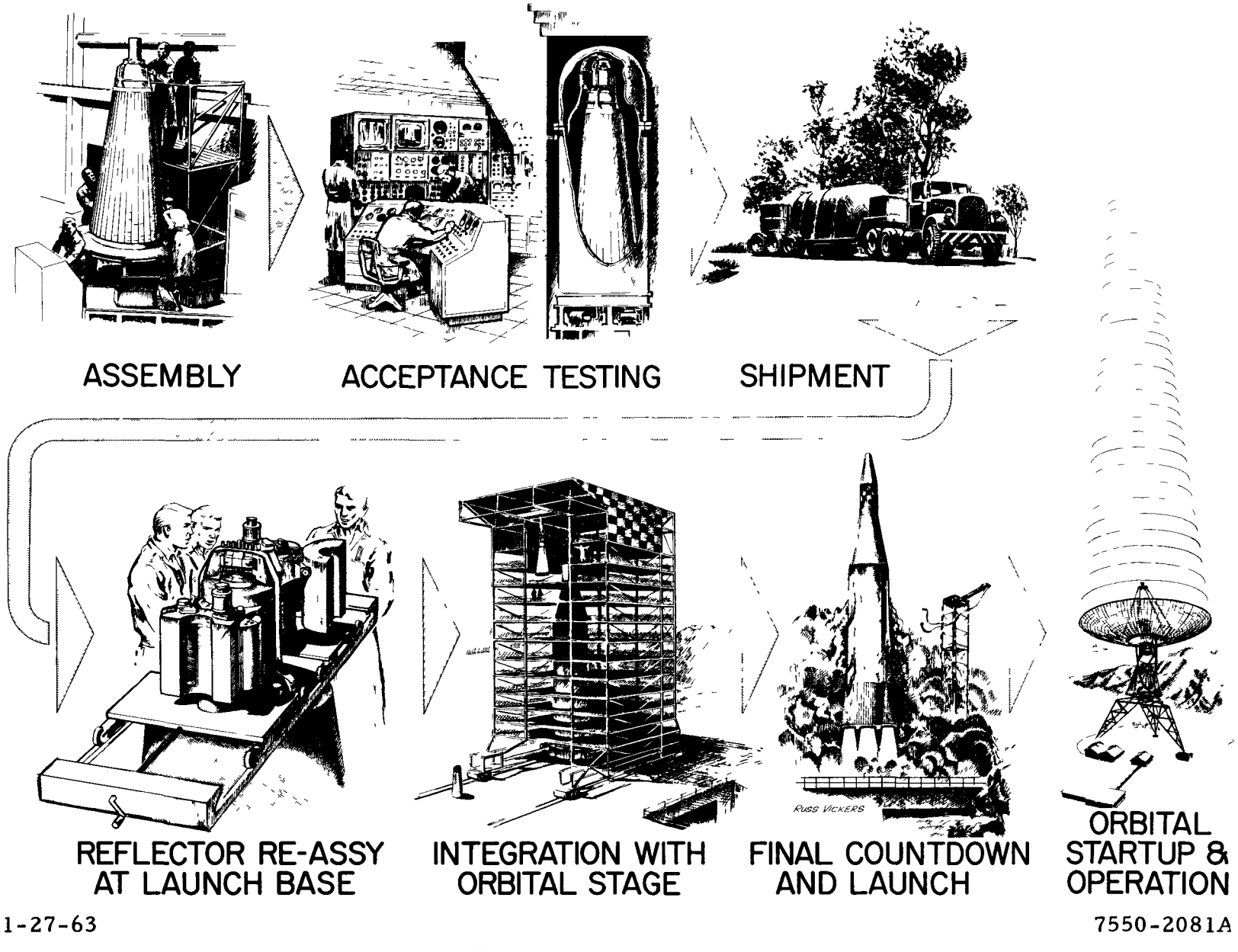

Figure 66. Factory-to-Flight Sequence

In the case of an earth satellite, the axis of the CRU will normally establish the pitch axis of the vehicle. It, therefore, may be necessary to have a very accurate alignment between the CRU and the vehicle. Allowable deviations in vehicle attitude will be reflected as rpm tolerances on the CRU and as allowable torques resulting from other angular momenta in the vehicle. At low altitudes, it may be feasible to obtain attitude control from natural restoring torques and an oscillation damper. At very high orbital altitudes, a dynamic attitude control will probably be necessary. In that case, a joint vehicle-APU study must be made so as to establish optimum induced torque specifications.

Ground handling equipment and launch pad complex modifications for the nuclear APU are minor if orbital startup is utilized. Telemetry for the startup must be supplied. Straight forward "go-no-go" checkout instrumentation will be available. No nuclear checkout at the launch pad would necessarily be anticipated; this could be covered in the acceptance test procedure before delivery.

If a prelaunch nuclear startup is desired, the system would be brought to power using a small 50-kw electrical heater built into the primary coolant loop. The power conversion equipment would be checked and the payload transferred to the NAPU. The reactor would be checked at very low power and then, just before launch, taken to full power as electrical heat is removed. If the mission is scrubbed, the NAPU or the entire final stage (depending on the separation provisions) must be placed in a shielded storage pit. A cleanup crew should also be available in case of a destructive booster abort. The SNAP unit factory-to-flight sequence is shown in Figure 66.

2. SAFETY

In considering the use of a nuclear auxiliary power system in space, the potential radiological hazards associated with its use must be evaluated. When anticipated by the appropriate design criteria, handling procedures, and operational limitations, it can be shown that these potential radiological hazards do not prevent the use of nuclear power in space. Throughout the design and development of SNAP, safety has provided the basis for many design decisions. In order to satisfy the objective of maximum possible safety of the SNAP space reactor systems, a set of safety design criteria for SNAP reactors was formulated. Compromises on the system design are necessary in order to obtain a

suitable balance between the safety of the system and the operational characteristics of reliability, simplicity, and weight. The safety design criteria for the SNAP space reactor systems are outlined below:

Safety and Ease of Handling

The reactor system will be designed so that personnel can handle, install, and repair the system before launch with safety.

Prevention of Accidental Criticality

The reactor system will be designed to prevent criticality of the reactor under any condition except controlled operation.

Inherent Shutdown

The reactor system will have inherent shutdown characteristics (i.e., negative temperature coefficient and fail-safe shutdown mechanisms to prevent reactor operation before or after mission time periods.

Orbital Startup

Reactor system full power operation need not begin until after a suitably safe orbit has been established.

Orbital Shutdown

After the mission has been completed and prior to reentry, the reactor may be shut down.

Reentry Burnup

Design of the reactor system and components will enhance the probability of high altitude reentry burnup and dispersal of SNAP reactor components.

The four major periods of the operational sequence, the particular safety problems of each, and their evaluation and resolution are discussed.

1. Shipment and Integration Period

During the shipment and integration of the Nuclear Auxiliary Power Unit into its payload and launch system, the possibility of accidental criticality and an uncontrolled power excursion must be prevented. The SNAP 2 reactor is specifically designed to allow the removal of the reactor's beryllium reflector and thus greatly increase the safety margin that must be overcome for accidental criticality. During shipment and integration the beryllium will be replaced with

a thick solid aluminum jacket such that accidental immersion in water, liquid hydrogen, or kerosene cannot cause criticality. Likewise, the proximity of installation personnel will not cause accidental criticality. During the shipment and integration period the radioactivity remaining in the core from the factory checkout operations will have decayed to a sufficiently low level that personnel working on or around the APU will be subjected to radiation levels below the AEC established occupational dose rate of 7.5 mr/hr.

By supplementing these physical constraints with carefully planned procedures and trained personnel, the potential of accidental criticality and personnel injury during the shipment and integration period can be even further reduced.

2. Launch Pad Operations Period

It is not expected to be necessary to operate the reactor at full power on the launch pad. The SNAP 2 APU is designed such that system operation and performance can be checked out with electrical power supplying the heat in place of the reactor. If future requirements necessitate complete nuclear operation on the launch pad, it can be accomplished.

Figure 67 shows the dose rate as a function of distance from the operating SNAP 2 reactor with air and inverse square distance attenuation and with 3 ft of concrete shielding. It can be seen from inspection of Figure 67 that the dose outside of normal chemical exclusion radius or inside a normal blockhouse installation is within the AEC occupational dose rate of 7.5 mr/hr.

If the mission is "held" after 30 minutes of reactor power operation on the launch pad, the dose as a function of distance and decay time is shown in Figure 68. After a few hours of decay, short time access to the base of a typical booster is not prohibitive. If access to a payload section is necessary, a gantry mounted maintenance shield is required. A possible configuration is shown in Figure 69. The 4-inch-thick lead maintenance shield is shown to reduce the dose at the payload region to about 100 mr/hr which allows several hours of payload access without excessive exposure.

If the mission is totally "scrubbed," the APU can be removed to a shielded storage well by means of a remotely operated manipulator and gantry.

In the case of a chemical accident after reactor operation or accompanied by an accidental power excursion, preliminary analysis indicates only minor

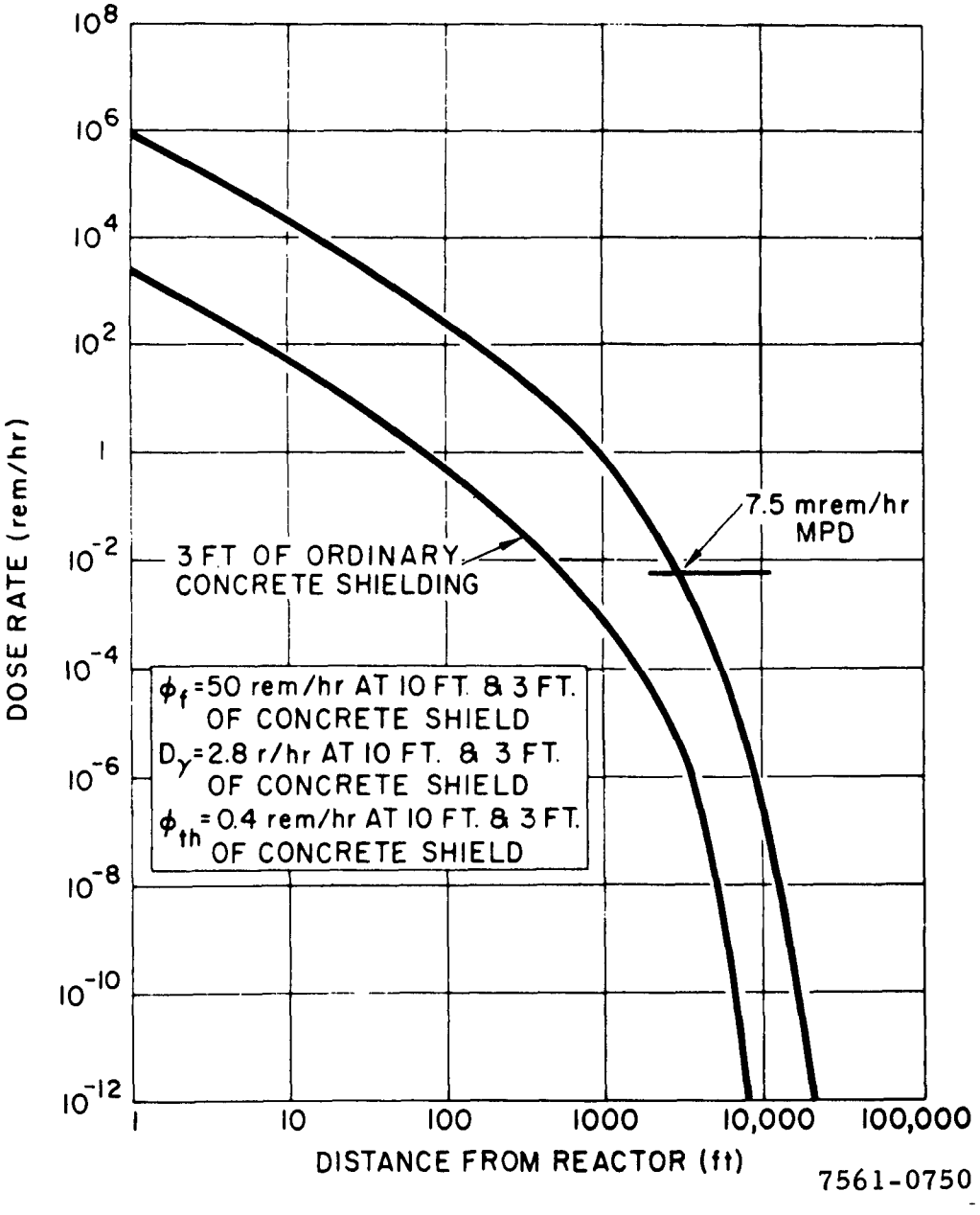

Figure 67. Total Dose Rate as a Function of Distance in Air from SNAP 2 During 50 kw Reactor Operation

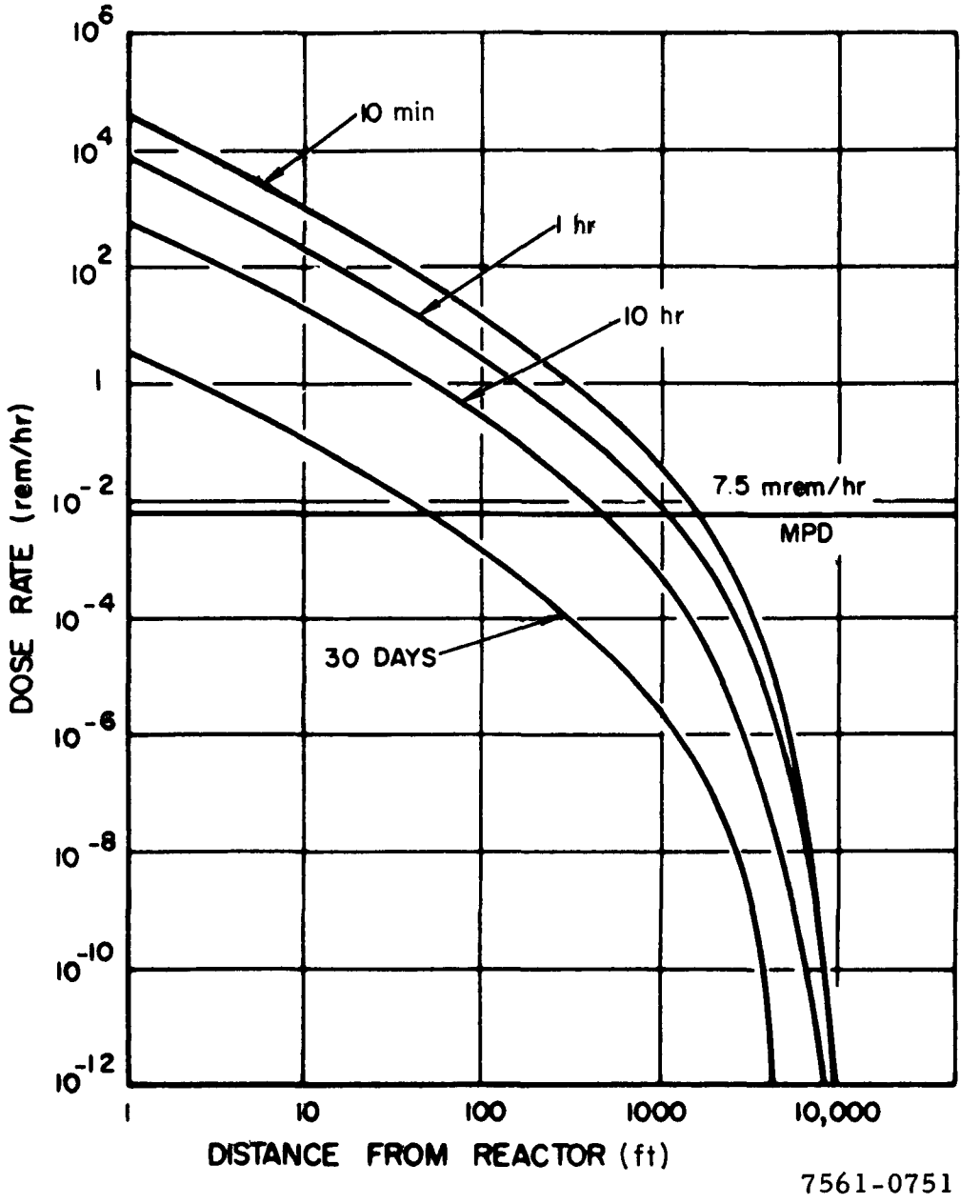

Figure 68. Gamma-Ray Dose Rate from SNAP 2 After 30 Minutes Operation at 50 kw

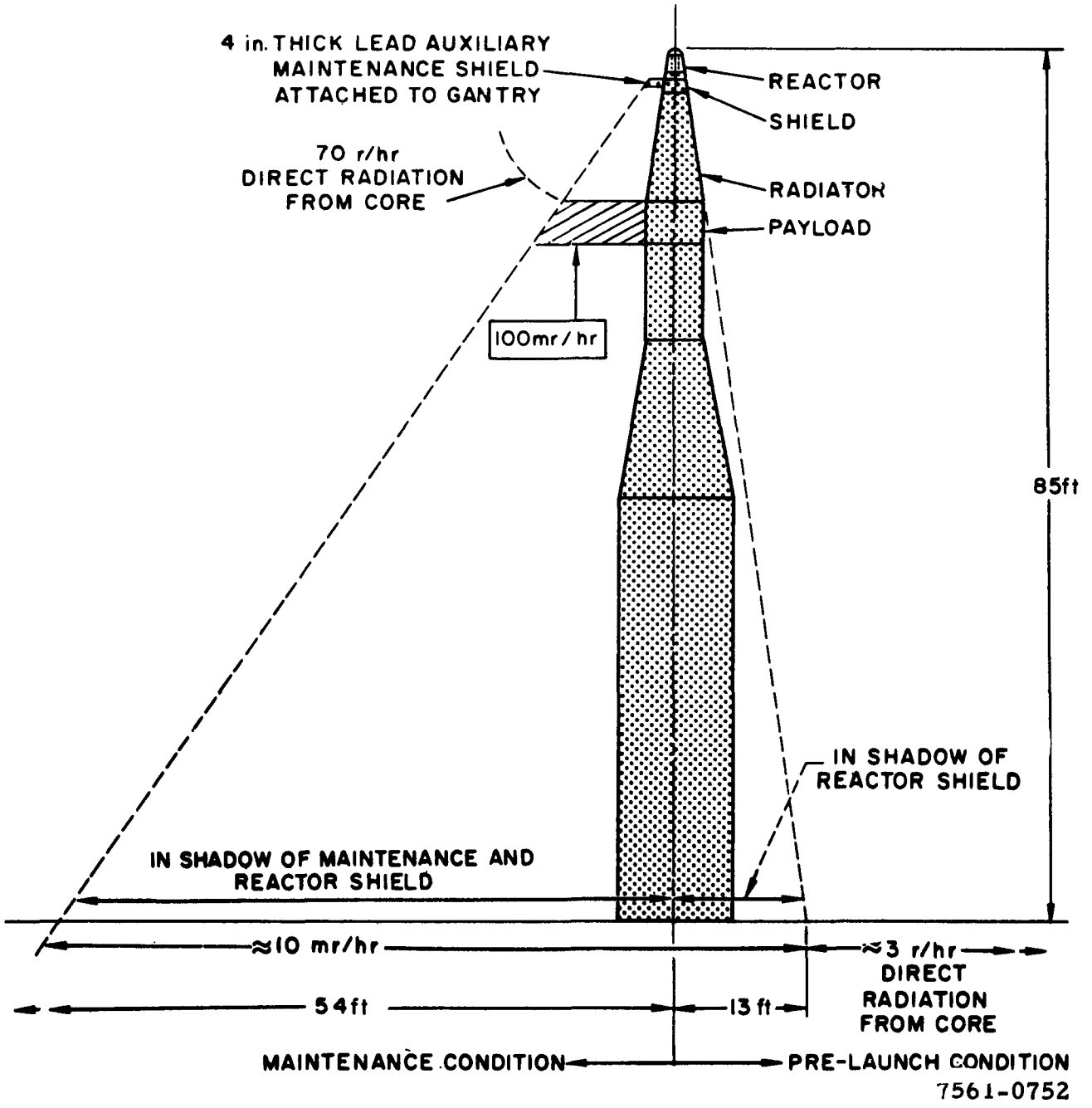

Figure 69. Dosage After 30 Min of Test Operation and 1-hr Decay

hazards outside the normal exclusion radius. Deposition of radioactivity within the exclusion radius could lead to temporary evacuation, but the combination of decay time and emergency decontamination procedures can restore the launch pad area to usefulness.

Again, even the worst case of launch pad abort during reactor power operation can be handled if appropriate equipment and procedures are made available.

3. Launch-to-Orbit Period

The significant problem during the launch to orbit period is the possible chemical explosion accompanied by an uncontrolled reactor power excursion. Only during the early stages of launch does the missile path pass over land. For this period, the hazards discussion for the launch pad period is applicable, which indicated only minor hazards outside the normal exclusion radius. After liftoff the dispersal and dilution factors for the altitudes associated with the missile path over land will further decrease these minor hazards. The remainder of the abort conditions for the launch phase will exist over an ocean region in non-populated areas and far from islands or major cities. The potential hazards to the general populace from a personnel as well as contamination standpoint is negligible over a complete range of possible abort conditions.

4. Reentry Period

In the first three periods considered, the hazards are at all times subject to control through site selection, meteorological limitations, emergency procedures, range safety, etc. The unique problem associated with reactor reentry results from the unpredictable location of reentry and the fact that radiation is undetectable by an unaware populace.

The objective of the SNAP development program is to design for fuel element high altitude burnup and dispersal to result from reentry heating. Preliminary calculations supplemented by arc-jet experiments indicate that this objective can be achieved. In order to evaluate the significance of contributing fission products to the earth's atmosphere through reentry burnup and dispersal of SNAP systems, the resultant buildup of Sr^{90} has been calculated. Figure 70 shows that the reentry of one SNAP 2 system each year after one year of operation will, after 60 years, result in an equilibrium Sr^{90} concentration in the earth's atmosphere that is about 1/240 of the level then existing from bomb

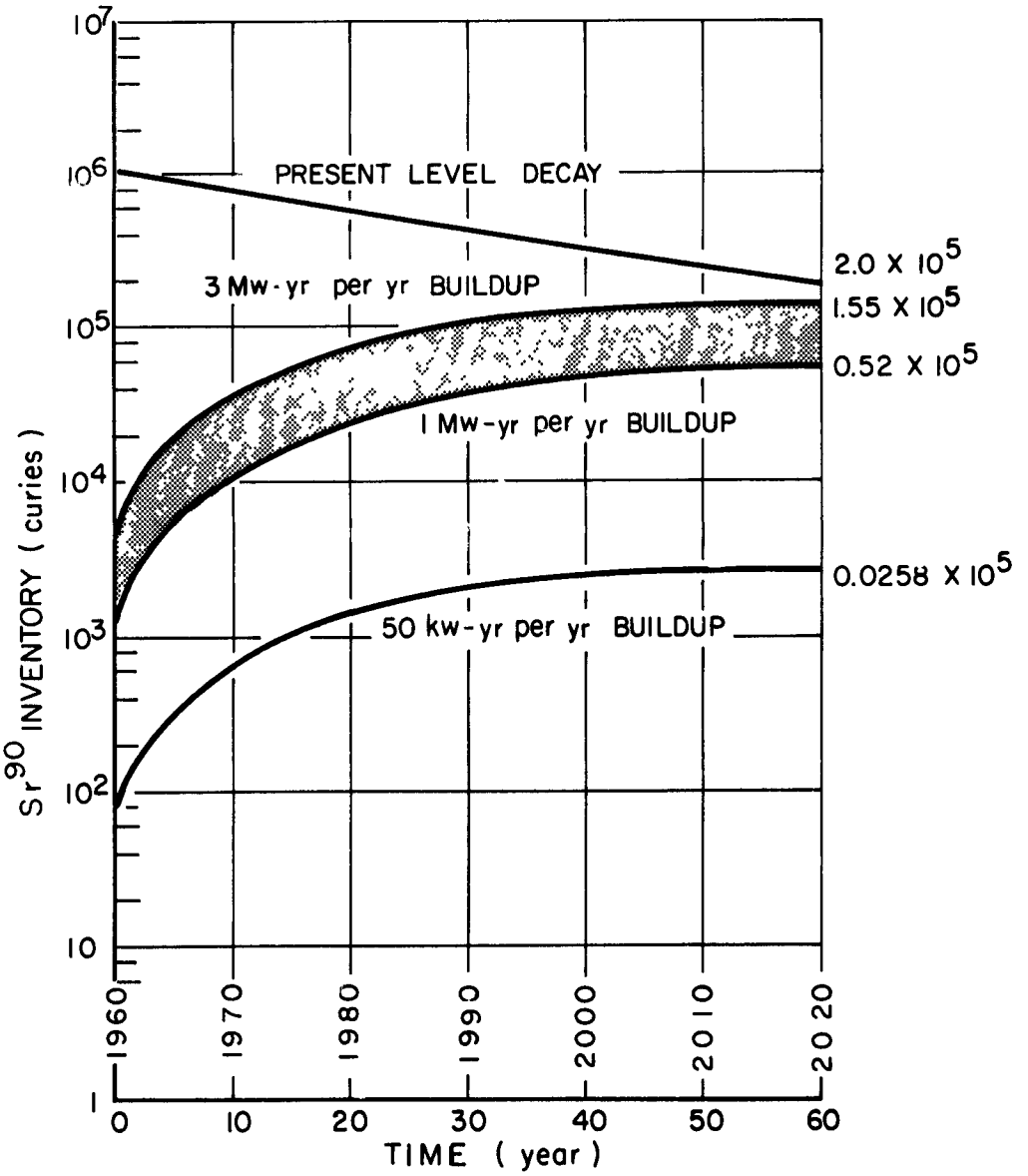

Figure 70. Comparison of Sr^{90} Inventory in Upper Atmosphere From PAST (pre 1960) Nuclear Tests and Possible Space Programs

testing prior to 1960. Or, in other words, SNAP 2 systems could be employed at the rate of 240 per year for the next 60 years and only contribute an amount equal to the Sr^{90} level remaining then from the bomb testing prior to 1960.

Until complete reentry burnup and high altitude dispersal have been demonstrated, there exists an immediately available solution to the hazards associated with the intact reentry of a SNAP system. The problem can be solved by allowing sufficient time for radioactive decay such that intact reentry does not constitute a radiological hazard. This decay time is achieved by limiting the use of SNAP systems to orbital altitudes which have the requisite orbital lifetime for decay. This approach must be supplemented by orbital startup of the system. This capability, which is a SNAP development objective, allows a complete safety appraisal of the orbit prior to system startup and fission product generation.

Figure 71 shows the relationship between dose rate, time for 25 r total dose, decay time, and orbital altitude as a function of distance from an intact SNAP 2 reactor. It can be seen that orbital lifetimes beyond 300 years or about 600 miles for a typical large vehicle, lead to negligible dose rates. Therefore, use of SNAP 2 in orbits of greater than 300 years duration coupled with orbital startup results in no reentry radiological hazard.

In conclusion, radiological hazards do not significantly limit the use of nuclear power in space. The use of high altitude orbits and orbital startup eliminate the reentry hazard by allowing long decay times prior to reentry.

Reentering systems with high altitude burnup and dispersal can be used in large numbers without appreciably contributing to the contamination of the earth's surface or atmosphere. The prelaunch and launch period hazards can be controlled through operational procedures and appropriate facilities and equipment.

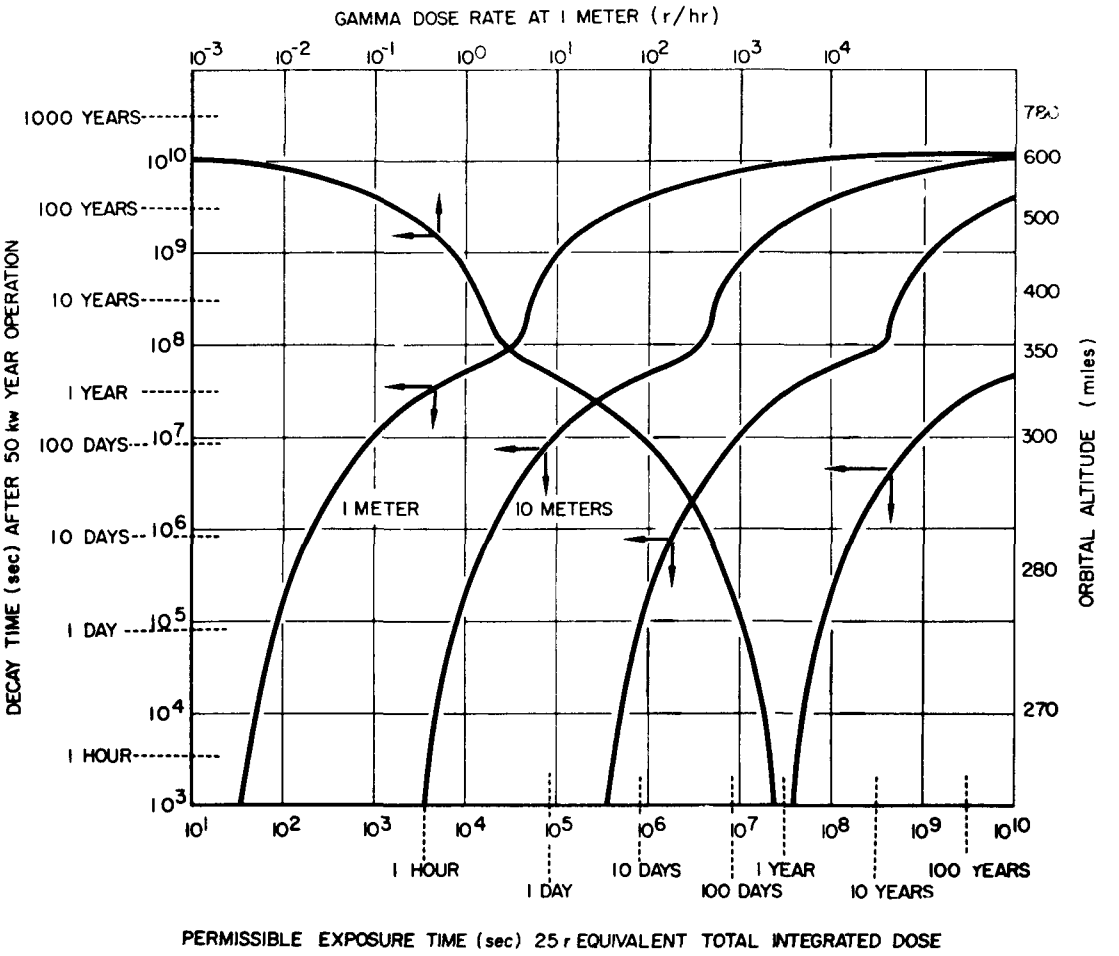

7569-0027

Figure 71. Permissible Exposure Time and Distance for Intact SNAP Reentry vs Decay Time in Orbit and Orbital Altitude

BIBLIOGRAPHY

1. The Elements of Nuclear Reactor Theory, Glasstone and Edlund, D. Van Nostrand Company, 1952.
2. Principles of Nuclear Reactor Engineering, S. Glasstone, D. Van Nostrand Company, 1955.
3. The Physical Theory of Neutron Chain Reactors, Weinberg and Wigner, University of Chicago Press, 1958.
4. Reactor Handbook, Interscience, 1960.
5. Propulsion Systems for Space Flight, W. R. Corliss, McGraw-Hill, 1960.
6. Space Power Systems, Edited by N. W. Snyder, Progress in Astronautics and Rocketry, Vol. 4, Academic Press, 1961.
7. "The Practical Application of Space Nuclear Power in the 1960's," J. R. Wetch, H. M. Dieckamp, and Lt. Col. G. M. Anderson (USAF), Presented to the International Astronautical Congress, August 1960, Stockholm, Sweden.
8. "Advanced Reactor Concepts for Nuclear Propulsion," F. E. Rom, Astronautics Journal, October 1956.
9. "A 20,000 kw Nuclear Turboelectric Power Supply for Manned Space Vehicle," NASA MEMO-2-20-59E, March 1959.
10. "Compact Reactors for Space Power," H. M. Dieckamp, R. Balent, and J. R. Wetch, Nucleonics, April 1961, p 73.
11. "The SNAP Program Present Status and Future Prospects," Lt. Col. G. M. Anderson, Presented at Atomic Industrial Forum, December 1960.
12. "Atoms in Space," Nucleonics, July 1960.
13. "Megawatt Power Levels Sought for Space," P. J. Klass, Aviation Week, August 22, 1960, p 69.
14. "SNAP 1A Targeted for 1961 Operation," Aviation Week, January 30, 1961, p 71.
15. "Systems Must be Flight Tested Soon," Missiles and Rockets, March 20, 1961, p 32.
16. "Nuclear Space Power Systems Utilizing Magnetohydrodynamics Vortices," Lewellen and Grabowsky, ARS Paper 1738-61.
17. "Hazards Associated with Nuclear Power Reactors in Space Applications," P. G. Lafyatis, ARS Paper 1754-61.
18. Nuclear Flight, Lt. Col. K. E. Grantz, Duell, Sloan and Pearce, 1960.
19. "Forecasts for Flight Vehicle Power," G. W. Sherman, SAE 297C, March 1961.
20. "A Binary Vapor Nuclear Power Plant," D. R. Sawle and J. Salisbury, ASME-60-WA-309, November 1960.

21. "Summary of SNAP Nuclear Space Power Systems," E. B. Baumeister, ARS-61-SA-52, June 1961.

22. "The Potential of the SNAP Reactors with Advanced Mercury Rankine Energy Conversion Systems," V. Kovacik, Presented at ANS Nucleonics in Flight Symposium, March 1961.

23. "300 kw Thermionic Generator by 67," W. Beller, Missiles and Rockets, October 3, 1960, p 30.

24. "Megawatt Electrical Power in Space," P. Ross, E. Ray, I. Taylor, Astronautics, December 1960, p 26.

25. "Trends in Turboelectric Power Generation for Space Vehicles," P. Ross and E. Ray, ASME, May 20, 1960.

26. "Space Nuclear Power Conversion System," C. E. Johnson, M. G. Coombs, and R. L. Hirsch, NAE-CON-IRE, May 2, 1959.

27. "Earth Satellite Mission for Electrical Propulsion," by E. E. Dangle, J. D. Gossett, and W. D. Hibbard Jr., paper No. 2225-61, American Rocket Society, Space Flight Report to the Nation, October 9-15, 1961.

28. "SNAP 8 – The First Electric Propulsion Power System," by P. I. Wood, D. L. Forrest, and B. M. Wilner, paper No. 2050-61, American Rocket Society, Space Flight Report to the Nation, October 9-15, 1961.

29. "Performance of Nuclear Electric Propulsion Systems in Space Exploration," by Evelyn W. Speiser, paper 2224-61, American Rocket Society, Space Flight Report to the Nation, October 9-15, 1961.

30. "Test-Bed Configurations for Flight Testing of SNAP 8 Powered Electrical Propulsion Systems," JPL Technical Report No. 32-190.

31. "Systems Engineering of a Nuclear Electric Spacecraft," by R. J. Beale, paper No. 2257-61, American Rocket Society, Space Flight Report to the Nation, October 9-15, 1961.

32. "Space Reactor Power," by J. R. Wetch and M. G. Coombs, paper 2167-61, American Rocket Society, Space Flight Report to the Nation, October 9-15, 1961.

33. "Nuclear Reactor Space Power Systems," by J. R. Wetch and M. G. Coombs, AIEE Aerospace Technical Conference, June 17-22, 1962, Denver, Colorado.

34. "Reactor Power for Communications Satellites," by A. B. Martin, AIF Conference, November 6-8, 1961, Chicago, Illinois.

35. G. Safanov, "Survey of Reacting Mixtures Employing U-235, Pu-239, and U-233 for Fuel and H_2O, D_2O, C, Be, and BeO for Moderators," R-259, January, 1954.

36. "Status of The SNAP 2 Reactor," by R. D. Keen and R. R. Eggleston, presented at the ARS Space Power Systems Conference, Santa Monica, California, September 27-30, 1960.

37. "SNAP 2 Power-Conversion Status," by D. L. Southam, presented at the Space Power Systems Conference, Santa Monica, California, September 27-30, 1960.

38. "SNAP 2 Radiative-Condenser Design," by M. G. Coombs and R. A. Stone, presented at the Space Power Systems Conference, September 27-30, 1960.

39. "SNAP 2 System and Vehicle Integration," D. J. Cockeram and R. L. Wallerstedt, presented at the Space Power Systems Conference, Santa Monica, California, September 27-30, 1960.

40. "SNAP Thermoelectric Systems," by A. W. Thiele and M. G. Coombs, presented at the Space Power Systems Conference, Santa Monica, California, September 27-30, 1960.

41. "The Application of SNAP Units in Current Space Vehicles," by J. R. Wetch and J. G. Lundholm, Jr., presented at the Space Power Systems Conference, Santa Monica, California, September 27-30, 1960.

42. "Problems Associated with the Development of a Thermionic Conversion Reactor," by R. L. Hirsch and J. W. Holland, presented at the Space Power Systems Conference, Santa Monica, California, September 27-30, 1960.

43. "Dynamic Versus Direct Conversion," by K. P. Johnson, presented at the Space Power Systems Conference, Santa Monica, California, September 27-30, 1960.

44. "Boiling Vs Non-Boiling Liquid Metal Cooled Reactors in Rankine Cycle Space Power Plants," by D. L. Cochran and Keith E. Buck, presented at the Space Power Systems Conference, Santa Monica, California, September 27-30, 1960.

45. Redesigned SNAP 8, Nucleonics, Vol 21, No. 7, July 1963.

46. Nuclear Reactor Systems, G. M. Anderson, Astronautics and Aerospace Engineering, May 1963.

47. Space Electrical Power, W. Scott and F. Schulman, Astronautics and Aerospace Engineering, May 1963.

48. Orbital Testing of SNAP Systems, Lt. Col. G. E. Austin, USAF, Astronautics and Aerospace Engineering, May 1963.

49. Thermionic Converters for Space Power, V. C. Wilson and R. C. Hamilton, Astronautics and Aerospace Engineering, May 1963.

50. Dynamic Energy Conversion, V. P. Kovacik, Astronautics and Aerospace Engineering, May 1963.

51. "SNAP 8 Reactor and Shield," by C. E. Johnson and C. A. Goetz, AIAA Electric Propulsion Conference, presented at Colorado Springs, Colorado, March 1963.

52. "Application of a SNAP Reactor Power Plant to a Manned Orbiting Space Station," by H. N. Rosenberg, AI-MEMO-7845, October 1962.

53. "Nuclear Space Power Systems - The SNAP Reactors," by R. E. Wimmer, AIEE Winter Meeting, New York, February 1962.

54. "Power Supply Aspects of the Mars Mission," by R. Balent and J. R. Wetch, presented at the American Astronautical Society, Symposium on the Exploration of Mars, Denver, June 1963.

ATOMICS INTERNATIONAL

A Division of North American Aviation, Inc., Canoga Park, California
Offices in: Washington, D.C./Geneva, Switzerland Affiliated with INTERATOM, Duisburg, Germany